Response to Editor:

Dear editor,

We really appreciate the efforts you made for improving the quality of our manuscript and your patience for giving us enough time to revise our manuscript during this extremely hard time. We tried our best to revise our manuscript according to the comments from two anonymous reviewers. The following major changes were made in our revised paper:

1. We found some mistakes in our program for mapping the MODIS classification system to CLM PFTs, which will lead to missing or double counting some PFT categories during the mapping process. Therefore, we corrected the program and re-ran all experiments. In addition, we used the IGBP classification scheme this time instead of using the Leaf Area Index Classification Scheme in MCD12C1 product as the original classification scheme for mapping considering the more detailed descriptions of legends in IGBP scheme. Some conclusions were also corrected based on the new results.

2. We added one more experiment named S5 to illustrate the contribution of LAI on trends of BVOC emission. In S5, we used the annually updated LAIv and the fixed meteorological inputs and PFT dataset for the year 2001. The analysis for S5 was already added into the revised paper.

3. We further compared our results with other studies to discuss the uncertainties of our estimation. We downloaded some long-term BVOC estimations from ECCAD database (https://eccad.aeris-data.fr) and compared them with our results to analyses the potential reason that results in the discrepancies between our results and other estimations. In addition, we collected the flux measurements from some recent studies (Bai et al., 2015;Bai et al., 2016;Bai et al., 2017) to validate our model and discuss the uncertainties induced by emission factor. Corresponding content has been added into the revised paper.

4. We removed the Section 3.5 in the previous version paper about "Comparison of BVOC emission with Anthropogenic Emission China". Considering the uncertainties behind our estimations, we decided to concentrate on BVOC emission estimation and discuss more about uncertainties instead of extending to discuss anthropogenic emissions. Some lengthy and less informative paragraphs are also removed in the revised paper.

The point-by-point responses to two reviewers' comments are given below.

Response to Referee #1

General comments: This paper presented the MEGAN-simulated biogenic volatile organic compound (BVOC) emissions in China and analysed the modelled contributions from changes in land cover and climate to the BVOC emissions. The modelled variations in isoprene emissions were further linked to the HCHO vertical column. The paper is well-written and has delivered the message about the potential importance of land cover changes in BVOC emissions in China.

Response: Thank you so much for your comments, and we really appreciate it. In the revised paper, we

did the following measurements to address your concerns as well as the other reviewer's concerns:

1. We found some mistakes in our program for mapping the MODIS classification system to CLM PFTs, which will lead to missing or double counting some PFT categories during the mapping process. Therefore, we corrected the program and re-ran all experiments. In addition, we used the IGBP classification scheme this time instead of using the Leaf Area Index Classification Scheme in MCD12C1 product as the original classification scheme for mapping considering the more detailed descriptions of legends in IGBP scheme. Some conclusions were also corrected based on the new results.

2. We added one more experiment named S5 to illustrate the contribution of LAI on trends of BVOC emission. In S5, we used the annually updated LAIv and the fixed meteorological inputs and PFT dataset for the year 2001. The analysis for S5 was already added into the revised paper.

3. We further compared our results with other studies to discuss the uncertainties of our estimation. We downloaded some long-term BVOC estimations from ECCAD database (https://eccad.aeris-data.fr) and compared them with our results to analyses the potential reason that results in the discrepancies between our results and other estimations. In addition, we collected the flux measurements from some recent studies (Bai et al., 2015;Bai et al., 2016;Bai et al., 2017) to validate our model and discuss the uncertainties induced by emission factor. Corresponding content has been added into the revised paper.

4. We removed the Section 3.5 in the previous version paper about "Comparison of BVOC emission with Anthropogenic Emission China". Considering the uncertainties behind our estimations, we decided to concentrate on BVOC emission estimation and discuss more about uncertainties instead of extending to discuss anthropogenic emissions. Some lengthy and less informative paragraphs are also removed in the revised paper.

The current format of the manuscript has been much focused on analysing the patterns simulated from the four different scenarios, but rather limited in understanding the uncertainties (e.g., uncertainties from satellite products or assigned emission factor or missing PFT) associated with the model simulation.

Response: Thank you so much for your comments. We double-checked the program for mapping the MODIS PFT to CLM PFT classification, and we found some mistakes in the program that led to missing or double counting some PFTs during the mapping process. Therefore, we corrected the program and re-ran the all experiments. In addition, we used the IGBP classification scheme this time instead of using the Leaf Area Index Classification Scheme in MCD12C1 product as the original classification scheme for mapping considering the more detailed descriptions of legends in IGBP scheme. So, we redesigned the mapping method.

The mapping method is in two steps. As presented in Table R1, we firstly mapped the IGBP classification to eight main vegetation categories: needleleaf evergreen forests, broadleaf evergreen forests, needleleaf deciduous forests, broadleaf deciduous forests, mixed forests, shrub, grass and crop according to the description of the legends. Then, eight main categories were mapped to the

classification of CLM/MEGAN for boreal, temperate and boreal climatic zones using the definition from Bonan et al. (2002). The climatic criteria for mapping is presented in Table R2, and the climatic information for mapping was from the climatology of the ERA Interim during 2001-2016 (Berrisford et al., 2011). The final special distribution of the percentages of PFTs is presented in Figure R1. The emission factors in this study are coming from the PFT-level emission factors presented in Table 2 of Guenther et al. (2012). The corresponding description is added at P4, L9 in the revised paper as:

"The PFT was used to determine the canopy structure and standard emission factors in MEGAN (Guenther et al., 2012). We adopted the default emission factors for PFTs described in Table 2 in Guenther et al. (2012). The PFT dataset in this study is obtained from the MODIS MCD12C1 land cover product (https://lpdaac.usgs.gov/products/mcd12c1v006/, Friedl and Sulla-Menashe, 2015). MODIS IGBP classification were mapped to the PFT classification of MEGAN or the Community Land Model (CLM) (Lawrence et al., 2011) based on the description of the legends in the user guide (Sulla-Menashe and Friedl, 2018) and the climatic criteria described in Bonan et al. (2002). The spatial distribution of percentage of PFTs in model grids is presented in Figure 1. According to the description of the legends, we firstly mapped the IGBP classification to eight main vegetation categories: 1) needleleaf evergreen forests, 2) broadleaf evergreen forests, 3) needleleaf deciduous forests, 4) broadleaf deciduous forests, 5) mixed forests, 6) shrub, 7) grass and 8) crop. The mapping method is described in Table S1 in the supplement. Eight main categories then were mapped to the classification of MEGAN/CLM for boreal, temperate and boreal climatic zones using the definition in Bonan et al. (2002). Table S2 in the supplement presents the climatic criteria for mapping, and the climatic information for mapping was from the ERA Interim climatology (https://www.ecmwf.int/en/forecasts/datasets/reanalysis-datasets/era-interim, Berrisford et al., 2011) Reanalysis dataset over 2001-2016."

Table R1. Look-up table for mapping the IGBP classification scheme to eight main vegetations categories.

Name	Value	Description	Percentages of Main Category
Needleleaf Evergreen Forest	1	Dominated by evergreen conifer trees (canopy >2m).	100% Needleleaf Evergreen Tree Forest
Broadleaf Evergreen Forest	2	Dominated by evergreen broadleaf and palmate trees (canopy >2m).	100% Broadleaf Evergreen Tree Forest
Needleleaf Deciduous Forest	3	Dominated by deciduous needleleaf (larch) trees (canopy >2m).	100% Needleleaf Deciduous Tree Forest
Broadleaf Deciduous Forest	4	Dominated by deciduous broadleaf trees (canopy >2m).	100% Broadleaf Deciduous Tree Forest
Mixed Forests	5	Dominated by neither deciduous nor evergreen (40-60% of each) tree type	100% Mixed Forests

		(canopy >2m).	
Closed Shrublands	6	Dominated by woody perennials (1-2m height) >60% cover.	100% Shrub
Open Shrublands	7	Dominated by woody perennials (1-2m height) 10-60% cover.	60% Shrub 40% Grass
Woody Savannas	8	Tree cover 30-60% (canopy >2m).	60% Mixed Forest 20% Shrub 20% Grass
Savannas	9	Tree cover 10-30% (canopy >2m).	30% Mixed Forest 35% Shrub 35% Grass
Grasslands	10	Dominated by herbaceous annuals (<2m).	100% Grass
Permanent Wetlands	11	Permanently inundated lands with 30-60% water cover and >10% vegetated cover.	40% Grass
Croplands	12	At least 60% of area is cultivated cropland.	100% Crop
Urban and Built-up Lands	13	At least 30% impervious surface area including building materials, asphalt, and vehicles.	None
Cropland/Natural Vegetation Mosaics	14	Mosaics of small-scale cultivation 40-60% with natural tree, shrub, or herbaceous vegetation.	60% Crop 20% Shrub 20% Grass
Permanent Snow and Ice	15	At least 60% of area is covered by snow and ice for at least 10 months of the year.	None
Barren	16	At least 60% of area is non-vegetated barren (sand, rock, soil) areas with less than 10% vegetation.	None

Table R2. The climatic criteria for mapping main vegetation categories to CLM PFTs [a].

Main Categories	Mapping Condition	Percentages of CLM PFTs
NET	T_c >-19 °C and GDD > 1200	100% NET Temperate
	T_c≤-19 °C or GDD ≤ 1200	100% NET Boreal
BET	T_c >15.5 °C	100% BET Tropical
	T_c≤15.5 °C	100% BET Temperate
NDT	None	100% NDT
BDT	T_c >15.5 °C	100% BDT Tropical
	-15.5 °C <T_c≤15.5 °C or GDD>1200	100% BDT Temperate
	T_c≤-15.5 °C or GDD ≤ 1200	100% BDT Boreal
Mixed Forest	T_c >15.5 °C	50% BET Tropical
		50% BDT Tropical
	-15.5 °C<T_c≤15.5 °C and GDD>1200	33.33% NET Temperate
		33.33% BET Temperate
		33.33% BDT Temperate
	T_c≤-15.5 °C or GDD ≤ 1200	33.33% NDT
		33.33% NET Boreal
		33.33% BDT Boreal
Shrub	T_c >-19 °C and GDD > 1200	100% BDS Temperate
	T_c≤-19 °C or GDD ≤ 1200	100% BDS Boreal
Grass	GDD<1000	100% C3 Arctic
	GDD>1000 and (Tc ≤ 22°C or Pmon≤25 mm)	100% C3
	GDD>1000 and Tc > 22°C and Pmon >25 mm	100% C4
Crop	None	100% Crop

[a] NET, Needleleaf Evergreen Trees; BET, Broadleaf Evergreen Trees; NDT, Needleleaf Evergreen Trees; BDT, Broadleaf Deciduous Trees; Tc, Temperature in the coldest month; GDD, growing-degree days above 5°C; Pmon, monthly precipitation.

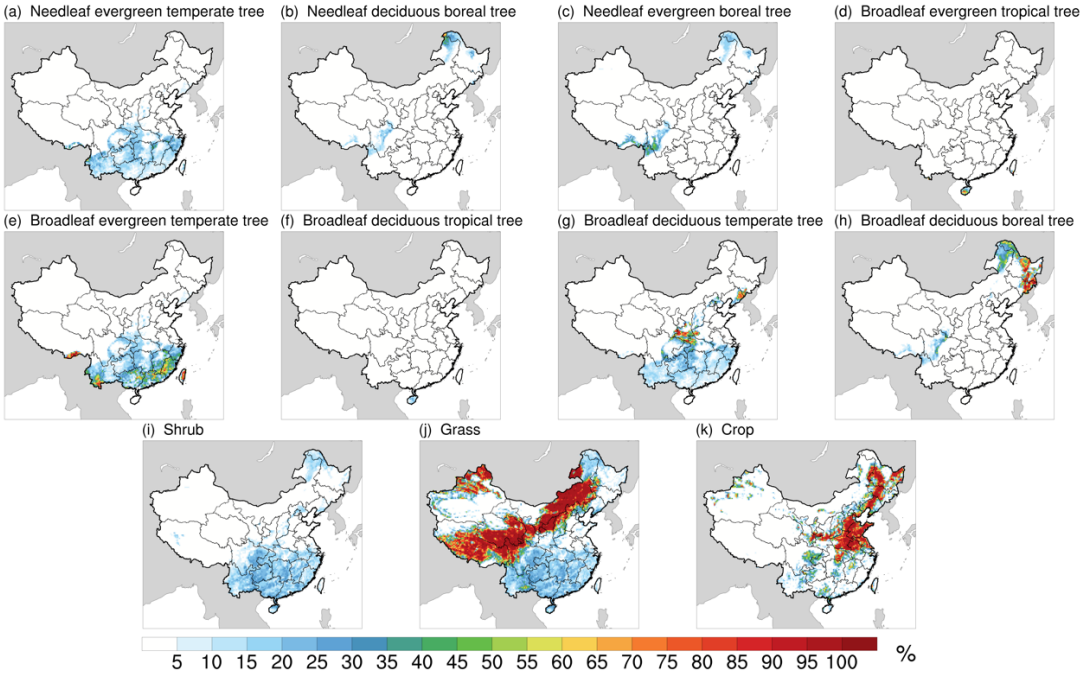

Figure R1. The percentage of different PFTs for the year 2016.

Then when the authors linked their simulated isoprene emission with the HCHO vertical column, the disagreement of these two has been mainly attributed to the AVOC, but I would think there could be also contributions from the uncertainties in the simulated BVOCs. From the maps with simulated BVOCs, I am a bit surprised to see that the north part of China with high LAI showed very low simulated emissions, especially monoterpene. Could this be linked to the misclassification of forest type?

Response: Thank you so much for comments. Firstly, we have added one more section to discuss the uncertainties by comparing our results with the flux measurements and other estimations from previous studies. Secondly, we updated the figure by presenting the annual averaged LAIv instead of growing season LAIv (May-Sep). As shown in the Figure R2, the annual averaged LAIv is not as high as the growing season averaged LAIv in northeast China. In addition, we also mapped the IGBP classification to PFTs with the new rules we designed and the distribution of different PFTs has been given in Figure R1. The main reason why the BVOC emission in northeastern China is low is the impact of local climate in this region. In the revised paper, we added northeastern China as one of the sub-regions for analyzing. As shown in Table 3 in the revised paper, the simulated growing season averaged temperature is about 13.74 °C in northeastern China, which is much lower than other regions, e.g. the simulated growing season averaged temperature is about 20.78 °C in the Qinling mountains. As shown in Figure R1, the tree cover fraction is not low in northeastern China, however, the unfavorable meteorological conditions lead to the low emission in this region.

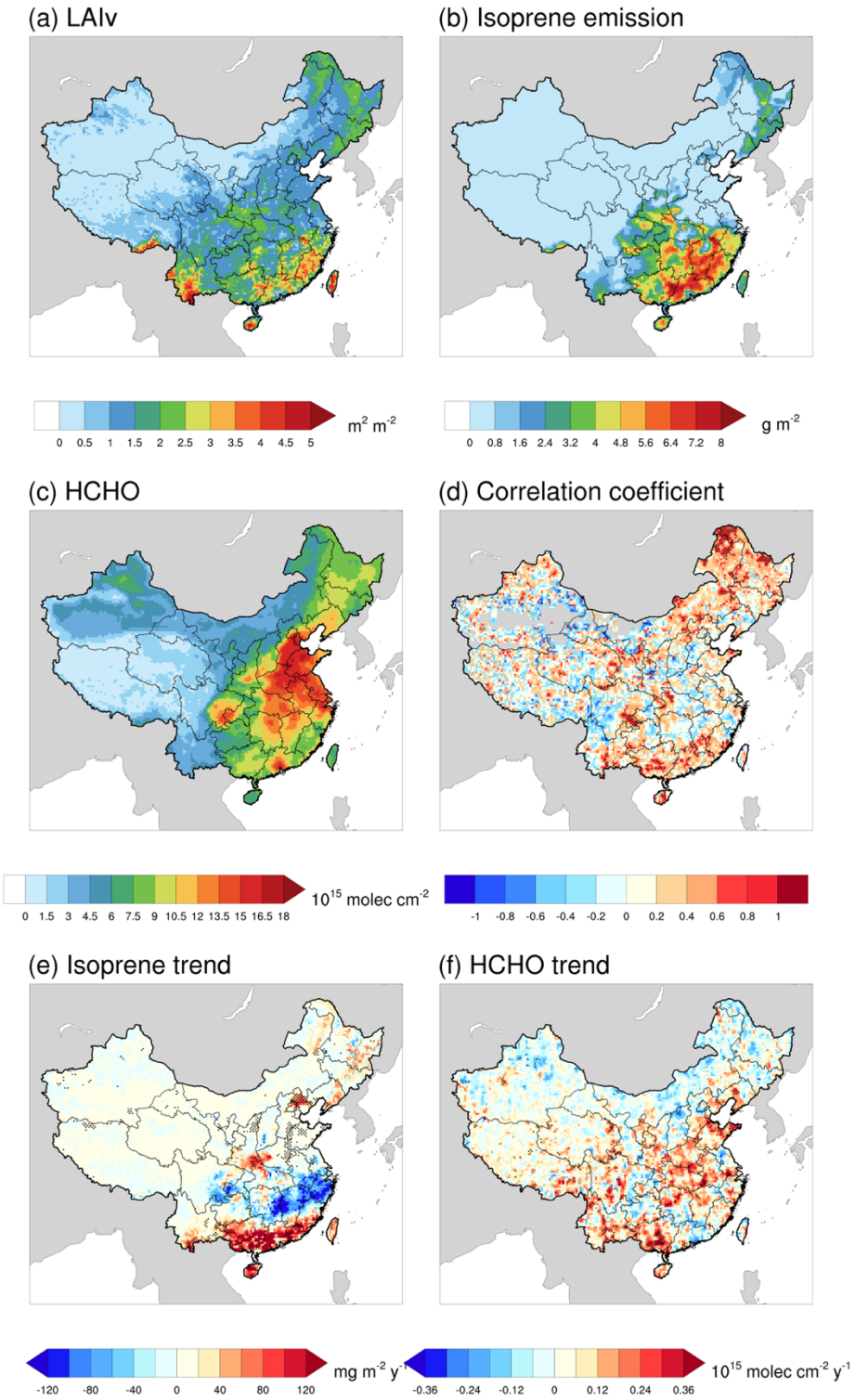

Figure R2. Comparison of estimated isoprene annual emission with the satellite derived tropospheric HCHO vertical column concentration by OMI during 2005-2016. (a), (b) and (c) illustrate the spatial distributions of annual mean LAI, isoprene emission and HCHO vertical columns (VC) by OMI respectively. (d) presents the

spatial distribution of the correlation coefficient between summertime isoprene emission and HCHO VC. (e) and (f) shows the increasing trend of isoprene and HCHO VC during 2005-2016.

Then in the east and/or at least North China Plain area, there is wide distribution of crops. Are crops specifically considered in MEGAN?

Response: Yeah, as shown in Figure R1, there is wide distribution of crops in North China Plain. The crops are considered as only one kind of PFT in the MEGAN, therefore, emission factors for all species of crops are same in our simulation.

In general, a map showing the spatial distribution of PFTs could be very useful for readers.

Response: Thank you so much for your comments. The spatial distribution of different PFTs has been given in Figure R1.

I also think it is crucial to compare the modelled emissions with a few sites' measurement data to illustrate the performance of the model before digging into analysing the changes of the emission patterns at the national scale and further linking to the HCHO column data.

Response: Thank you so much for your precious time and your comments. We collected the flux measurements in China from some recent studies (Bai et al., 2015;Bai et al., 2016;Bai et al., 2017) and use them to validate and analyze the uncertainties of our estimation. The details about the flux measurements has been given in Table R3. In addition, we also compared our results with other similar studies to discuss the source of uncertainties in this study. The discussion about the uncertainties in this study has been added at P11, L11 in the revised paper as:

"The comparison of isoprene and monoterpenes emission estimations between our estimations and previous studies is presented in Table 5. The estimations of isoprene emission range from 4.65 Tg to 33.21 Tg, and the estimations of monoterpenes emission range from 3.16 Tg to 5.6 Tg in China. Multiple factors including emission factor, algorithm, meteorological and land cover inputs can lead to the discrepancy of these estimations. We listed the inputs of these estimations in Table 6 to fully understand the discrepancies between our results and other estimations.

The setting of inputs in this study is relatively close to the study by Stavrakou et al. (2014) and CAMS-GLOB-BIO biogenic emission inventories (https://eccad3.sedoo.fr/#CAMS-GLOB-BIO) that adopted the method described by Sindelarova et al. (2014). However, the estimation of isoprene emission in this study is about 86.6%-122.3% higher than their estimations, and the estimation of monoterpene emission is about 23.5% and 31.3% higher than that from CAMS-GLOB-BIO v3.1 and v1.1, respectively. We further compared our results with two versions of CAMS-GLOB-BIO inventories. Figure 10 and Figure 11 present the trends of isoprene emission and monoterpenes emission respectively from S1 and S3 in this study, CAMS-GLOB-BIO inventory v 1.1 and v 3.1 during 2001-2016. As shown in Figure 10 and

Figure 11, S3 shows similar spatial patterns and magnitude of changing trend of isoprene and monoterpenes emission with CAMS-GLOB-BIO v 1.1 and CAMS-GLOB-BIO v3.1, e.g. three datasets all showed a strong increasing trend in Yunnan province, and S1 shows much more stronger changing trends comparing with other three datasets with annually updated LAI and PFT datasets. The meteorological inputs for CAMS-GLOB-BIO v1.1 and v3.1 are ERA-Interim and ERA-5 reanalysis data, respectively, and the WRF model used in this study was also driven by ERA-Interim reanalysis data. Therefore, the four datasets have the similar source of meteorological inputs. In addition, these estimations all adopted the same PFT level emission factors from Guenther et al. (2012). Therefore, the potential reason for the differences of isoprene and monoterpenes emission among the datasets in Figure 10 and Figure 11 is the discrepancies of PFT and LAI inputs. CAMS-GLOB-BIO also adopted the annually updated LAI inputs developed by Yuan et al. (2011) based on MODIS MOD15A v5 LAI product, but the two versions of CAMS-GLOB-BIO inventory didn't show a same level strong increasing trend with S1. The increasing trend of LAI in China is agreed by multiple LAI products but with different rates (Piao et al., 2015; Chen et al., 2020). In this study, we adopted the latest MODIS LAI product of version 6, and a strong increasing trend of LAI in China has been found by using this product (Chen et al., 2019). Therefore, an increasing trend of BVOC emission induced by LAI should be seen in the estimation with annually updated LAI inputs, but the magnitude of this trend is also affected by the magnitude of changing trend of LAI products. The PFT map used in this study is coming from MODIS land cover product, which is a mesoscale satellite product with the highest resolution of 500m. Besides the product itself, the method for converting the original land cover classification system to PFT classification system is also important. Hartley et al. (2017) illustrated that the cross-walking table for converting land cover class maps to PFT fractional maps can lead to 20%-90% uncertainties for gross primary production estimation in land surface model by using different vegetation fractions for mixed pixels, and the BVOC emission estimation has the same issue. In this study, we assumed that the pixels that were assigned as vegetation is 100% covered by that kind of vegetation (Table S3 in the supplement). Therefore, it will lead to the overestimation of vegetation cover rate for mixed pixels, which can lead to higher BVOC emission.

The emission factor is also an important source of uncertainties, and it decided the spatial patterns of emission rates together with the PFT distribution. In order to understand the role of emission factor, the flux measurements of isoprene and monoterpenes from the campaigns conducted during 2010 to 2016 in China (Bai et al., 2015; Bai et al., 2016; Bai et al., 2017) were collected and compared with model results in this study. The details of these campaigns are provided in Table 7, and the emission factors that were retrieved from the observations are also listed for these sites. Most samples were collected during the daytime every 3 hours according to the descriptions of the measurements (Bai et al., 2015;Bai et al., 2016;Bai et al., 2017), therefore, we averaged the model results during 8:00 A.M. to 20 A.M in local time with a three hours interval for comparison. As shown in the (a) and (b) of Figure 12, the modeled fluxes of isoprene and monoterpenes with the default emission factors in this study didn't capture the variability of the observations. The ME, MB and RMSE are 1.60, 1.59 and 2.31 mg m-2 h-1 for isoprene and 0.21, -0.003 and 0.32 mg m-2 h-1 for monoterpenes. When we adopted the emission

factor retrieved from observations (Bai et al., 2015;Bai et al., 2016;Bai et al., 2017), the simulated isoprene and monoterpenes fluxes showed relatively good consistence with the observations by using the same activity factor from this study (γ in equation (1)) as shown in (c) and (b) of Figure 12. The ME, MB and RMSE are 0.44, 0.41 and 0.57 mg m-2 h-1 for isoprene and 0.32, 0.14 and 0.49 mg m-2 h-1 for monoterpenes after adopting the observation-based emission factors, and the statistic parameters for isoprene simulation are largely improved. Although the MB and ME of monoterpenes simulation are increased, but the simulated monoterpenes flux showed better agreement with observations (Figure 12). Therefore, it is clear that our calculation of activity factors is in a reasonable range, but the emission factor is the main source of uncertainties. The PFT level emission factors used in this study from Guenther et al. (2012) represents the globally averaged emission factor for PFTs, and it is relatively easy to use the them with the satellite PFT products. Therefore, the most studies listed in Table 6 adopted the PFT/landuse level emission factors. Our validation showed that the accurate emission factor based on observations could largely improve the performance of MEGAN model, but it also requires abundant efforts to conduct measurements. However, the measurements listed in Table 7 are still very limited for describing the spatial discrepancies of ecosystems in China, so we still used the default emission factors in MEGAN model. The estimations by Li et al. (2013, 2020) used the species level emission factors and Vegetation Atlas of China for 2007 to describe the spatial distribution of BVOC emission potentials, and they concluded the reason why their estimations were far higher than other studies is the high emission factors they adopted. Therefore, the same validations by using canopy-scale BVOC flux measurements are also needed for these studies to validate and constrain the emission factors they used.

Meteorological input is also a source of uncertainties for BVOC emission estimation. As shown in Figure 12, the modeled isoprene and monoterpenes fluxes are still generally higher than observations when observation-based emission factors were used. One potential reason for this phenomenon is the overestimation of temperature and radiation as described in Section 2.3. The sensitivity tests by Wang et al. (2011) showed that the about 1.89 °C discrepancy of temperature can result in -19.2 to 23.2% change of isoprene emission and -16.2 to 18.5% change of monoterpenes emission for Pearl River Delta region during July, where is also a hotspot for BVOC emission in this study. They also found that 115.8 W m-2 discrepancy of DSW can result in -31.4 to 36.2% change of isoprene emission and -14.3 to 16.8% change of monoterpenes emission for the same region. The BVOC emission in this study might be overestimated because of the overestimated temperature and DSW in meteorological inputs. However, inaccurate emission factors could lead to over 100% uncertainties, which is more significant than the uncertainties induced by meteorological inputs."

Table R3. Detailed descriptions of the flux measurements used in this study and corresponding campaigns.

Reference	Site Location	Sample Collection Time	Ecosystem Type	Isoprene Emission Factor ($mg\ m^{-2}\ h^{-1}$)	Monoterpenes Emission Factor ($mg\ m^{-2}\ h^{-1}$)

Bai et al. (2015)	Changbai Mountain (42°24′ N, 128°6′)	28 June -9 July 2010; 19 July -30 July 2010; 12 Aug.- 25 Aug. 2010; 19 June - 30 June 2011; 10 July -16 July 2011; 22 July - 29 July 2011; 5 Sep. - 8 Sep. 2011.	Mixed forest	4.3	0.32
Bai et al. (2016)	An Ji, Zhejiang (30°40′15″ N, 119°40′15″)	7 July-13 July 2012; 20 Aug.-26 Aug. 2012; 25 Sep.-1 Oct. 2012; 28 Oct.- 5 Nov. 2012.	Moso bamboo forest	3.3	0.008
Bai et al. (2017)	Taihe, Jiangxi (26°44′48″ N, 115°04′13″)	22 May -28 May 2013; 29 June - 6 July 2013; 6 Aug. -13 Aug. 2013; 7 Sep. -11 Sep. 2013; 18 Jan. -19 Jan. 2014; 23 July - 27 July 2014; 2 Nov. - 7 Nov. 2015; 31 Dec. 2015 -4 Jan. 2016.	Subtropical Pinus forest	0.71	1.65

Specific comments:

P2 L5-6, please indicate at which spatial scale we can see cropland dominates the reduction of isoprene.

Response: Thank you for your comments. We have revised this sentence as:

"For instance, the global cropland expansion has been estimated to dominate the reduction of isoprene, the dominant BVOC species, in last century (Lathière et al., 2010; Unger, 2013) although there are large uncertainties associated with these estimates."

P2 L10, the authors mentioned that the greening in China has been linked to "maintain and expand forests". Did they change plant species when expanding forest? And can you see this level of land use change in the MODIS PFT product?

Response: Thank you for your comments. Currently, it is not possible to distinguish the specific species of trees using MODIS since the spatial resolution of MODIS sensor is not high enough to do so. So, we can't see the species-level change through the MODIS PFTs. Our estimation is mainly based on the PFT level change.

P3 L2, suggest to delete "accurately". You have not evaluated the modelled BVOC against the measurements.

Response: Thank you so much for your advice, and the word "accurately" has been deleted in the revised paper.

P4L2-4, here you might need to specify where these emission factors are from? How much of these emission factors covered the measurements from China? I did a quick google search and could already see some measurement data available for different ecosystems in China.
https://www.sciencedirect.com/science/article/pii/S1352231017302947
https://www.sciencedirect.com/science/article/pii/S1352231015305173
https://www.sciencedirect.com/science/article/pii/S0269749119346081?via%3Dihub

Response: Thank you so much for your comments. The emission factors in this study are the default values of the MEGAN 2.1 provided by Guenther et al. 2012. Since we didn't have an ability to distinguish the species of the trees using the MODIS images, we didn't consider using the species-based emission factors. It is true that this will induce the uncertainty of emission amount, and we have added some discussion for this in the revised paper. As mentioned above, we used the flux measurements of BVOC from some recent studies to validate our model and discuss the uncertainties induced by emission factors. The performance of model can be improved by updating the emission factors according to our results. When we adopted the emission factor retrieved from observations (Bai et al., 2015; Bai et al., 2016;Bai et al., 2017), the simulated isoprene and monoterpenes fluxes showed relatively good consistence with the observations by using the same activity factors from this study shown in (c) and (b) in Figure R3. However, these studies only covered very limited numbers of ecosystems in China. Since our work is focusing on the impact of land cover change and vegetation biomass change on BVOC emission, so using the default emission factor is also able to discuss the change of BVOC induced by vegetation development.

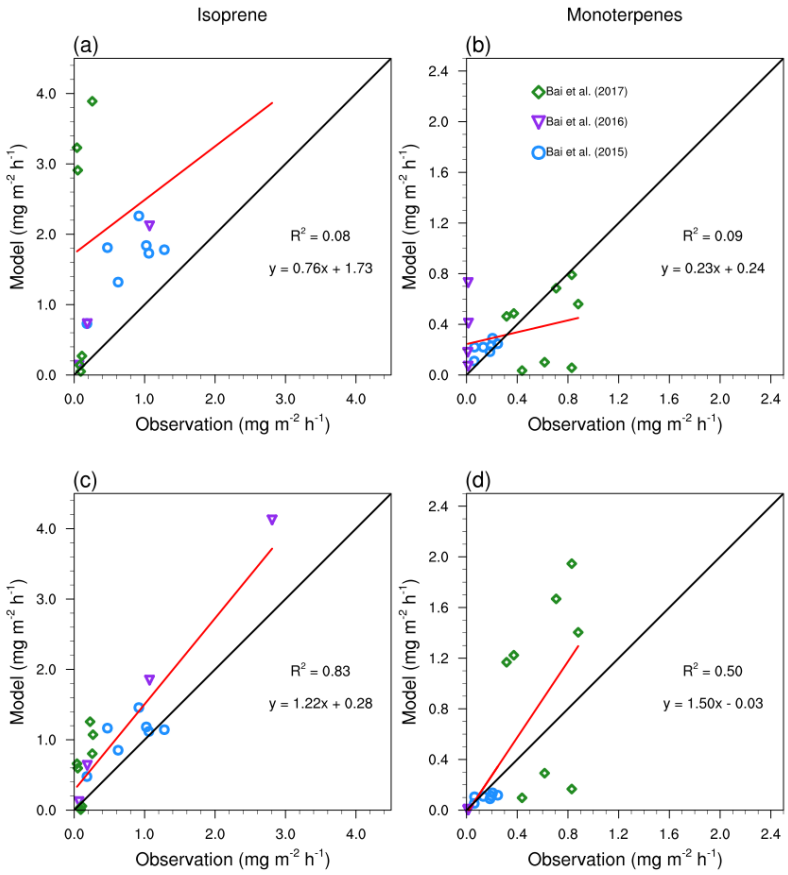

Figure R3. Validation of the model with flux measurements in China. (a) and (b) show the performance of the MEGAN model with the default emission factors. (c) and (d) show the performance of the MEGAN model with the emission factors derived from observations.

P4 L8, "The Cce(=0.57) is a factor to xx" what does this mean?

Response: As described by Guenther et al. (2006), the C_{ce} is a parameter in MEGAN model that sets the emission factor to unity at the standard conditions. It has no physical meaning and was used to normalize the emission factors.

P4 L9, how can LAI define leaf age in MEGAN?

Response: Thank you so much for your comments. The leaf-age factor,γ_{age}, in MEGAN is described in detail in Guenther et al. (2006). For the evergreen canopies, γ_{age} is constant. For the deciduous canopies, the leaves are divided into four stages of new leaf, growing leaf, mature leaf and old leaf since the emission capacity of leaf is diverse with leaf age(Guenther et al., 1991;Monson et al., 1994;Guenther et al., 2006). According to Guenther et al. (2006), the γ_{age} is defined as:

$$\gamma_{age} = F_{new}A_{new} + F_{gro}A_{gro} + F_{mat}A_{mat} + F_{old}A_{old}$$

where A_{new}, A_{gro}, A_{mat} and A_{old} are the relative emission rates for new, growing, mature and old foliages. F_{new}, F_{gro}, F_{mat} and F_{old} are the fractions of different sorts of leaves and are defined by the change of LAI between the current time step (LAIc) and the previous time step (LAIp). F_{new}=0, F_{gro}=0.1, F_{mat}=0.8 and F_{old}=0.1 when LAIc equals LAIp. When LAIp> LAIc, the fractions in different stages are as:

$$\begin{cases} F_{new} = 0 \\ F_{gro} = 0 \\ F_{old} = [(LAIp - LAIc)/LAIp] \\ F_{old} = 1 - F_{old} \end{cases}$$

In the cases of LAIp<LAIc, the fractions are calculated as:

$$\begin{cases} F_{new} = 1 - (LAIp/LAIc) \\ F_{gro} = 1 - F_{new} - F_{mat} \\ F_{mat} = LAIp/LAIc \\ F_{old} = 0 \end{cases}$$

.

P4 L13, Is soil moisture used as inputs for model? If so, please clarify.

Response: Thanks for your comments. The soil moisture is simulated by the WRF model and will be considered in the calculation. We have followed your comments and clarify this part in the revised paper in P4, L20:

"The hourly meteorological fields including temperature, downward shortwave radiation (DSW), wind speed, surface pressure, precipitation and water vapor mixing ratio were provided by the Weather Research and Forecast (WRF) Model V3.9 (Skamarock et al., 2008) simulations."

P4 L17-18, LAI is a 'modelled' product from other satellite products and potentially has large uncertainty in itself. I wonder if the LAI has been filtered by the quality flags before using as inputs for MEGAN and how the model deals with the LAI gap if there is no data for many 8-days?

Response: Thank you so much for your comments. We used all available values in MODIS LAI products, and we didn't use the quality filter at the first place to ensure the model can be driven by continued LAI field. The model didn't have ability to deal with the LAI gap, but this problem can be solved by using some interpolation technics when preparing the inputs. In this study, we didn't use interpolation method to fill the gaps to avoid introducing artificial uncertainties especially for trend analysis.

P4 L21-23, Could you list what PFTs you have in your simulations (or showing a map), and also how MODIS PFTs were reclassified to the CLM group? I think this information is important for readers to understand the spatial pattern.

Response: Thank you so much for your comments. We already provided the method we adopted to reclassify the MODIS IGBP classification to the CLM group in the revised paper. The spatial distribution of different PFTs has been given in Figure R1.

P7 L18-19, the reasons why the simulated MT is so much lower than the previous estimations needs to dig in-depth. Like I mentioned early, could it be linked to the misclassification of PFTs or very different emission factors assigned? In Table 3, the modelled isoprene is very low than Li et al., 2013, can the authors describe a bit about why?

Response: Thank so much for your comments. As mentioned above, we re-mapped the IGBP classification to PFTs with the new rules we designed and the distribution of different PFTs has been given in Figure R1. Currently, our estimation of 33.99 Tg is relatively moderate comparing to other studies (Table R4). In addition, the studies by Li et al. (2013, 2020) showed the highest amounts of isoprene and monoterpenes emissions comparing to other studies. Therefore, in the revised paper, we listed the inputs of different studies to analyze the potential reasons for the discrepancies among these studies. As shown in Table R5, the estimations by Li et al. (2013, 2020) used the species level emission factors and Vegetation Atlas of China for 2007 to describe the spatial distribution of BVOC emission potentials, which is quite different from other studies adopting the PFT-level emission factors and satellite PFT products. They themselves concluded the reason why their estimations were far higher than other studies was because of the high emission factors they adopted. Therefore, the same validations by using canopy-scale BVOC flux measurements are also needed for these studies to validate and constrain the emission factors they used.

Table R4. Comparison of isoprene and monoterpene emissions (Tg) in China with previous studies.

Data Source	Isoprene	Monoterpene	Study period	Method or Model
This study	15.94 (±1.12)	3.99 (±0.17)	2001-2016	MEGAN
Stavrakou et al. (2014)	7.17 (±0.30)	-	2007-2012	MEGAN-MOHYCAN
Li et al. (2013)	23.4	5.6	2003	MEGAN
Li et al. (2020)	33.21	6.35	2008-2018	MEGAN
CAMS-GLOB-BIO v1.1	7.67	3.04	2001-2016	MEGEN

(Sindelarova et al., 2014)				
CAMS-GLOB-BIO v3.1 (Sindelarova et al., 2014)	8.54	3.23	2001-2016	MEGAN
Fu and Liao (2012)	10.87	3.21	2001-2006	GEOS-Chem-MEGAN
Tie et al. (2006)	7.7	3.16	2004	Guenther et al. (1993)
Klinger et al. (2002)	4.65	3.97	2000	Guenther et al. (1995)
Guenther et al. (1995)	17	4.87	1990	Guenther et al. (1995)

Table R5. Comparison of inputs for BVOC estimation with previous studies.

Reference	Emission Factor Type	Emission Factor Reference	PFT/Land use	LAI/Biomass	Meteorology	Model/Algorithms
This study	PFT level emission factors	Guenther et al. (2012)	MODIS MCD12C1 v6	MODIS MCD15A2H v5	WRF Model v3.9	MEGANv2.1
Stavrakou et al. (2014)	PFT level emission factors	Guenther et al. (2006)	Ramankutty and Foley (1999)	MODIS MOD15A2 v5	ERA-Interim Dataset	MEGAN-MOHYCAN
Li et al. (2013)	Vegetation genera/species level emission factors	Li et al. (2013)	Vegetation Atlas of China for year 2007	MEGAN database for 2003	MM5 Model v3.7	MEGAN
Li et al. (2020)	Vegetation genera/species level emission factors	Li et al. (2013)	Vegetation Atlas of China for year 2007	Estimations based on surveys and statistics	WRF Model v3.8	MEGAN
CAMS-GLOB-BIO v1.1 (Sindelarova et al., 2014)	PFT level emission factors	Guenther et al. (2012)	16 plant functional types consistent with the Community Land Model	MODIS MOD15A2 v5	ERA-Interim Dataset	MEGAN

CAMS-GLOB-BIO v3.1 (Sindelarova et al., 2014)	PFT level emission factors	Guenther et al. (2012)	16 plant functional types consistent with the Community Land Model	MODIS MOD15A2 v5	ERA-5 Dataset	MEGAN
Fu and Liao (2012)	PFT level emission factors	Guenther et al. (1995) Lathière et al. (2006) Levis et al. (2003) Bai et al. (2006)	MODIS MCD12Q1 v5	MODIS MOD15A2 v5	GEOS-4 Meteorology	GEOS-Chem-MEGAN
Tie et al. (2006)	Landuse level emission factors	Landuse-based emission rates	USGS 1km land use data	/	WRF model	Guenther et al. (1993)
Klinger et al. (2002)	Vegetation genera/species level emission factors	Klinger et al. (2002)	Province-level Forest Inventory	/	Monthly meteorology database by (Leemans and Cramer, 1991)	Guenther et al. (1995)
Guenther et al. (1995)	PFT level emission factors	Guenther et al. (1995)	Grided Global Ecosystem Types	Estimations from NPP	Monthly meteorology database by (Leemans and Cramer, 1991)	Guenther et al. (1995)

P9 L23, might need to add one or two sentences in the method section why p > 0.9 is statistically significant. I did not get it here.

Response: Thank you so much for comments. The probability we used here is defined as:

probability = 1 – p,

where p is the 2-sided p value after MK test (https://mailman.ucar.edu/pipermail/ncl-talk/2015-May/002594.html). Since this may confuse the readers, we adopted the original 2-sided p value from MK tests in the revised paper.

P12 L11-12, "The lack of long-term in-situ observations of BVOC in China..." I think this might be the case for most of countries where we don't have dataset being representative at the whole country level,

but I think the authors should definitely compare the modelled with in-situ data for a few representative sites to evaluate the model performance. In China, there are some sites where you can find the ecosystem-level BVOC measurement data for comparison, like some links I provided in the previous comments.

Response: Thank you so much for comments. Luckily, some flux measurements were conducted in China and published in recent years. We collected theses flux measurements from some recent studies (Bai et al., 2015;Bai et al., 2016;Bai et al., 2017) and use them to validate and analyze the uncertainties of our estimation. The details about the flux measurements has been given in **Table R3**.

According to our validation, the performance of model can be improved by updating the emission factors. When we adopted the emission factor retrieved from observations (Bai et al., 2015; Bai et al., 2016;Bai et al., 2017), the simulated isoprene and monoterpenes fluxes showed relatively good consistence with the observations by using the same activity factors from this study shown in (c) and (b) in Figure R3. This indicates that emission factors are an important source of uncertainties in this study, on the other hand, it also demonstrates our calculation of activity factor in the model is in a relatively reasonable range. However, these studies only covered very limited numbers of ecosystems in China. Our work is focusing on the impact of land cover change and vegetation biomass change on BVOC emission. The increasing trend of tree cover fraction will increase the BVOC emission with the reasonable activity factors, and the role of emission factors is to decide how strong the trend can be. So, using the default emission factor is also able to discuss the change of BVOC induced by vegetation development.

P12 L12-18, this part should be in the method section.

Response: Thanks for your comments. This part has been introduced in the Section 2.4, so we removed the repeated information here and rephrased this paragraph as:

"The OMI HCHO VC product from 2005-2016 developed by BIRA-IASB (De Smedt et al., 2015) was used in this study. The interannual variability of isoprene emission estimated in this study was evaluated by comparing the isoprene emission with the summer (June-August) averaged HCHO VC."

P13 L5, ". . . are marked with black dots" it is difficult to see these dots though.

Response: Thanks for your comments. As shown in Figure R2, we used relatively sparser and more conspicuous dots to illustrate the grids that passed the t test in the revised paper.

Conclusion, it is rather lengthy at this moment and includes large section of discussion as well. Please make it more concise.

Response: Thanks for your comments. We have removed some lengthy paragraphs in the revised paper,

and we were more focused on discussing the detail of methods and uncertainties.

Response to Referee #2

The study by Wang and co-workers investigates the impact of satellite-based land use changes on biogenic VOC emissions in China over 16 years (2001-2016). They report positive emission trends of 1-1.5% per year over the whole country, which are attributed, for a major part, to changes in vegetation. The strongest BVOC trends are reported in Qianling mountains and in south China, where the BVOC emissions increased by more than ~60% in 2016 relative to 2001. Further comparison of BVOC interannual variability with HCHO columns from the OMI instrument over the studied period in summertime exhibited positive temporal correlation over forested regions. This study addresses an interesting subject for Atmospheric Chemistry and Physics journal. However, there are weaknesses and limitations in the present study, which raise doubts regarding the validity of the conclusions. Furthermore, the presentation is often difficult to follow, mostly due to insufficient mastery of the English language. To my view, the manuscript will need a major revision before it becomes suitable for publication. My main concerns are listed below:

Response: Thank you so much for your precious time and we really appreciate your comments. We have tried to address your concerns by taking the following measures:

1. We found some mistakes in our program for mapping the MODIS classification system to CLM PFTs, which will lead to missing or double counting some PFT categories during the mapping process. Therefore, we corrected the program and re-ran the all experiments. In addition, we used the IGBP classification scheme this time instead of using the Leaf Area Index Classification Scheme in MCD12C1 product as the original classification scheme for mapping considering the more detailed descriptions of legends in IGBP scheme. Some conclusions were also corrected based on the new results.

2. We added one more experiment named S5 to illustrate the contribution of LAI on trends of BVOC emission. In S5, we used the annually updated LAIv and the fixed meteorological inputs and PFT dataset for the year 2001. The analysis for S5 has been added into the revised paper.

3. We further compared our results with other studies to discuss the uncertainties of our estimation. We downloaded some long-term BVOC estimations from ECCAD database (https://eccad.aeris-data.fr) and compared them with our results to analyses the potential reason that results in the discrepancies between our results and other estimations. In addition, we collected the flux measurements from some recent studies (Bai et al., 2015;Bai et al., 2016;Bai et al., 2017) to validate our model and discuss the uncertainties induced by emission factor. Corresponding content has been added into the revised paper.

4. We removed the Section 3.5 in the previous version paper about “Comparison of BVOC emission with Anthropogenic Emission China”. Considering the uncertainties behind our estimations, we decided to concentrate on BVOC emission estimation and discuss more about uncertainties instead of extending to discuss anthropogenic emissions. Some lengthy and less informative paragraphs are also removed in

the revised paper.

(i) Important input datasets required for calculating BVOC emissions using MEGAN model (e.g. PFTs) are not shown. Annual maps of the MODIS PFTs and LAI should be provided, as well as their trends. Without such information, it is impossible to assess the driving factors for the changes and therefore for the validity of the claims. Furthermore, it is not clearly mentioned whether a unique emission factor per PFT has been used (Table 2 of Guenther et al. 2012) or if a map of standard emission factors has been used.

Response: Thank you so much for your comments. The spatial distribution of different PFTs has been shown in Figure R1, which is also provided in the revised paper. Besides the spatial distribution of PFTs, the trend of main PFTs and LAIv are also provided here (Figure R4) as well as in the revised paper.

The method for converting MODIS classification system to CLM PFTs is added at P4, L8 as:

"The PFT was used to determine the canopy structure and standard emission factors in MEGAN (Guenther et al., 2012). We adopted the default emission factors for PFTs described in Table 2 in Guenther et al. (2012). The PFT data source in this study is obtained from the MODIS MCD12C1 land cover product (https://lpdaac.usgs.gov/products/mcd12c1v006/, Friedl and Sulla-Menashe, 2015). MODIS IGBP classification were mapped to the PFT classification of MEGAN or the Community Land Model (CLM) (Lawrence et al., 2011) based on the description of the legends in the user guide (Sulla-Menashe and Friedl, 2018) and the climatic criteria described in Bonan et al. (2002). The spatial distribution of percentage of PFTs in model grids is presented in Figure 1. According to the description of the legends, we firstly mapped the IGBP classification to eight main vegetation categories: 1) needleleaf evergreen forests, 2) broadleaf evergreen forests, 3) needleleaf deciduous forests, 4) broadleaf deciduous forests, 5) mixed forests, 6) shrub, 7) grass and 8) crop. The mapping method is described in Table S1 in the supplement. Eight main categories then were mapped to the classification of MEGAN/CLM for boreal, temperate and boreal climatic zones using the definition by Bonan et al. (2002). Table S2 in the supplement presents the climatic criteria for mapping, and the climatic information for mapping was from the climatology of the ERA Interim (https://www.ecmwf.int/en/forecasts/datasets/reanalysis-datasets/era-interim, Berrisford et al., 2011) Reanalysis dataset over 2001-2016."

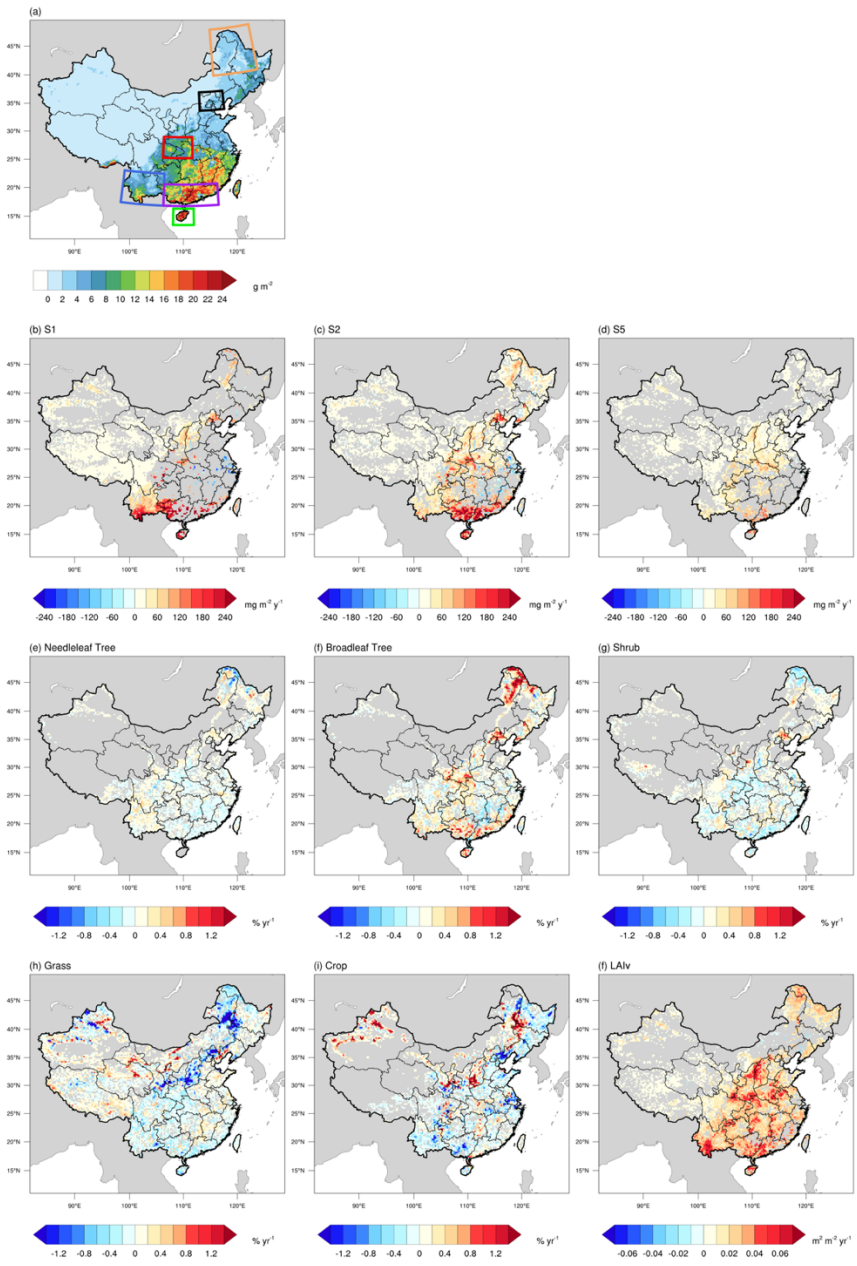

Figure R4. Spatial distribution of BVOC emission in 2001 (b) and the changing trends of annual emission rate (S1, S2 and S5), cover fractions of main PFTs and LAIv.

(ii) I have my doubts regarding the almost negligible isoprene trends due to meteorology suggested by Figure 3 (simulations S3 and S4). The scale in this figure does not allow to see any changes elsewhere than in the Tibetan Plateau. Elsewhere, the color (grey) corresponds to no value. In order to explain the emission trend in S3 and S4, trends of the main drivers of the BVOC emission trends, namely, air temperature, solar radiation and leaf area index should be analysed. In addition, the simulated trend in surface temperature and radiation should be compared to the corresponding trends of the in situ

temperature and solar radiation data used for the evaluation of the WRF model simulation in Section 2.3.

Response: Thank you so much for your comments. We have adopted your suggestions and took some measures to improve the way to convey information. As shown in Figure R5, we changed the way we presented the spatial patterns of trends, and we used the black dots to mark the regions with statistically significant trends and keep the non-significant trends for other the regions. For the meteorological drivers, we also gave the trends of growing season 2-meter temperature (T2) and downward shortwave radiation (DSW) (Figure R6). Furthermore, the details of land cover changes, LAI and meteorological conditions were also presented and analyzed for the regional analysis.

We also added the following description in P5, L12:

"The trends of growing season averaged T2 and DSW from model results as well as in-situ measurements are presented in Figure 3. The model and the in-situ measurements show similar patterns for T2. For instance, the model and observations both show an increasing trend in regions like the Tibetan Plateau, southern China and a decreasing trend in eastern and northeastern China. For DSW, the model presented a dimming trend in northeastern and eastern China and a brightening trend in southeastern and central China, and the limited number of radiation observation sites show a similar pattern of trend with model results. In general, the WRF simulation successfully captured the long-term meteorological variabilities and is reasonable to use for estimating the impact of climatic variability on BVOC emission in China for this study."

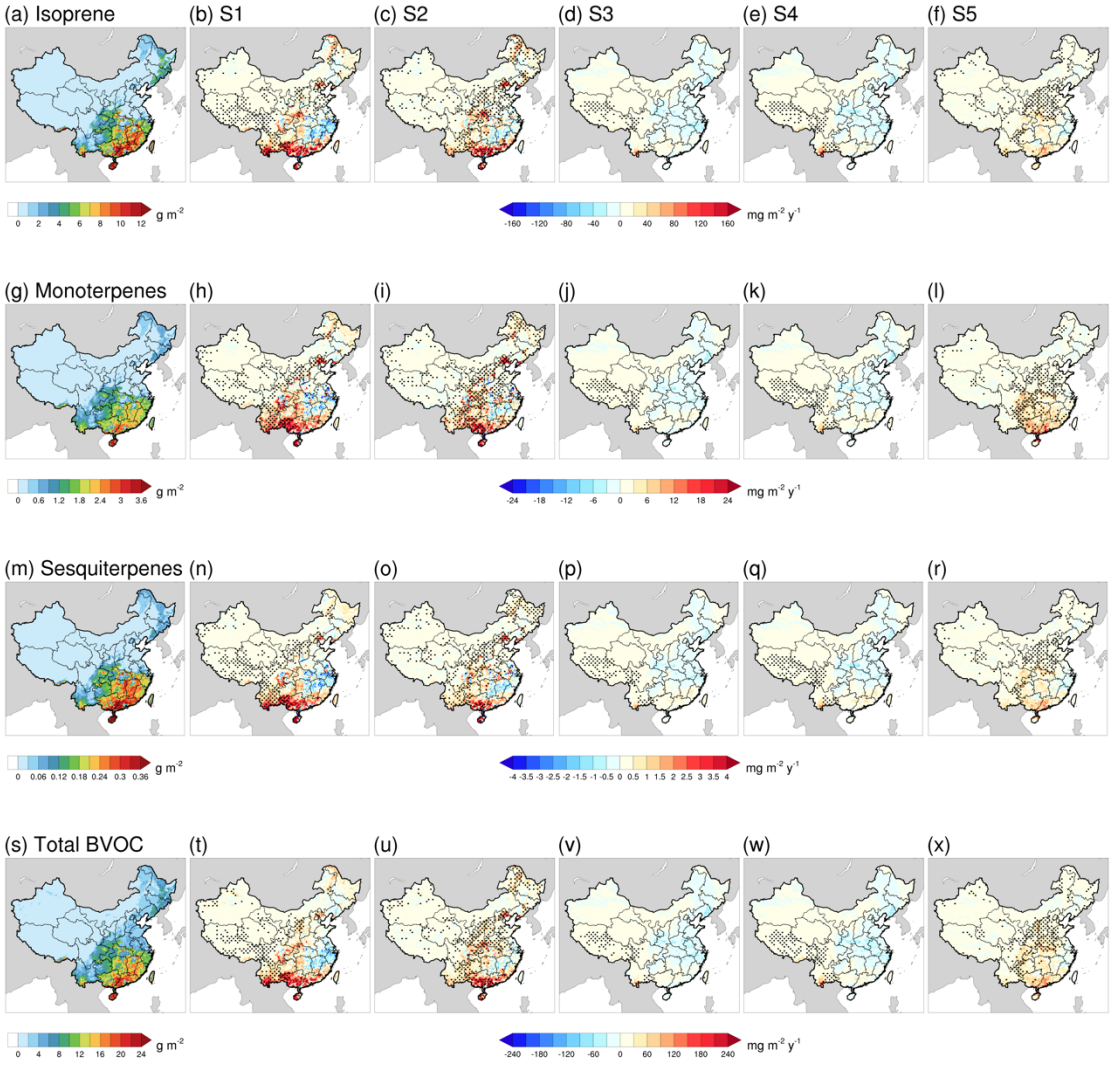

Figure R5. The horizontal distributions of isoprene, monoterpenes, sesquiterpenes and total BVOCs emissions of China in 2001 are showed in figure (a), (g), (m) and (s), respectively. The rest columns of figures present the changing trend of isoprene (b-f), monoterpenes (h-l), sesquiterpenes (n-r) and total BVOCs (t-x) in S1, S2, S3, S4 and S5, respectively. The Mann-Kendall test were used to mark the grids where the p is smaller than 0.1.

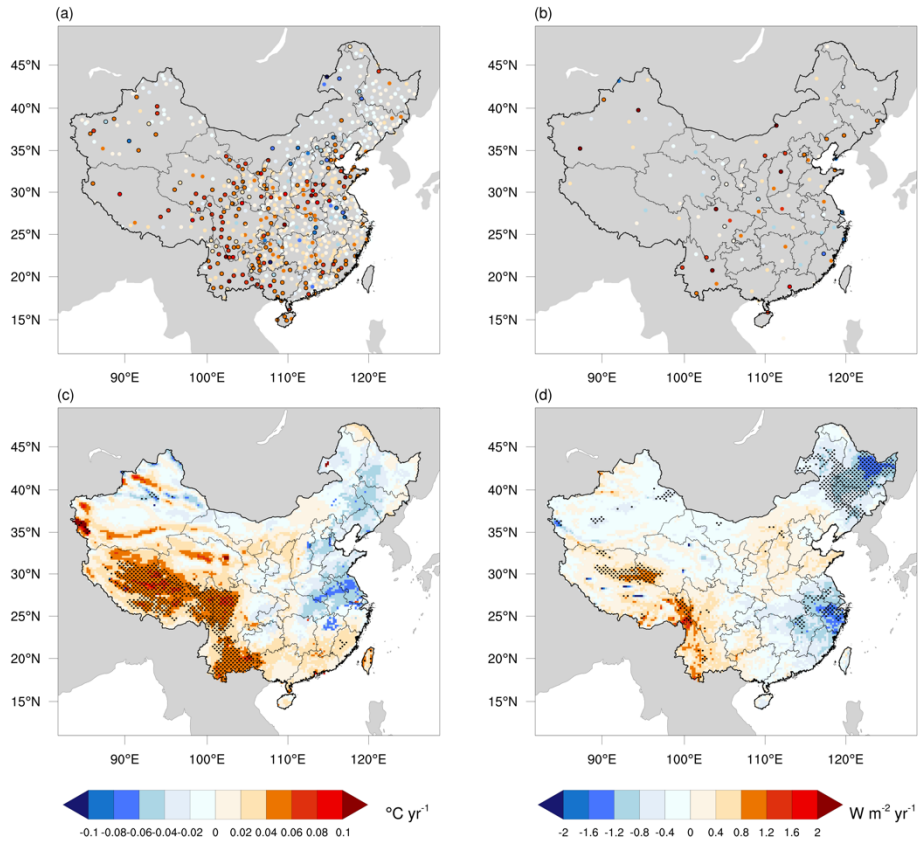

Figure R6. The trend of growing season averaged 2-meter temperature (T2) and downward shortwave radiation (DSW). (a) and (b) are for in-situ T2 and DSW, respectively, and the sites with statistically significant trend are marked by black circles. (c) and (d) are for the WRF simulated T2 and DSW, respectively, and the regions with statistically significant trend are illustrated by shadow.

(iii) There is not convincing evidence for the very low monoterpene emission derived in this study compared to previous work (Table 3). The invoked reasons, e.g. interannual variations, horizontal resolution, etc. (page 7, lines 81-20) are not convincing. The reasons of the discrepancy should be investigated through detailed comparisons e.g. with the MEGAN inventory and similar studies e.g. Sindelarova et al. (2014). These datasets are accessible via the ECCAD database (https://eccad.aeris-data.fr).

Response: Thank you so much for your comments. After re-runing our experiments, our estimation of monoterpenes emission is about 3.99 Tg, which is close to or even higher than other studies. In addition, we have compared our results with the CAMS-GLOB-BIO inventories of BVOC emission from ECCAD database as shown in Figure R7 and Figure R8, and we concluded that the discrepancy between our estimation with CAMS-GLOB-BIO inventories is the PFT and LAI inputs. The meteorological

inputs for CAMS-GLOB-BIO v1.1 and v3.1 are ERA-Interim and ERA-5 reanalysis data, respectively, and the WRF model used in this study was also driven by ERA-Interim reanalysis data. Therefore, the four datasets have the similar source of meteorological inputs. In addition, these estimations all adopted the same PFT level emission factors from Guenther et al. (2012). Therefore, the potential reason for the differences between our estimation and CAMS-GLOB-BIO inventories is the discrepancies of PFT and LAI inputs. The following discussion have been added in P11, L16:

"The setting of inputs in this study is relatively close to the study by Stavrakou et al. (2014) and CAMS-GLOB-BIO biogenic emission inventories (https://eccad3.sedoo.fr/#CAMS-GLOB-BIO) that adopted the method described by Sindelarova et al. (2014). However, the estimation of isoprene emission in this study is about 86.6%-122.3% higher than their estimations, and the estimation of monoterpene emission is about 23.5% and 31.3% higher than that from CAMS-GLOB-BIO v3.1 and v1.1, respectively. We further compared our results with two versions of CAMS-GLOB-BIO inventories. Figure 10 and Figure 11 present the trends of isoprene emission and monoterpenes emission respectively from S1 and S3 in this study, CAMS-GLOB-BIO inventory v 1.1 and v 3.1 during 2001-2016. As shown in Figure 10 and Figure 11, S3 shows similar spatial patterns and magnitude of changing trend of isoprene and monoterpenes emission with CAMS-GLOB-BIO v 1.1 and CAMS-GLOB-BIO v3.1, e.g. three datasets all showed a strong increasing trend in Yunnan province, and S1 shows much more stronger changing trends comparing with other three datasets with annually updated LAI and PFT datasets. The meteorological inputs for CAMS-GLOB-BIO v1.1 and v3.1 are ERA-Interim and ERA-5 reanalysis data, respectively, and the WRF model used in this study was also driven by ERA-Interim reanalysis data. Therefore, the four datasets have the similar source of meteorological inputs. In addition, these estimations all adopted the same PFT level emission factors from Guenther et al. (2012). Therefore, the potential reason for the differences of isoprene and monoterpenes emission among the datasets in Figure 10 and Figure 11 is the discrepancies of PFT and LAI inputs. CAMS-GLOB-BIO also adopted the annually updated LAI inputs developed by Yuan et al. (2011) based on MODIS MOD15A v5 LAI product, but the two versions of CAMS-GLOB-BIO inventory didn't show a same level strong increasing trend with S1. The increasing trend of LAI in China is agreed by multiple LAI products but with different rates (Piao et al., 2015;Chen et al., 2020). In this study, we adopted the latest MODIS LAI product of version 6, and a strong increasing trend of LAI in China has been found by using this product (Chen et al., 2019). Therefore, an increasing trend of BVOC emission induced by LAI should be seen in the estimation with annually updated LAI inputs, but the magnitude of this trend is also affected by the magnitude of changing trend of LAI products. The PFT map used in this study is coming from MODIS land cover product, which is a mesoscale satellite product with the highest resolution of 500m. Besides the product itself, the method for converting the original land cover classification system to PFT classification system is also important. Hartley et al. (2017) illustrated that the cross-walking table for converting land cover class maps to PFT fractional maps can lead to 20%-90% uncertainties for gross primary production estimation in land surface model by using different vegetation fractions for mixed pixels, and the BVOC emission estimation has the same issue. In this study, we assumed that the pixels that were assigned as vegetation is 100% covered by that kind of vegetation (Table S2 in the

supplement). Therefore, it will lead to the overestimation of vegetation cover rate for mixed pixels, which can lead to higher BVOC emission. ”

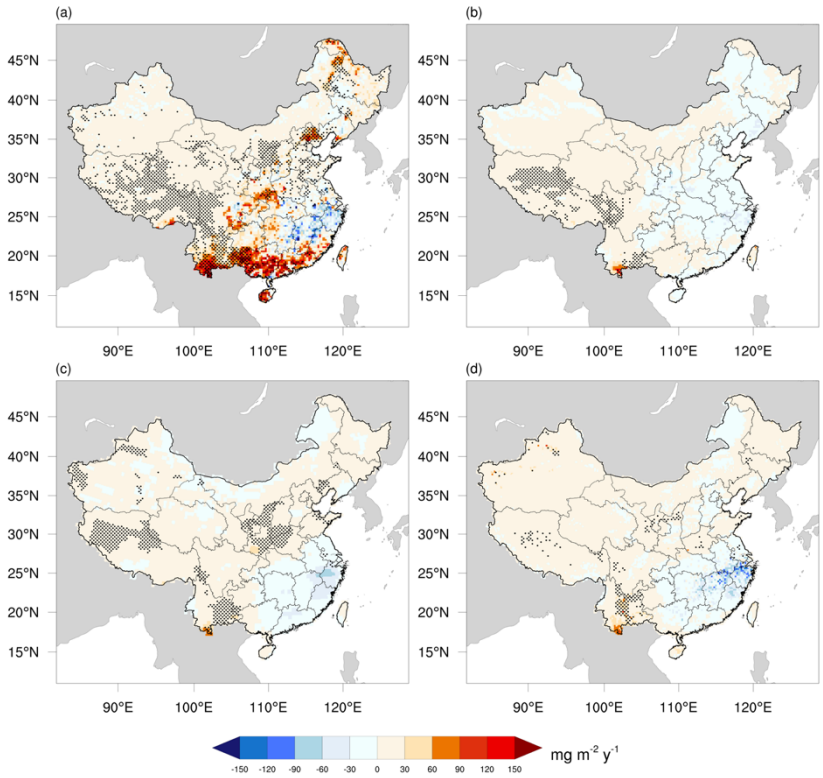

Figure R7. Comparison of the trend of isoprene emission between this study (S1) and other estimations during 2001-2016. (a) and (b) is for S1 and S3 respectively in this study, and (c) and (d) are for CAMS-GLOB-BIO v 1.1 and CAM-GLOB-BIO v3.1, respectively.

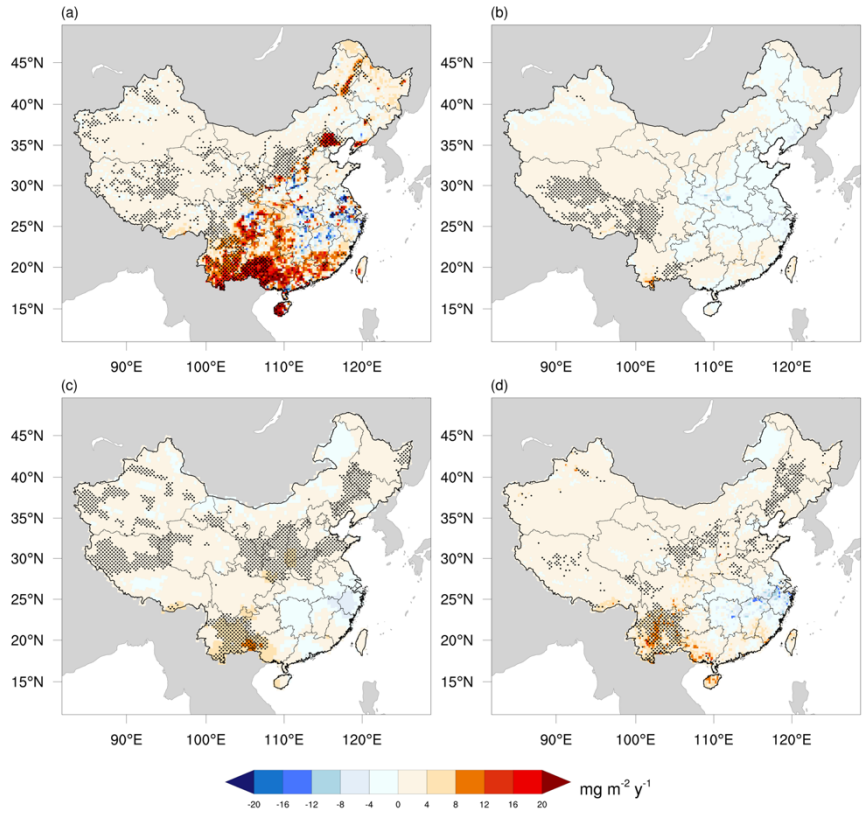

Figure R8. Comparison of the trend of monoterpenes emission between this study (S1) and other estimations during 2001-2016. (a) and (b) is for S1 and S3, respectively, in this study, and (c) and (d) are for CAMS-GLOB-BIO v 1.1 and CAM-GLOB-BIO v3.1, respectively.

(iv) The strong trends inferred over the Qinling mountains and over Southern China need further discussion. Can you put compare this result to past studies? What is the respective roles played by LAI and PFT cover trends?

Response: Thank you for your comments. As mentioned above, we compared our results with the CAMS-GLB-BIO inventories. As shown in Figure 5 above, an increasing trend of isoprene emission can be found in CAMS-GLOB-BIO v 1.1 inventory but with relative low magnitude comparing with our estimation. For further discuss the trends of BVOC emission in these regions, we listed the change of annual emission amount in S1, S2 and S5 scenarios, cover fractions of main PFTs, LAIv, growing season temperature and DSW in these regions in Table 3 and Table 4 in the revised paper. In addition, we also added one more experiment named S5 with annually updated LAIv inputs and fixed the meteorological conditions as well as PFT input to investigate the contribution of LAI trend on BVOC emission trend. The results of S5 has been added into the revised paper.

Specific comments/Language corrections

p.2, l.3-7: The sentence is too long, considering splitting into two and rephrasing.

Response: Thank you for your comments. This sentence has been re-written as:

"Besides the climatic factors, the land cover change also plays a key role in the variability of BVOC emission (Stavrakou et al., 2014; Unger, 2013; Chen et al., 2018). For instance, cropland expansion has been estimated to dominate the reduction of isoprene, the dominant BVOC species, in last century (Lathière et al., 2010; Unger, 2013) although there are large uncertainties associated with these estimates."

p.2, l.5: add space between '2014' and 'Chen'

Response: Thank you. We have followed your advice.

p.2, l.12: 'a corresponding impact', replace by 'changes'

Response: Thank you. We have followed your advice.

p.3, l.10: remove 'observed'

Response: Thank you. We have followed your comments.

p.3, l.10: 'regional ecosystem isoprene emission', change to 'isoprene emission at regional to global scales'

Response: Thank you. We have followed your advice.

p.3, l.11: 'reported the', change to 'reported an'

Response: Thank you. We have followed your advice.

p.3, l.12: read 'detected by the Ozone'

Response: Thank you. We have followed your advice.

p.3, l.14-15: rephrases as follows: 'Here we used the long-term OMI 2005-2016 record to estimate the interannual isoprene variability in China'

Response: Thank you. We have followed your advice.

p.3, l.19: add reference Guenther et al.(2012)

Response: Thank you. We have followed your advice.

p.3, l.20: add more references, e.g. Bauwens et al.(2018) and Messina et al.(2016)

Response: Thank you. We have added these references.

p.3, l.23: read ’uses the fundamental’

Response: Thank you. We have followed your advice.

p.4, l.1: read ’the standard emissions factor, and the emission activity factor for the chemical species i’

Response: Thank you. We have followed your advice.

p.4, l.3: ’(PFT) distribution from the Community Land...’

Response: Thank you. We have followed your advice.

p.4, l.5: replace ’expresses it as’ by ‘can be written as’

Response: Thank you. We have followed your advice.

p.4, l.8: ’equal to 1 at standard conditions (Guenther et al. (2006)’

Response: Thank you. We have followed your advice.

p.4, l.9: please specify the source of the LAI dataset

Response: Thank you. We have added the link of website of MODIS LAI products (https://lpdaac.usgs.gov/products/mcd15a2hv006/) in this sentence.

p.4, l.9: replace ’and the leaf age in MEGAN’ by a new sentence: ’It is used to define the leaf age response function as described in Guenther et al.(2012).’

Response: Thank you. We have followed your advice.

p.4, l.10: the test should read ’Guenther et al. (1991, 1993, 2012)’

Response: Thank you. We have followed your advice.

p.4, l.14: remove ’factor’

Response: Thank you. We have followed your advice.

p.4, l.18: ’adopted’, change to ’used’

Response: Thank you so much. We have followed your advice.

p.4, l.18: ’in this study’, missing reference for the LAI datasets used

Response: Thank you so much. We have followed your advice and added the reference of MODIS LAI product.

p.4, l.20: missing reference for the dataset

Response: Thank you so much. We have followed your advice and added the reference of MODIS VCF product.

p.4, l.22: change ’data’ to ’dataset’

Response: Thank you. We have followed your advice.

p.4, l.22: ’land cover product’ missing reference.

Response: Thank you so much. We have followed your advice and added the reference of MODIS land cover product.

p.4, l.24: ’described in’

Response: Thank you. We have followed your advice.

p.4, l.24: using the climatology of ERA-interim dataset’, change to ’using the ERAInterim climatology’

Response: Thank you. We have followed your advice.

p.5, l.1: ’during 2001-2016’, change to ’over 2001-2016’

Response: Thank you. We have followed your advice.

p.5, l.5: 'The meteorological simulation is', change to 'The model was'

Response: Thank you. We have followed your advice.

p.5, l.10: 'using the in-situ', change to 'using in-situ'

Response: Thank you. We have followed your advice.

p.5, l.13: 'monthly averaged'

Response: Thank you. We have followed your advice.

p.5, l.15: -2 in Wm-2 should be superscript

Response: Thank you. We have followed your advice.

p.5, l.15: among 98 sites, and the overestimations', change to 'for 98 studied sites. The overestimation'

Response: Thank you. We have followed your advice.

p.5, l.17: 'the lack of aerosol radiation effect and cloud simulation', not clear what is meant here

Response: Thank you so much for your comments. We have modified this sentence as:

"The overestimation of DSW simulation is a common issue in multiple simulation studies and may be induced by the lack of physical processes for aerosol radiation effect (Wang et al., 2011; Situ et al., 2013; Wang et al., 2018)."

p.5, l.23: 'Our', change to 'The'

Response: Thank you. We have followed your advice.

p.6, l.1: 'Observations'

Response: Thank you. We have followed your advice.

p.6, l.3: 'and was retrieved'

Response: Thank you. We have followed your advice.

p.6, l.4-5: 'The detailed...De Smedt et al. (2015)'. Please remove sentence (repetition)

Response: Thank you. We have followed your advice.

p.6, l.6: 'temporally stable', what about the row anomaly? This effect should be mentioned.

Response: Thank you. We have added the following description in the revised paper:

"We used the monthly Level-3 HCHO VC product with 0.25° × 0.25° spatial resolution, and the rows affected by the row anomaly since June 2007 have been filtered in this product (De Smedt et al., 2015; Jin and Holloway, 2015). Since the OMI instrument is temporally stable (Dobber et al., 2008; De Smedt et al., 2015), the OMI HCHO VC product is suitable for long-term analysis (Jin and Holloway, 2015) and was used to primarily validate our estimation of isoprene emission variability."

p.6, l.9: change 'anthropogenic source' to 'anthropogenic VOC'

Response: Thank you. We have followed your advice.

p.6, l.10: 'in the forest regions without obvious anthropogenic impact', replace by 'over forests in summertime'

Response: Thank you. We have followed your advice.

p.6, l.21: 'between 2001 to 2016', change to 'between 2001 and 2016'

Response: Thank you. We have followed your advice.

p.6, l.25: This has been already mentioned, please avoid repetitions

Response: Thank you. We have followed your advice and removed that sentence.

p.6, l.26-27: sentence not clear

Response: Thank you. We have rephrased this sentence as:

"Therefore, the indirect impact of meteorological conditions on BVOC emission through affecting biomass and phenology was not considered in this study."

p.7, l.6-8: what do you mean by 'results' and corresponding results'? State clearly what you did

Response: Thank you. We have followed your advice and rephase this sentence as:

"The trend analysis and the MK tests in this study were implemented using the trend_manken (https://www.ncl.ucar.edu/Document/Functions/Built-in/trend_manken.shtml) function of the NCAR Command Language (NCL, https://www.ncl.ucar.edu/)."

p.7, l.15: 'S1...conditions', repetition

Response: Thank you. We have followed your advice and removed the sentence.

p.7, l.18: 'other estimations', missing references

Response: Thank you. About this part, we have moved the comparison with other studies to section 3.4 as an independent section. The references of studies we used for comparison has been listed in Table 5 as.

"Table 5. Comparison of isoprene and monoterpene emissions (Tg) in China with previous studies.

Data Source	Isoprene	Monoterpene	Study period	Method or Model
This study	15.94 (±1.12)	3.99 (±0.17)	2001-2016	MEGAN
Stavrakou et al. (2014)	7.17 (±0.30)	-	2007-2012	MEGAN-MOHYCAN
Li et al. (2013)	23.4	5.6	2003	MEGAN
Li et al. (2020)	33.21	6.35	2008-2018	MEGAN
CAMS-GLOB-BIO v1.1 (Sindelarova et al., 2014)	7.67	3.04	2001-2016	MEGEN
CAMS-GLOB-BIO v3.1 (Sindelarova et al., 2014)	8.54	3.23	2001-2016	MEGAN
Fu and Liao (2012)	10.87	3.21	2001-2006	GEOS-Chem-MEGAN
Tie et al. (2006)	7.7	3.16	2004	Guenther et al. (1993)
Klinger et al. (2002)	4.65	3.97	2000	Guenther et al. (1995)

Guenther et al. (1995)	17	4.87	1990	Guenther et al. (1995)

”

p.7, l.24: ’increasing rates of these species’, replace by ’trends’

Response: Thank you. We have followed your advice.

p.7, l.25: ’despite the direct impact of meteorological conditions’, not clear

Response: Thank you so much. We have removed this sentence in the revised paper.

p.8, l.11: Rewrite as ’The average annual total BVOC emission over 2009-2016 is by 50% higher than over 2001-2008.’ Is that what you mean?

Response: Thank you so much for your comments. That’s what we mean, and we have rewritten this sentence following your suggestion.

p.8, l.13: ’are by 11.3%’

Response: Thank you. We have followed your advice.

p.8, l.21: ’S4 is 23.5%’, change to ’S4 is by 23.5%

Response: Thank you. We have followed your advice.

p.8, l.23: ’by 29.9%’

Response: Thank you. We have followed your advice.

p.8, l.25-26: poor language

Response: Thank you. We will rephrase this sentence.

p.9, l.15: ’landcover’, change to ’land cover’

Response: Thank you. We have followed your advice.

p.9, l.15: read ’contribute up to 20%, and taken together more than 30% to the estimated...’

Response: Thank you. We have followed your advice.

p.10, l.6: ’driven’, change to ’driven’

Response: Thank you. We have followed your advice.

p.10, l.10-12: Sentence could be removed

Response: Thank you. We have followed your advice.

p.10, l.15: superscripts for m-2 y-1

Response: Thank you. We have followed your advice.

p.10, l.20: read ’broadleaf trees, needleleaf trees and other vegetation’

Response: Thank you. We have followed your advice.

p.10, l.25: ’percent’, replace by ’percentage’

Response: Thank you. We have followed your advice.

p.10, l.13-24: too many numbers in this paragraph make the reading difficult, consider removing some of the numbers and rewriting

Response: Thank you so much for your suggestion. We will rephrase this paragraph.

p.11, l.4-7: too many numbers in the text, consider introducing them in a table

Response: Thank you. We will consider your advice and add a suitable table or graph.

p.11, l.11: ’in (Figure 3)’, change to ’in Figure 3’

Response: Thank you. We have followed your advice.

p.11, l.23: ’dominate factor’, read ’dominant factor’

Response: Thank you. We have followed your advice.

p.12, l.2: 'suffering from poor air quality'

Response: Thank you. We have followed your advice.

p.12, l.2: add space between 'years' and 'Yang'

Response: Thank you. We have followed your advice.

p.12, 13: 'in rural regions with minimal anthropogenic influence', change to 'over forests'

Response: Thank you. We have followed your advice.

p.12, l.18: 'summer-average isoprene emission estimated in our study to evaluate our estimation of interannual variability of isoprene emission', poor wording.

Response: Thank you. We have rephrased this sentence as:

"The interannual variability of isoprene emission estimated in this study was evaluated by comparing the isoprene emission with the summer (June-August) averaged HCHO VC."

p.13, l.1: 'anthropogenic sources', missing reference

Response: Thank you. We have added the reference in the revised paper.

p.13, l.5: 'correlation can be found', change to 'correlation is found'

Response: Thank you. We have followed your advice.

p.13, l.10: 'anthropogenic sources', missing reference

Response: Thank you. We have removed this sentence from the revised paper.

p.13, l.20: 'greatest increasing trend', change to 'strongest positive trend'

Response: Thank you. We have followed your advice.

p.14, l.4: 'the mega-city areas', read 'in megacities'

Response: Thank you. We have removed this section.

p.15, l.1: read ’from 2001 to 2016’

Response: Thank you. We have followed your advice.

p.15, l.1: read ’as inputs in the MEGAN’

Response: Thank you. We have followed your advice.

p.15, l.1: ’the long-term’, remove ’the’

Response: Thank you. We have followed your advice.

p.15, l.11: here and elsewhere in the manuscript, use one instead of two decimals

Response: Thank you. We have followed your advice.

p.15, l.18: ’there’?

Response: Thank you so much for your comments. We have removed this sentence from the revised paper.

p.15, l.21: ’during 200-2010’, missing reference

Response: Thank you so much for your comments. We have removed this sentence from the revised paper.

p.15, l.22: ’there has been in a increasing trend’, do you mean ’showed an increasing trend’?

Response: Thank you so much for your comments. We have removed this sentence from the revised paper.

p.15, l.24: read ’assess’

Response: Thank you. We have followed your advice.

p.16, l.6: remove the references (they are already mentioned before)

Response: Thank you. We have followed your advice.

p.16, l.6-10: repetition of l.20-25 of page 14, not necessary

Response: Thank you. We have followed your advice and removed this sentence.

p.23: Table 3, the estimates reported in Li et al. are in TgC, not in Tg, please correct

Response: Thank you so much. We have corrected this in the revised paper.

p.26: Difficult to read, I suggest splitting into a figure with 4 panels (a, f, k, p) and another figure with the trends. The regions in panel (r) are barely visible. Please improve.

Response: Thank you. We added one more figure to illustrate the interest regions and present the trend of BVOC emission.

p.27: It is very difficult to distinguish the colors corresponding to broadleaf and needleleaf trees, please adapt. In the caption, please correct typos for the names of provinces.

Response: Thank you. We have added one figure to present the spatial distribution of broadleaf trees and needle leaf trees. The typos in the caption have been corrected.

Reference

Bai, J., Guenther, A., Turnipseed, A., and Duhl, T.: Seasonal and interannual variations in whole-ecosystem isoprene and monoterpene emissions from a temperate mixed forest in Northern China, Atmospheric Pollution Research, 6, 696-707, https://doi.org/10.5094/APR.2015.078, 2015.

Bai, J., Guenther, A., Turnipseed, A., Duhl, T., Yu, S., and Wang, B.: Seasonal variations in whole-ecosystem BVOC emissions from a subtropical bamboo plantation in China, Atmospheric Environment, 124, 12-21, https://doi.org/10.1016/j.atmosenv.2015.11.008, 2016.

Bai, J., Guenther, A., Turnipseed, A., Duhl, T., and Greenberg, J.: Seasonal and interannual variations in whole-ecosystem BVOC emissions from a subtropical plantation in China, Atmospheric Environment, 161, 176-190, 10.1016/j.atmosenv.2017.05.002, 2017.

Guenther, A., Karl, T., Harley, P., Wiedinmyer, C., Palmer, P., and Geron, C.: Estimates of global terrestrial isoprene emissions using MEGAN (Model of Emissions of Gases and Aerosols from Nature), Atmos. Chem. Phys, 6, 3181-3210, 2006.

Guenther, A. B., Monson, R. K., and Fall, R.: Isoprene and monoterpene emission rate variability: Observations with eucalyptus and emission rate algorithm development, Journal of Geophysical

Research: Atmospheres, 96, 10799-10808, 10.1029/91JD00960, 1991.

Guenther, A. B., Jiang, X., Heald, C. L., Sakulyanontvittaya, T., Duhl, T., Emmons, L. K., and Wang, X.: The Model of Emissions of Gases and Aerosols from Nature version 2.1 (MEGAN2.1): an extended and updated framework for modeling biogenic emissions, Geoscientific Model Development, 5, 1471-1492, 10.5194/gmd-5-1471-2012, 2012.

Monson, R. K., Harley, P. C., Litvak, M. E., Wildermuth, M., Guenther, A. B., Zimmerman, P. R., and Fall, R.: Environmental and developmental controls over the seasonal pattern of isoprene emission from aspen leaves, Oecologia, 99, 260-270, 10.1007/BF00627738, 1994.

Land cover change dominates decadal trends of biogenic volatile organic compound (BVOC) emission in China

Hui Wang[1, 2], Qizhong Wu[1], Alex B. Guenther[2], Xiaochun Yang[1], Lanning Wang[1], Tang Xiao[3], Jie Li[3], Jinming Feng[4], Qi Xu[1], Huaqiong Cheng[1]

[1]College of Global Change and Earth System Science, Joint Center for Global Changes Studies, Beijing Normal University, Beijing 100875, China
[2]Department of Earth System Science, University of California, Irvine, CA 92697, USA
[3]State Key Laboratory of Atmospheric Boundary Layer Physics and Atmospheric Chemistry, Institute of Atmospheric Physics, Chinese Academy of Sciences, Beijing 100029, China
[4]Key Laboratory of Regional Climate-Environment for Temperate East Asia, Institute of Atmospheric Physics, Chinese Academy of Sciences, Beijing 100029, China
Correspondence to: Qizhong Wu (wqizhong@bnu.edu.cn) & Lanning Wang (wangln@bnu.edu.cn)

Abstract. Satellite observations reveal that China has been leading the global greening trend in the past two decades. We assessed the impact of land cover change on total BVOC emission in China during 2001-2016 and found that the land cover change from 2001 to 2016 can lead to a significant increasing trend of 0.50% y^{-1}.~~09% yr-1 with increases~~ of ~~1.35, 1.25 and 1.43 % yr-1 for~~ total BVOC emission in China. Main BVOC classes of isoprene, ~~monoterpenes~~monoterpene and sesquiterpene all had increasing trends of 0.64, 0.44 and ~~sesquiterpenes, respectively. Comparison of~~0.39 % y^{-1}. The BVOC emission level in 2016 can be 11.7% higher than that in 2001 because of higher tree cover fraction and vegetation biomass. Considerable heterogeneity was found on regional scales, and the BVOC emission level during 2013-2016 would be 8.6%~19.3% higher than that during 2001-2004 in the regions including 1) northeastern China, 2) Beijing and its surrounding areas, 3) the Qinling Mountains, 4) Yunnan province, 5) Guangxi-Guangdong provinces and 6) Hainan island because of land cover change. The comparison among different scenarios showed that vegetation ~~change~~ changes resulting from land cover management is the main driver of BVOC emission change in China. ~~Considerable heterogeneity was observed on regional scales, with the highest increasing trends of BVOC emission found in the Qinling Mountains and in the south of China. The BVOC emission for the year 2016~~ Climate variability contributed significantly to interannual variations but not the long-term trend. In the standard scenario, that considers both land cover change and climate variability, a statistic significant increasing trend still can be found in the regions including Beijing and its surroundings, Yunnan provinces and Hainan island, and BVOC emission total amount in these ~~two~~ regions ~~was enhanced by 61.89 and 67.64% compared to~~during 2013-2016 is 11.0%-17.2% higher, that ~~of~~during 2001~~, respectively~~-2004. We compared the long-term HCHO vertical columns (VC) from the satellite-based Ozone Monitoring Instrument (OMI) with the estimation of isoprene emission in summer. The results showed statistically significant positive correlation coefficients over the regions with high vegetation cover fractions. In addition, the isoprene emission and HCHO VC both showed statistically significant increasing trends in the south of China where these two variables have high positive correlation coefficients. This result supports our estimation of the variability and trends of BVOC emission in China. ~~Although anthropogenic sources comprise ~63% NMVOC emissions in China, the~~The continued increase of BVOC will enhance the importance of considering BVOC when making policies for controlling ozone pollution in China along with ongoing efforts to reduce anthropogenic emissions.

Style Definition: EndNote Bibliography: Font: (Default) DengXian Light, 10 pt
Formatted: Font color: Text 1
Formatted: Font color: Text 1
Formatted: Font color: Text 1
Formatted: Font color: Text 1
Formatted: Font color: Text 1
Formatted: Font color: Text 1
Formatted: Font color: Text 1
Formatted: Font color: Text 1, Superscript
Formatted: Font color: Text 1
Formatted: Font color: Text 1
Formatted: Font color: Text 1
Formatted: Font color: Text 1
Formatted: Font color: Text 1
Formatted: Font color: Text 1
Formatted: Font color: Text 1
Formatted: Font color: Text 1
Formatted: Font color: Text 1
Formatted: Font color: Text 1
Formatted: Font: Not Bold, Font color: Text 1, English (United States)

1 Introduction

Biogenic Volatile Organic Compounds (BVOCs) play an important role for air quality and the climate system due to their large emission amount and reactivity (Guenther et al., 1995; Guenther, 2006). BVOCs are important precursors of ozone and secondary organic aerosols (SOAs) (Kavouras et al., 1998; Claeys et al., 2004), therefore, it is important to understand the variability of BVOC emission and its impact on air quality and the climate system. The emission of BVOC is controlled by multiple environmental factors like temperature, radiation, CO_2 concentration ~~of CO_2~~ and other stresses, ~~and~~therefore it is affected by climate changes (Guenther et al., 1995; Arneth et al., 2007; Penuelas and Staudt, 2010). Besides the climatic factors, the land cover change also plays a key role in the variability of BVOC emission (Stavrakou et al., 2014; Unger, ~~2014;~~2013; Chen et al., 2018~~), e.g.,~~). For instance, the global cropland expansion has been estimated to dominate the reduction of isoprene, the dominant BVOC species, in last century (Lathière et al., 2010; Unger, 2013) although there are large uncertainties associated with these estimates.

China has been greening in recent decades (Piao et al., 2015). A recent study points out that China accounts for 25% of the net increase of global leaf area during 2000-2017 (Chen et al., 2019). The increase of forest area plays a dominant role in greening in China with multiple programs to maintain and expand forests (Zhang et al., 2016; Bryan et al., 2018; Chen et al., 2019). The enhancement of vegetation cover rate and biomass can lead to the increase of BVOC emission ~~in China~~ and induce ~~a corresponding impact~~changes on local air quality and the climate system. Previous studies have investigated the long-term emission trend of dominant BVOC species like isoprene in China (Fu and Liao, 2012; Li and Xie, 2014; Stavrakou et al., 2014; Chen et al., 2019). Li and Xie (2014) estimated the historical BVOC emissions during 1981-2003 in China using the national forest inventory records and reported that the BVOC emission increased at a rate of 1.27% ~~yr~~y^{-1}. Another estimation by Stavrakou et al. (2014) showed an upward trend of 0.42% ~~yr~~y^{-1} of isoprene emission in China during 1979-2005 driven by the increasing temperature and solar radiation, moreover, the upward trend of isoprene emission reached 0.7% ~~yr~~y^{-1} when considering the replacement of cropland with forest. A recent study by Chen et al. (2018) concluded that the global isoprene emission decreased by 1.5% because of the tree cover change during 2000-2015, but in China, the isoprene emitted by broadleaf trees and non-trees increased by 3.6% and 5.4%, respectively. However, these studies have limitations in representing annual changes of vegetation, e.g., Li and Xie (2014) used fixed LAI input of year 2003 over the whole study period of 1981-2003.

Considering the significant land cover change and greening trend in China, it is necessary to thoroughly investigate the impact of intense reforestation on BVOC emission in China. In this study, we used the latest annually continuous land cover products Version 6 by the MODerate-resolution Imaging Spectroradiometer

Formatted: Font color: Text 1
Formatted: Font color: Text 1
Formatted: Font color: Text 1
Formatted: Font color: Text 1
Formatted: Font color: Text 1
Formatted: Font color: Text 1
Formatted: Font color: Text 1
Formatted: Font color: Text 1
Formatted: Font color: Text 1, Superscript
Formatted: Font color: Text 1
Formatted: Font color: Text 1, Superscript
Formatted: Font color: Text 1
Formatted: Font color: Text 1, Superscript
Formatted: Font color: Text 1

(MODIS) sensors as well as the Model of Emissions of Gases and Aerosols from Nature (MEGAN, Guenther et al. 2012) model to investigate BVOC emission in China from 2001 to 2016. By annually updating the vegetation information of MODIS observations, we could accurately estimate interannual variability of BVOC emission to assess the impact of greening trend on BVOC in China during 2001-2016.

~~There are no~~A long-term in-situ observation of BVOC is not available in China currently to ~~validate our estimation of~~investigate interannual variability of BVOC emission, however, satellite formaldehyde (HCHO) observations provide an opportunity to validate the interannual variability of isoprene, the dominant compound among BVOC species that accounts for almost half of total BVOC emission in China (Li et al., 2013). Since HCHO is an important proxy of isoprene in forest regions with no significant anthropogenic impact, satellite ~~observed~~ HCHO columns are widely used to derive ~~regional ecosystem~~ isoprene emission at regional to global scales (Palmer et al., 2003; Marais et al., 2012; Stavrakou et al., 2015; Kaiser et al. 2018). Zhu et al. (2017b) reported ~~the~~an increasing trend of HCHO vertical columns (VC) detected by the Ozone Monitoring Instrument (OMI) driven by increasing cover rate of local forest in the northwestern ~~US.~~United States. Stavrakou et al. (2018) also used the long-term HCHO VC to investigate the annual variability of BVOC induced by climate variability. ~~We have~~Here we used the long-term ~~HCHO record from~~ OMI 2005-2016 ~~by OMI~~record to ~~assess our estimation of annual~~estimate the interannual isoprene variability in China.

2 Data and Method

2.1 MEGAN Model

MEGAN (Guenther et al., 2006; Guenther et al., 2012) is the most widely used model for calculating BVOC emission from regional to global scales (Müller et al., 2008; Li et al., 2013; Sindelarova et al., 2014; Chen et al., 2018~~).~~; Bauwens et al. 2018; Messina et al. 2016). The offline version of the MEGAN v2.1 (Guenther et al., 2012) model, available at https://bai.ess.uci.edu/megan, was used to estimate the BVOC emission in China from 2001 to 2016. MEGAN v2.1 calculates emissions for 19 major compound categories ~~using~~uses the fundamental algorithm:

$$F_i = \varepsilon_i \gamma_i \quad (1)$$

where Fi, εi and γi represent the emission amount, the standard ~~emission~~emissions factor, and emission activity factor of chemical species i. The standard emission factor in this study is based on the plant functional type (PFT) distribution~~, and the PFT scheme in MEGAN v2.1 is the scheme adopted in~~ from the Community

Formatted: Font color: Text 1
Formatted: Font color: Text 1
Formatted: Font color: Text 1
Formatted: Font color: Text 1
Formatted: Font color: Text 1
Formatted: Font color: Text 1
Formatted: Font color: Text 1
Formatted: Font color: Text 1
Formatted: Font color: Text 1
Formatted: Font color: Text 1
Formatted: Font color: Text 1
Formatted: Font color: Text 1
Formatted: Font color: Text 1
Formatted: Font color: Text 1
Formatted: Font: Times, Font color: Text 1
Formatted: Font color: Text 1
Formatted: Font color: Text 1
Formatted: Font color: Text 1
Formatted: Font color: Text 1
Formatted: Font color: Text 1
Formatted: Font color: Text 1
Formatted: Font color: Text 1
Formatted: Font color: Text 1
Formatted: Font color: Text 1
Formatted: Font color: Text 1
Formatted: Font color: Text 1
Formatted: Font color: Text 1
Formatted: Font color: Text 1
Formatted: Font color: Text 1
Formatted: Font color: Text 1

Land Model 4.0 (Lawrence et al., 2011). The emission activity factor γi accounts for the impact of multiple environmental factors and ~~expresses it~~can be written as:

$$\gamma_i = C_{CE} LAI \gamma_{p,i} \gamma_{T,i} \gamma_{A,i} \gamma_{SM,i} \gamma_{C,i} \qquad (2)$$

where $\gamma_{p,i}$, $\gamma_{T,i}$ $\gamma_{A,i}$ $\gamma_{SM,i}$ and $\gamma_{C,i}$ represent the activity factors for light, temperature, leaf age, soil moisture and CO_2 inhibition impact. The Cce (=0.57) is a factor to set the γi equal to 1 at ~~the~~ standard conditions~~.~~ (Guenther et al., 2006). The LAI is the leaf area index, and ~~defines~~it is used to define the amount of foliage and the leaf age response function as described in ~~MEGAN.~~Guenther et al. (2012). The light and temperature response algorithms in MEGAN v2.1 are from Guenther et al. (1991~~), Guenther et al. (~~, 1993~~) and Guenther et al. (~~, 2012), which described enzymatic activities controlled by temperature and light conditions. The CO_2 inhibition algorithm is from Heald et al. (2009), and only the estimation of isoprene emission considers the impacts of soil moisture and CO_2 concentration. The detailed descriptions of these ~~factor~~ algorithms can be found in Guenther et al. (2012) and Sakulyanontvittaya et al. (2008).

2.2 Land Cover Datasets.

The land cover parameters for driving MEGAN including LAI, PFT and vegetation cover fraction (VCF) were provided by satellite datasets. The MODIS MOD15A2H for 2001 (https://lpdaac.usgs.gov/products/mod15a2hv006/, Myneni et al., 2015a) and MCD15A2H for 2002-2016 LAI (https://lpdaac.usgs.gov/products/mcd15a2hv006/, Myneni et al., 2015b) datasets were ~~adopted~~used in this study. The parameter LAIv in MEGAN is calculated as:

$$LAIv = \frac{LAI}{VCF} \qquad (3)$$

where VCF is provided by MODIS MOD44B datasets~~.~~ (https://lpdaac.usgs.gov/products/mod44bv006/, Dimiceli et al., 2015).

The PFT was used to determine the canopy structure and standard emission factors in MEGAN (Guenther et al., 2012). ~~The PFT data~~ We adopted the default emission factors for PFTs described in Table 2 in Guenther et al. (2012). The PFT dataset in this study is obtained from the MODIS MCD12C1 land cover product~~,~~ (https://lpdaac.usgs.gov/products/mcd12c1v006/, Friedl and Sulla-Menashe, 2015). MODIS IGBP classification were mapped to the PFT classification ~~were converted to~~ of MEGAN ~~PFT classification~~ or the Community Land Model (CLM) (Lawrence et al., 2011) based on the description of the legends in the user guide (Sulla-Menashe and Friedl, 2018) and the climatic criteria described ~~by~~in Bonan ~~Gordon~~ et al. (2002~~)~~). The spatial distribution of percentage of PFTs in model grids is presented in Figure 1. According to the description of the legends, we firstly mapped the IGBP classification to eight main vegetation categories: 1)

Formatted: Font color: Text 1
Formatted: Font color: Text 1
Formatted: Font color: Text 1
Formatted: Font color: Text 1
Formatted: Font color: Text 1
Formatted: Font color: Text 1
Formatted: Font color: Text 1
Formatted: Font color: Text 1
Formatted: Font color: Text 1
Formatted: Font color: Text 1
Formatted: Font color: Text 1
Formatted: Font color: Text 1
Formatted: Font color: Text 1
Formatted: Font color: Text 1
Formatted: Font color: Text 1
Formatted: Font color: Text 1
Formatted: Font color: Text 1
Formatted: Font color: Text 1
Formatted: Font color: Text 1
Formatted: Font color: Text 1
Formatted: Font color: Text 1
Formatted: Font color: Text 1
Formatted: Font color: Text 1
Formatted: Font color: Text 1
Formatted: Font color: Text 1
Formatted: Font color: Text 1
Formatted: Font color: Text 1
Formatted: Font color: Text 1
Formatted: Font color: Text 1
Formatted: Font color: Text 1
Formatted: Font color: Text 1
Formatted: Font: Times New Roman, Font color: Text 1
Formatted: Font color: Text 1
Formatted: Font color: Text 1
Formatted: Font color: Text 1
Formatted: Font color: Text 1
Formatted: Font color: Text 1
Formatted: Font color: Text 1
Formatted: Font color: Text 1
Formatted: Font: 12 pt, Not Bold, Font color: Text 1

needleleaf evergreen forests, 2) broadleaf evergreen forests, 3) needleleaf deciduous forests, 4) broadleaf deciduous forests, 5) mixed forests, 6) shrub, 7) grass and 8) crop. The mapping method is described in Table S1 in the supplement. Eight main categories then were mapped to the classification of MEGAN/CLM for boreal, temperate and boreal climatic zones using the definition in Bonan et al. (2002). Table S2 in the supplement presents the climatic criteria for mapping, and the climatic information for mapping was from the ERA Interim climatology ~~of ERA-interim dataset (~~(https://www.ecmwf.int/en/forecasts/datasets/reanalysis-datasets/era-interim, Berrisford et al., 2011) ~~during~~Reanalysis dataset over 2001-2016. ~~We adopted the default emission factors of different PFTs described in Guenther et al. (2012).~~

2.3 Meteorological Datasets

The hourly meteorological fields including temperature, downward shortwave radiation (DSW), wind speed, surface pressure, precipitation and water vapor mixing ratio were provided by the Weather Research and Forecast (WRF) Model V3.9 (Skamarock et al., 2008) simulations. The ~~meteorological simulation is~~model was driven by ERA-Interim reanalysis data (Berrisford et al., 2011) with 27 km horizontal spatial resolution and 39 vertical layers. The physical schemes were presented in supplemental Table ~~S1~~S3.

Since light and temperature conditions are the main environmental drivers of BVOC emission (Guenther et al., 1993; Sakulyanontvittaya et al., 2008), we assessed the reliability of the WRF simulated ~~downward shortwave radiation (~~DSW~~)~~ and 2-meter temperature (T2) using ~~the~~ in-situ observations from 98 radiation observation sites and 697 meteorology observation sites in China. The in-situ observations ~~used in this study~~ are from the National Meteorological Information Center (http://data.cma.cn/). We converted the hourly model outputs and daily observations to monthly ~~average~~averaged values from 2001 to 2016 for comparison. For DSW, the average mean bias (MB), mean error (ME) and root mean square error (RMSE) are 40.37 (± 20.81), 43.55 (± 17.52) and 49.79 (± 17.70) W m^{-2} ~~among~~for 98 studied sites~~, and the~~. The overestimation of DSW simulation is a common issue in multiple simulation studies and may be induced by the lack of physical processes for aerosol radiation ~~affect and cloud simulation~~effect (Wang et al., 2011; Situ et al., 2013; Wang et al., 2018). For T2, the average MB, ME and RMSE are -1.19 (± 2.87), 2.40 (± 2.14) and 2.65 (± 2.11) °C among 697 sites over China. We also compared the monthly anomalies of DSW and T2 from the model simulation and observation to validate the interannual variability of meteorological fields simulated by WRF. As shown in Figure 2, the results indicate that the model accurately reproduced the interannual variability of DSW and T2, and the correlation coefficients of DSW and T2 anomaly between the simulation and observation reached 0.77 and 0.88, respectively. ~~Our~~The trends of growing season averaged T2 and DSW from model results as well as in-situ measurements are presented in Figure 3. The model and the in-situ

Formatted: Font color: Text 1
Formatted: Font color: Text 1
Formatted: Font color: Text 1

measurements show similar patterns of T2. For instance, the model and observations both show an increasing trend in regions like the Tibetan Plateau and southern China as well as a decreasing trend in eastern and northeastern China. For DSW, the model presented a dimming trend in northeastern and eastern China and a brightening trend in southeastern and central China, and the limited number of radiation observation sites show a similar pattern of trend with model results. In general, the WRF simulation successfully captured the long-term meteorological variabilities and is reasonable to use for estimating the impact of climatic variability on BVOC emission in China for this study.

2.4 Satellite Formaldehyde ~~Observation~~(HCHO) Observations

The satellite HCHO VC used in this study is from the Belgian Institute for Space Aeronomy (BIRA-IASB) and ~~is~~was retrieved using the differential optical absorption spectroscopy (DOAS) algorithm (De Smedt et al., 2012; De Smedt et al., 2015). ~~The detailed description of the BIRA-IASB OMI HCHO product can be found in De Smedt et al. (2015), and we~~We used the monthly Level-3 HCHO VC product with 0.25° × 0.25° spatial resolution~~., and the rows affected by the row anomaly since June 2007 have been filtered in this product (De Smedt et al., 2015; Jin and Holloway, 2015)~~. Since the OMI instrument is temporally stable (Dobber et al., 2008; De Smedt et al., 2015), the OMI HCHO VC product is suitable for long-term analysis (Jin and Holloway, 2015) and was used to primarily validate our estimation of isoprene emission variability. The major sources of tropospheric HCHO are biogenic VOC, anthropogenic ~~source~~VOC and open fires (Zhu et al., 2017a). Since biogenic isoprene is the dominant source of HCHO ~~in the forest regions without obvious anthropogenic impact~~over forests in summertime (Palmer et al., 2003), we used HCHO as the proxy of isoprene to validate the interannual variability of isoprene estimates.

2.5 Scenarios and Analysis Method

We designed ~~four~~five scenarios (S1-~~S4~~S5) to investigate the impact of land cover change and climatic conditions on BVOC emission. The configurations of the ~~four~~five scenarios are shown in Table 1~~, and~~:

1) S1 was considered as the standard or "full" scenario with both annually updated land cover parameters (LAIv and PFT) and meteorological conditions.

2) S2 used the fixed meteorological conditions of the year 2001 and annually updated land cover parameters to investigate solely the impact of the ecosystem and land cover variability on BVOC emission.

3) S3 and S4 adopted the land cover conditions of the year 2001 and 2016 respectively with annually updated meteorological fields to characterize the effect of climate variability on BVOC emission and compare the difference in BVOC emission induced by vegetation change in China between 2001 ~~to~~and 2016.

Formatted: Font color: Text 1
Formatted: Font: Times, Font color: Text 1
Formatted: Font: Times, Font color: Text 1
Formatted: Font color: Text 1
Formatted: Font color: Text 1
Formatted: Font color: Text 1
Formatted: Font color: Text 1
Formatted: Font color: Text 1
Formatted: Font color: Text 1
Formatted: Font color: Text 1
Formatted: Font color: Text 1
Formatted: Font color: Text 1
Formatted: Font color: Text 1, Not Highlight
Formatted: Font: Times, Font color: Text 1
Formatted: Font color: Text 1
Formatted: Font color: Text 1
Formatted: Font color: Text 1
Formatted: Font color: Text 1
Formatted: Font color: Text 1
Formatted: Font color: Text 1
Formatted: Font color: Text 1
Formatted: Font color: Text 1
Formatted: Font color: Text 1

4) In S5, meteorological conditions as well as PFT input is fixed, and LAIv input is annually updated to investigate the contribution of LAI trend to BVOC emission trend.

The climatic variability can affect the growth of vegetation and then affect LAI values (Piao et al., 2015). In this study, the interaction between climate and ecosystem is not considered in the offline MEGAN model, which means the meteorological conditions, e.g. precipitation, will not affect the LAI values. ~~The LAI input for MEGAN model in this study was obtained from the remote sensed LAI products.~~ Therefore, ~~when the time of the meteorological condition is inconsistent with that of the LAI input,~~ the indirect impact of meteorological conditions on BVOC emission through affecting biomass and phenology ~~were neglected. We used the experiments with the inconsistent LAI and meteorological conditions to investigate the direct effect of climatic variability on BVOC emission~~was not considered in this study.

The chemical species emissions estimated by MEGAN were grouped into four major categories including isoprene, monoterpene, sesquiterpene and other VOCs since the terpenoids account for the majority of total BVOC emission and have known impacts on atmospheric oxidants and SOA (Wang et al., 2011). The trend analysis in this study was done following the Theil-Sen trend estimation method and the results were tested by the Mann-Kendall non-parametric trend test~~,~~ (MK test). The trend analysis and the ~~corresponding results~~MK tests in this study were ~~calculated~~implemented using the trend_manken (https://www.ncl.ucar.edu/Document/Functions/Built-in/trend_manken.shtml) function of the NCAR Command Language (NCL, https://www.ncl.ucar.edu/).

3 Results and Discussion

3.1 The Variability of BVOC Emission in China During 2001-2016

As shown in Table 2, the average annual emission during 2001-2016 of isoprene, monoterpene, sesquiterpene and other VOCs estimated from S1 are ~~7.56 (±0.74),~~ 15.94 (±1.37 (±0.12), 3.99 (±0.17), 0.50 (±0.~~16 (±0.0203~~) and ~~6.73~~13.84 (±0.~~4678~~) Tg, respectively. Isoprene is the dominant species and accounts for about half of the total BVOC emission in China. ~~S1 is~~ As shown in Figure 4, the ~~standard scenario that includes both annually updated meteorological fields and vegetation conditions. In comparison with previous studies (Table 3), our estimation of isoprene emission is very close to the results by Stavrakou et al. (2014) and Tie et al. (2006) while our estimation of monoterpene emission is considerably (57 to 72%) lower than other estimations. Multiple factors including interannual variations, horizontal resolution, meteorological and land cover inputs can lead to the discrepancy of these estimations.~~

~~The total~~ estimated BVOC emission in S2 has a statistically significant increasing trend ~~with rates of 1.09 and 1.19% yr-1 for the S1 and~~ without considering the annual variability of meteorological conditions. The

Formatted: Font color: Text 1
Formatted: Font color: Text 1
Formatted: Font color: Text 1

increasing rates of isoprene, monoterpenes, sesquiterpenes and total BVOC emission in S2 scenarios ~~(d in Figure 2),~~are 0.64, 0.44, 0.39 and 0.50 % y^{-1}, respectively. ~~The increasing rate of isoprene, monoterpene and sesquiterpene are 1.35, 1.25 and 1.43% yr-1 respectively for the S1 scenario. In comparison, the increasing rates of these species in the S2 scenario are higher than those in the S1 scenario with 1.58, 1.51 and 1.61 % yr-1 for isoprene, monoterpene and sesquiterpene despite the direct impact of meteorological conditions. Although the~~The S1 scenario considers the impact of annual meteorological variability~~,~~ as well as the surface vegetation change, and the BVOC emission in S1 is ~~still~~ in ~~a significant~~an upward trend ~~driven by the increasing forest area and leaf mass. The lack of~~but didn't pass the significance test of $p < 0.1$. There's no a significant trend of BVOC emission for both S3 and S4, with fixed landcover and annually updated meteorological conditions, demonstrates that meteorology was not ~~an important~~the direct driver of BVOC emission ~~change~~trend in China during this period. Climatic conditions could affect the BVOC emission indirectly by affecting the growth of vegetation and controlling BVOC emission (Peñuelas et al., 2009), which is not considered in the model used in this study. ~~Therefore, our results only represent the direct impact of meteorological conditions on BVOC emission~~The estimated total BVOC emission in S5 also has a statistically significant increasing trend of 0.26% y^{-1} ($p<0.05$) without considering the annual variability of meteorological conditions, which is purely caused by the increase of LAI during 2001-2016.

~~3.2 The Impact of Land Cover Changes and Meteorological Variability~~

The surface vegetation change had a significant influence on BVOC emissions in China during 2001-2016~~.~~ according to our estimation. In S2, the interannual variability of total BVOC emission is primarily determined by the surface vegetation change resulting in a nearly linear increasing trend of BVOC emission. The average annual emission of total BVOC during ~~the later eight years (~~2009-2016~~)~~ is ~~8.50~~3.9% (1.29 Tg) higher than that during ~~the previous eight years (~~2001-2008~~). The~~ in S2, and the average annual emissions of isoprene, monoterpene and sesquiterpene during the previous eight years are ~~11.3% (~~by 5.0~~.79~~% (0.75 Tg), ~~11.9~~3.5% (0.~~15~~13 Tg) and ~~11.5~~3.1% (0.02 Tg) higher than those during next eight years, respectively. The comparison of S3 and S4 results further demonstrate the importance of vegetation development on BVOC emission considering the interannual variability of meteorological conditions. S3 and S4 adopted the same annually updated meteorological field but the fixed land cover information of the year 2001 and 2016, respectively. The fluctuation of meteorological factors leads to an interannual ~~fluctuation~~variability of BVOC emission in S3 and S4, but the increase of vegetation cover rate in 2016 results in BVOC emissions that are much higher than that in 2001 ~~under the same meteorological conditions~~. As presented in Table 2, the average total BVOC emissions are ~~14.2 (±0.70~~31.77 (±1.54) and ~~17.6 (±0.89~~35.48 (±1.76) Tg in S3 and S4, respectively, and the total BVOC emission in S4 is ~~23.5~~by 11.7% (3.~~35~~71 Tg) higher than that in S3. The emissions of isoprene,

Formatted: Font color: Text 1

monoterpene and sesquiterpene with the land cover information of the year 2016 are ~~29.9~~by 14.1% (2.~~00~~07 Tg), ~~27.4~~9.0% (0.34 Tg) and ~~26.7~~8.5% (0.04 Tg) higher than those estimated based on the land cover information of the year 2001, respectively.

~~The comparison among different scenarios indicates that the land cover change has comparative impact on annual BVOC variability with the meteorological fluctuation. The coefficient of variance (CV) of total BVOC emission in S3 and S4 is about 5% during 2001-2016, which is due to the interannual meteorological variability. Furthermore, as shown in Figure 2, the largest discrepancy in total BVOC emission in S3 and S4 appears between the year 2014 and 2016, with the total BVOC emission in the year 2016 being 21.1 % and 22.5 % higher than that of the year 2014 in S3 and S4, respectively. In general, the interannual variability of meteorological conditions leads to ~20% difference in BVOC emission during our study period. In contrast, the CV of total BVOC in S2 is 5.74%, which is close to that of 5% in S3 and S4, showing that interannual variability is dominated by meteorology even though the trend is dominated by landcover. Moreover, the largest discrepancy of total BVOC in S2 (23.9%) occurred between the year 2002 and 2016 and is very close to that estimated solely for meteorological conditions. However, as mentioned above, the comparison here only considered the direct impact of meteorological conditions, and the meteorological conditions also can affect the growing process and phenology which can influence BVOC emission indirectly (Peñuelas et al., 2009). Considering the direct and indirect impact of climatic conditions as well as land cover change, the CV of total BVOC in the "full" scenario S1 is 8.15%, which is higher than the other scenarios. The highest and lowest total BVOC emission in S1 are in year 2016 and 2010, respectively, with 2016 being 34.60% (5.00 Tg) higher than 2010. These results show that both landcover and meteorology can individually contribute ~20%, and together over 30%, to the estimated annual variability in China BVOC emissions within this 16-year time period.~~

3.~~3~~2 The Regional Variability of BVOC Emission in China

The hotspots of BVOC emission are mainly located in the northeast, central and south of China where the forest is widely distributed and the climate is warm and favorable for emitting BVOC as shown in Figure 5. The Changbai Mountains, the Qinling Mountains, the southeast and southwest China forest regions, southeast Tibet, Hainan and Taiwan islands are the regions with highest BVOC emission in 2001~~, which is broadly consistent with the previous estimations (Tie et al., 2006; Li et al., 2013).~~

..The spatial ~~distributions~~patterns of statistically significant (p~~></~~ < 0.~~9~~1) changing trends in S1-~~S4~~S5 are also presented for individual categories in Figure 5. ~~In general, the~~The spatial distributions of trends of different species in ~~S1 and~~ S2 ~~are highly consistent~~ all shows a national wide significantly increasing trend since the vegetation development is the main driver of the increasing trend of BVOC emission~~. A strong positive trend~~

Formatted: Font color: Text 1
Formatted: Font color: Text 1
Formatted: Font color: Text 1
Formatted: Font color: Text 1
Formatted: Font color: Text 1
Formatted: Font color: Text 1
Formatted: Font color: Text 1
Formatted: Font color: Text 1
Formatted: Font color: Text 1
Formatted: Font color: Text 1
Formatted: Font color: Text 1
Formatted: Font color: Text 1
Formatted: Font color: Text 1
Formatted: Font color: Text 1
Formatted: Font color: Text 1
Formatted: Font color: Text 1
Formatted: Font color: Text 1
Formatted: Font color: Text 1
Formatted: Font color: Text 1
Formatted: Font color: Text 1
Formatted: Font color: Text 1

~~is found~~ (c, i, o and u in Figure 5). In the full scenario of S1, the ~~Qinling Mountains, southern China (Guangdong and Guangxi provinces) and southwestern China (Yunnan province), on the other hand, the strong negative~~area with statistically significant trend is ~~found at the boundary of Jiangxi and Hunan provinces.~~less than that in S2 considering the impact of meteorological variability. S5 also shows a national wide significantly increasing trend of BVOC emission but with smaller rates comparing to S2 (f, l, r and x in Figure 5). While a positive increasing trend induced by meteorology is also found in Tibet, western Sichuan and southeastern Yunnan province in S3 and S4, ~~and it is clear that most of the trend hotspots in S2 do not overlap with those in S3 and S4, which further indicates that the vegetation development is the main driver of BVOC increasing trend in S1, the "full" scenario, rather than meteorological conditions.~~which is induced by the warming climate and stronger downward shortwave radiation as presented in Figure 3.

~~We chose three main~~ The spatial patterns of changing trends of total BVOC emission and landcover parameters are presented in Figure 6. The cover fraction of broadleaf trees shows a strong increasing trend in regions ~~to~~ including northeastern, central and southern China, meanwhile, the grass and crop cover faction show a decreasing trend in the same regions. The crop cover rates also show an increasing trend in northeastern China, Shan Xi, Gansu and Xinjiang Provinces by replacing the grass there. Besides the change of PFTs, a national wide increasing trend of LAIv was also found for most regions in China.

In order to understand the regional discrepancies of changing trend of BVOC emission and its drivers, we chose six interest regions to further analyze ~~the hotspots of changing BVOC trend driving by the vegetation change, as shown in Figure 3r~~. As shown in (a) of Figure 6, six regions includes 1) northeastern China (orange frame in Figure 6a, 45.5-54N, 118-130E), 2) Beijing and its surrounding areas (black frame in Figure 6a, 39-42.5N, 114-120E), 3) Qinling Mountains (red frame in Figure 6a, 30-~~35N, 104~~34N, 105.5-112E), ~~the boundary region of Jiangxi and Hunan provinces (24.5-29N, 112-115E) and southern China, mainly~~4) Yunnan Province (blue frame in Figure 6a, 21-27N, 97.5-106E), 5) Guangxi ~~and~~ Guangdong provinces (~~21-24.5N,~~ purple frame in Figure 6a, 21-25N, 106-117E~~,~~) and 6) Hainan island (green frame in Figure 6a, 17.5-20.5N, 108-112E). The annual changes of vegetation conditions (~~PFT~~PFTs and ~~LAI) and~~ LAIv), the annual emission ~~rate in these three regions~~flux and growing season averaged temperature and DSW are presented in Figure 7 and Figure 8, and the averaged values and trends of above variables are listed in Table 3 and Table 4. In general, six regions all show that the woody vegetations replaced the herbaceous vegetations with a significantly increasing trend of annual LAIv. Since the broadleaf trees tend to have a higher emission potential than grass or crop (Guenther et al., 2012), the transformation of land cover from grass or crop to broadleaf tree is expected to enhance the emission of BVOC by increasing the landscape average emission factor. ~~. The (a), (b) and (c) in Figure 4 illustrate the vegetation and BVOC emission change in Qinling~~

Formatted: Font color: Text 1
Formatted: Font: Times, 12 pt, Not Bold, Font color: Text 1, English (United States)
Formatted: Font color: Text 1
Formatted: Font color: Text 1
Formatted: Font: Times, 12 pt, Not Bold, Font color: Text 1, (Asian) Chinese (China), (Other) English (United States)
Formatted: Font color: Text 1
Formatted: Font: Times, 12 pt, Not Bold, Font color: Text 1, English (United States)
Formatted: Font color: Text 1
Formatted: Font: Times, 12 pt, Not Bold, Font color: Text 1, English (United States)
Formatted: Font color: Text 1
Formatted: Font color: Text 1
Formatted: Font: Times, 12 pt, Not Bold, Font color: Text 1, (Asian) Chinese (China), (Other) English (United States)
Formatted: Font: Times, 12 pt, Not Bold, Font color: Text 1, (Asian) Chinese (China), (Other) English (United States)
Formatted: Font: Times, 12 pt, Not Bold, Font color: Text 1, (Asian) Chinese (China), (Other) English (United States)
Formatted: Font color: Text 1
Formatted: Font: Times, 12 pt, Not Bold, Font color: Text 1, (Asian) Chinese (China), (Other) English (United States)
Formatted: Font color: Text 1
Formatted: Font color: Text 1
Formatted: Font: Times, 12 pt, Not Bold, Font color: Text 1, (Asian) Chinese (China), (Other) English (United States)
Formatted: Font color: Text 1
Formatted: Font color: Text 1
Formatted: Font: Times, 12 pt, Not Bold, Font color: Text 1, (Asian) Chinese (China), (Other) English (United States)
Formatted: Font color: Text 1
Formatted: Font: Times, 12 pt, Not Bold, Font color: Text 1, (Asian) Chinese (China), (Other) English (United States)
Formatted: Font color: Text 1
Formatted: Font color: Text 1
Formatted: Font color: Text 1
Formatted: Font color: Text 1
Formatted: Font color: Text 1
Formatted: Font: Times, 12 pt, Not Bold, Font color: Text 1, English (United States)
Formatted: Font: Times, 12 pt, Not Bold, Font color: Text 1, English (United States)
Formatted: Font color: Text 1

~~Mountains, southern China and the boundary of Jiangxi and Hunan provinces, respectively~~As shown in Table 3 and Table 4, the broadleaf tree cover fraction increased in a rate of 0.15~0.32 % y^{-1}, and the grass cover fraction decreased in a rate of 0.11~0.37% y^{-1} among the six regions during 2001-2016. Except for the northeastern China we defined, other five regions all show a decreasing trend of 0.04~0.26% y^{-1} for the crop cover faction. As a result, the total tree cover fraction during the last four years (2013-2016) is 11.0, 82.5, 6.1, 5.7, 5.9 and 8.0 % higher than that during first four years (2001-2004) for northeastern China, Beijing and its surroundings, Qinling Mountains, Yunnan Province, Guangxi-Guangdong provinces and Hainan Island, respectively, and the LAIv for these regions also increased by 14.8 ~ 26.4 %. Correspondingly, the annual BVOC emission flux in six regions all show a significantly increasing trend without considering the variability of meteorology in S2. The mean annual BVOC emission flux for the last four years (2013-2016) is 8.6%~9.8% higher than that for the first four years (2001-2004) in the regions defined above except for Beijing and its surrounding areas, where the change of the annual BVOC emission flux reached 19.3% with the tree cover fraction increased by 82.5%. If we only consider the contribution of LAI change, as described in the scenario S5, above sub-regions except for Guangxi-Guangdong provinces still show a statistically significant increasing trend of BVOC emission without considering the variability of meteorology, and the contributions of the LAIv change to BVOC emission increasing trend is about 25%-66% in these regions. ~~As shown in Figure 3, the Qinling Mountains and southern China are the regions with high BVOC emission as well as a significant increasing trend of BVOC emission. The mean emission flux in the Qinling Mountains of approximately 3.91 g m-2 yr-1 in 2001 increased by 61.9 and 40.4 % to 6.33 and 5.49 g m-2 yr-1 in S1 and S2 in 2016, respectively. Southern China also shows a strong enhancement of BVOC emission. The mean emission rate is about 4.11 g m-2 yr-1 in 2001 and increased by 67.6 and 47.4 % to 6.89 and 6.06 g m-2 yr-1 in S1 and S2 respectively in 2016. Interestingly, the vegetation change patterns are notably different in the two regions. We grouped the PFTs used to estimate BVOC emission into three main categories, broadleaf tree, needleleaf tree and other vegetations. As shown in Figure 4a, the total vegetation cover fraction increased by 0.105, from 0.578 in 2001 to 0.683 in 2016, in the Qinling Mountains region. All three of the PFTs categories contributed to the increasing vegetation cover trend in the Qinling Mountains from 2001 to 2016 including 0.207 to 0.262 (0.055 increase) for broadleaf trees, 0.004 to 0.007 (0.003 increase) for needleleaf trees and 0.366 to 0.414 (.048 increase) for other vegetation. The percent contribution of each PFT category to the total vegetation cover fraction increase was about 52% for broadleaf trees, 3% for needleleaf trees and 45% for other vegetation. In contrast, there is only a small (0.017) change in total vegetation cover fraction in Southern China where the total vegetation cover fraction increased from 0.225 in 2001 to 0.242 in 2016. The major vegetation change in this region, as shown in Figure 4b, is the~~

Formatted: Font: Times, 12 pt, Not Bold, Font color: Text 1, English (United States)

Formatted: Font color: Text 1

~~deforestation that leads to the decrease of broadleaf forest and the increase of other vegetation, primarily cropland, from 2001 to 2005 followed by the decline in other vegetation since 2006 along with the increase in broadleaf tree cover fraction since 2007. The cover fractions of broadleaf tree, needleleaf tree and other vegetation in southern China changed from 0.127, 0.0001 and 0.097 in 2001 to 0.179, 0.0002 and 0.0626 in 2016, respectively. As a result, the 0.0522 broadleaf tree cover fraction plus the small 0.0001 needleleaf tree cover fraction increase was partially offset by the 0.0353 vegetation cover fraction decrease of other vegetation~~The changing trend of the annual BVOC emission flux is different in S1 when the impact of meteorological variability is taken into account. The simulated T2 and DSW during the growing season do not show a significantly trend in most regions we chose. As shown in Figure 7 and Figure 8, the variabilities of the temperature and DSW during the growing season controlled the variability of BVOC flux in S1. When the meteorological variability is considered, there are still three regions we defined above that show a significantly increasing trend of BVOC emission: 1) Beijing and its surrounding areas, 2) Guangxi-Guangdong Provinces and 3) Hainan island. In Beijing and its soundings, the changing trend of the annual BVOC emission flux is 0.04 and 0.03 g m^{-1} y^{-1} in S2 and S1, respectively, and the mean annual BVOC emission flux in last four years still shows a large increase of 16.6% comparing that in first four years in this region. A significantly increasing trend of temperature of 0.03 °C y^{-1} were found in southwestern China region, therefore, the increasing trend of the annual BVOC emission flux is 0.1 g m^{-1} y^{-1} in S1, which is higher than that in S2 of 0.04 g m^{-1} y^{-1}. The BVOC flux in last four years is about 17.2% higher than that in first four years in southwestern China. In Hainan island, the changing trend of the annual BVOC emission flux is 0.13 and 0.12 g m^{-1} y^{-1} in S2 and S1, respectively, and the annual BVOC emission flux in last four years is 11.0% higher than that in first four years.

~~BVOC emission shows a statistically significant negative trend at the boundary region of Hunan and Jiangxi province in (Figure 3). As shown in Figure 4c, there was a BVOC emission decreasing trend from 2001 to 2010 and an increasing trend from 2011 to 2016 as a result of changes in the broadleaf tree cover fraction. As mentioned above, broadleaf tree has a relatively higher BVOC emission potential compared to other PFTs, therefore, the change of broadleaf tree cover rate induced by anthropogenic activities is expected to affect local BVOC emission as shown in Figure 4. Compared to the lowest point of 0.177 in 2010, the cover fraction of broadleaf tree in this region recovers to 0.21 in 2016, which is still lower than the 2001 value of 0.224. In S2, the average emission rate of BVOC in this region in 2016 is 5.32 g m-2 yr-1 and is 2.91% lower than that in 2001 of 5.48 g m-2 yr-1. The lowest average emission rate during the study period appears in 2010 because of the lowest cover fraction of broadleaf trees. However, in S1 with the impact of meteorological variability, the average emission rate in 2016 is 5.89 g m-2 yr-1. This is 7.48% higher than the average emission rate in~~

Formatted: Font: Times, 12 pt, Not Bold, Font color: Text 1, (Asian) Chinese (China), (Other) English (United States)

~~2001 of 5.48 g m-2 yr-1, but the lowest average emission rate of 4.49 g m-2 yr-1 is still in 2010. In general, it is clear that land cover change is a dominate factor impacting the interannual variability of BVOC emission on a decadal scale in regions undergoing rapid landcover change as has been suggested by previous studies (Unger, 2014; Chen et al., 2018).~~

The estimated increase of BVOC in the regions like the Qinling Mountains and southern China are expected to affect regional air quality. For the Qinling Mountains and surrounding areas, as estimated by Li et al. (2018) using the WRF-chem model, the average contribution of BVOC to O_3 could reach 16.8 ppb for the daily peak concentration and 8.2 ppb for the 24h concentration in the urban region of Xi'an, one of the biggest cities near the Qinling Mountains suffering from poor air quality in recent years (Yang et al., 2019). For ~~southern China~~Guangxi-Guangdong Provinces, Situ et al. (2013) reported that BVOC emission could contribute an average 7.9 ppb surface peak O_3 concentration for the urban area in the Pearl River Delta region, and the contribution from BVOC even reached 24.8 ppb over PRD in November. Since BVOC plays an important role in local air quality, the change of BVOC emission may have an even greater effect on the local ozone pollution. For instance, the simulation study by Li et al. (2018) also found that the urban region of Xi'an is VOC-limited because of the abundant NOx emission there. Therefore, the increase of BVOC emission in the Qinling Mountains would further favor the formation of O_3 in the urban region of Xi'an.

3.43 Comparison of Estimates of Isoprene Emission and Satellite Derived Formaldehyde Column Concentration

~~The lack of long-term in-situ observations of BVOC in China makes it difficult to validate the variability and trend estimation of BVOC emission in this study. However, since biogenic isoprene is the dominant precursor of formaldehyde in rural regions with minimal anthropogenic influence (Palmer et al., 2003), remotely sensed HCHO observation can used as a proxy of isoprene emission to assess the interannual variability of isoprene emission.~~ The OMI HCHO VC product from 2005-2016 developed by BIRA-IASB (De Smedt et al., 2015) was used in this study~~, and we compared~~. The interannual variability of isoprene emission estimated in this study was evaluated by comparing the isoprene emission with the summer (June-August) ~~average~~averaged HCHO VC~~ records with the summer average isoprene emission estimated in our study to evaluate our estimation of interannual variability of isoprene emission~~.

The ~~average growing season~~annually averaged LAI during 2005-2016 presented in Figure 9a indicates the spatial distribution of vegetation in China. However, the spatial pattern of estimated isoprene emission (Figure 9b) differs from the spatial distribution of vegetation because of the variability of emission potentials among different PFTs in the MEGAN model as well as the climatic conditions. The spatial pattern of average summertime HCHO VC observed by the OMI sensor during 2005-2016 is also presented in Figure 9c. The highest summer HCHO concentrations in the US are mainly distributed in rural forest regions dominated by

Formatted: Font color: Text 1

biogenic emission (Palmer et al., 2003), while the highest summer HCHO concentrations in China are mainly distributed in developed regions like North China Plain where HCHO concentration is dominated by anthropogenic sources. (Smedt et al., 2010). There is a moderate HCHO VC of about 6-10 $\times 10^{15}$ molec cm^{-2} in the vegetation dominated regions of China.

The grid level correlation coefficients between the average summer HCHO VC and isoprene emission estimated in our study are shown in Figure 9d, and the grids with statistically significant correlations ($p >= < 0.91$, N=12) grids are marked with black dots. A positive correlation can beis found in the northeast, central and south of China where there are relatively high vegetation cover rates and low anthropogenic influence. In contrast, there's almost no statistically significant correlation in the high HCHO VC regions like the North China Plain which is dominated by anthropogenic emissions. In addition, there is also no significant correlations between isoprene emission and HCHO VC in regions like the Pearl River Delta where HCHO concentration is controlled by both biogenic and anthropogenic sources. However, the distribution of statistically significant positive correlated points is not completely consistent with the vegetation distribution indicated by LAI because ofdue to the absence of consideration of physical and chemical processes, including transportation, diffusion, and chemical reactions. The grids with significant correlation are mostly distrusted in or near rural regions with high vegetation biomass indicating that our estimations can represent the annual variation of isoprene emission.

The increasing trends of isoprene and HCHO VC during 2005-2016 are presented in (e) and (f) of Figure 9, and the statistically significant ($p >= < 0.91$) grids are marked with black dots. The increasing trend pattern of isoprene emission during 2005-2016 is basically consistent with that during 2001-2016, which has been described in the previous sectionSection 3.2, and it is clear that central and southern China areis the regionsregion with the greatest increasingstrongest positive trend (> 0.06 g m-2 yr-1). For HCHO, developed regions such as the North China Plain have an increasing trend because of the increase of human activities (Smedt et al., 2010), there is also an obvious increasing trend of HCHO VC in the developed Yunnan and Guangxi provinces in the south of China. Moreover, these regions, especially Guangxi province also show a statistically significant positive correlation between isoprene emission and HCHO VC as presented in Figure 9d. This indicates that biogenic emissions might be the main driver of the increased HCHO in Guangxi province.

3.54 Comparison of BVOC Emission with Anthropogenic Emissionother studies and uncertainties discussion

The comparison of isoprene and monoterpenes emission estimations between our estimations and previous studies is presented in Table 5. The estimations of isoprene emission range from 4.65 Tg to 33.21 Tg, and

Formatted: Font color: Text 1
Formatted: Font color: Text 1
Formatted: Font color: Text 1
Formatted: Font color: Text 1, Superscript
Formatted: Font color: Text 1
Formatted: Font color: Text 1
Formatted: Font color: Text 1
Formatted: Font color: Text 1
Formatted: Font color: Text 1
Formatted: Font color: Text 1
Formatted: Font color: Text 1
Formatted: Font color: Text 1
Formatted: Font color: Text 1
Formatted: Font color: Text 1
Formatted: Font color: Text 1
Formatted: Font color: Text 1
Formatted: Font color: Text 1
Formatted: Font color: Text 1
Formatted: Font color: Text 1
Formatted: Font color: Text 1
Formatted: Font color: Text 1
Formatted: Font color: Text 1
Formatted: Font color: Text 1
Formatted: TA_Main_Text, Space Before: 0 pt, After: 0 pt, Line spacing: 1.5 lines

the estimations of monoterpenes emission range from 3.16 Tg to 5.6 Tg in China. Multiple factors including emission factor, meteorological and land cover inputs can lead to the discrepancy of these estimations. We listed the inputs of these estimations in Table 6 to fully understand the discrepancies between our results and other estimations.

Formatted: Font: Times, 12 pt, Font color: Text 1

Formatted: Font: Times, 12 pt, Font color: Text 1

~~China has initiated a series of pollution control policies in recent years (Zheng et al., 2018; Ma et al., 2019) and achieved success in controlling some air pollutants, especially PM2.5 (Ma et al., 2019; Yu et al., 2019; Xu et al., 2019). However, the ozone pollution is still severe in China especially the mega-city areas (Li et al., 2019; Xu et al., 2019). It is widely known that NOx and VOC are the precursors of ground level ozone pollution (Seinfeld and Pandis, 2012). NOx emission in China increased from 2010 to 2012 and then declined rapidly since 2013 because of the emission control policies, and the national-level NOx emission is about 22.50 Tg in 2016 and is ~15 % lower than that in 2010 (Zheng et al., 2018). On the other hand, as shown in Figure 6, the average anthropogenic volatile organic compounds (AVOC) emission during 2010-2016 was about 27.9 Tg in China (Zheng et al., 2018), which is ~70% higher than the average emission of BVOC during the same period investigated by this study. It is clear that the anthropogenic source currently dominates non-methane volatile organic compound (NMVOC) emissions in China. In addition, the spatial distribution of remotely sensed HCHO VC (Figure 5) also indicates the dominant role of anthropogenic NMVOC emission.~~

~~The urban areas in China are generally in the VOC-limited condition and decreasing/increasing local NOx/VOC emission would correspondingly promote the formation of ozone (Tang et al., 2010; Li et al., 2018; Li et al., 2019). Both AVOC and BVOC show the increasing trend since 2010, as shown in Figure 6, with an increase of 9.7% for AVOC and 34.6% for BVOC from 2010 to 2016, respectively. Combined with the decreasing trend of NOx emission, the overall changes of precursors are expected to make it more difficult to control ozone pollution. In addition, there are multiple studies pointing out the interactions between anthropogenic emission and biogenic emission on ozone pollution in mega cities including Beijing (Pang et al., 2009;Shao et al., 2009), Shanghai (Geng et al., 2011), Guangzhou (Situ et al., 2013) and Xi'an (Li et al., 2018). The current trends in biogenic as well as anthropogenic emissions suggest that biogenic emissions will play an even more important role in future air pollution in China.~~

The setting of inputs in this study is relatively close to the study by Stavrakou et al. (2014) and CAMS-GLOB-BIO biogenic emission inventories (https://eccad3.sedoo.fr/#CAMS-GLOB-BIO) that adopted the method described by Sindelarova et al. (2014). However, the estimation of isoprene emission in this study is about 86.6%-122.3% higher than their estimations, and the estimation of monoterpene emission is about 23.5% and 31.3% higher than that from CAMS-GLOB-BIO v3.1 and v1.1, respectively. We further

compared our results with two versions of CAMS-GLOB-BIO inventories. Figure 10 and Figure 11 present the trends of isoprene emission and monoterpenes emission respectively from S1 and S3 in this study, CAMS-GLOB-BIO inventory v 1.1 and v 3.1 during 2001-2016. As shown in Figure 10 and Figure 11, S3 shows similar spatial patterns and magnitude of changing trend of isoprene and monoterpenes emission with CAMS-GLOB-BIO v 1.1 and CAMS-GLOB-BIO v3.1, e.g. three datasets all showed a strong increasing trend in Yunnan province, and S1 shows much more stronger changing trends comparing with other three datasets with annually updated LAI and PFT datasets. The meteorological inputs for CAMS-GLOB-BIO v1.1 and v3.1 are ERA-Interim and ERA-5 reanalysis data, respectively, and the WRF model used in this study was also driven by ERA-Interim reanalysis data. Therefore, the four datasets have the similar source of meteorological inputs. In addition, these estimations all adopted the same PFT level emission factors from Guenther et al. (2012). Therefore, the potential reason for the differences of isoprene and monoterpenes emission among the datasets in Figure 10 and Figure 11 is the discrepancies of PFT and LAI inputs. CAMS-GLOB-BIO also adopted the annually updated LAI inputs developed by Yuan et al. (2011) based on MODIS MOD15A v5 LAI product, but the two versions of CAMS-GLOB-BIO inventory didn't show a same level strong increasing trend with S1. The increasing trend of LAI in China is agreed by multiple LAI products but with different rates (Piao et al., 2015; Chen et al., 2020). In this study, we adopted the latest MODIS LAI product of version 6, and a strong increasing trend of LAI in China has been found by using this product (Chen et al., 2019). Therefore, an increasing trend of BVOC emission induced by LAI should be seen in the estimation with annually updated LAI inputs, but the magnitude of this trend is also affected by the magnitude of changing trend of LAI products. The PFT map used in this study is coming from MODIS land cover product, which is a mesoscale satellite product with the highest resolution of 500m. Besides the quality of the product, the method for converting the original land cover classification system to PFT classification system is also important. Hartley et al. (2017) illustrated that the cross-walking table for converting land cover class maps to PFT fractional maps can lead to 20%-90% uncertainties for gross primary production estimation in land surface model by using different vegetation fractions for mixed pixels, and the BVOC emission estimation has the same issue. In this study, we assumed that the pixels that were assigned as vegetation is 100% covered by that kind of vegetation (Table S1 in the supplement). Therefore, it will lead to an overestimation of vegetation cover rate for mixed pixels, which can lead to higher BVOC emission.

The emission factor is also an important source of uncertainties, and it decided the spatial patterns of emission rates together with the PFT distribution. In order to understand the role of emission factor, the flux measurements of isoprene and monoterpenes from the campaigns conducted during 2010 to 2016 in China (Bai et al., 2015; Bai et al., 2016; Bai et al., 2017) were collected and compared with model results in this

Formatted: Font: Times, 12 pt, Not Bold, Font color: Text 1, English (United States)

Formatted: Font: Times, 12 pt, Not Bold, Font color: Text 1, English (United States)

Formatted: Font: Times, 12 pt, Not Bold, Font color: Text 1, English (United States)

study. The details of these campaigns are provided in Table 7, and the emission factors that were retrieved from the observations are also listed for these sites. Most samples were collected during the daytime every 3 hours according to the descriptions of the measurements (Bai et al., 2015;Bai et al., 2016;Bai et al., 2017), therefore, we averaged the model results during 8:00 A.M. to 20 A.M in local time with a three hours interval for comparison. As shown in the (a) and (b) of Figure 12, the modeled fluxes of isoprene and monoterpenes with the default emission factors in this study didn't capture the variability of the observations. The ME, MB and RMSE are 1.60, 1.59 and 2.31 mg m^{-2} h^{-1} for isoprene and 0.21, -0.003 and 0.32 mg m^{-2} h^{-1} for monoterpenes. When we adopted the emission factor retrieved from observations (Bai et al., 2015;Bai et al., 2016;Bai et al., 2017), the simulated isoprene and monoterpenes fluxes showed relatively good consistence with the observations by using the same activity factor from the model (γ in equation (1)) as shown in (c) and (b) of Figure 12. The ME, MB and RMSE are 0.44, 0.41 and 0.57 mg m^{-2} h^{-1} for isoprene and 0.32, 0.14 and 0.49 mg m^{-2} h^{-1} for monoterpenes after adopting the observation-based emission factors, and the statistic parameters for isoprene simulation are largely improved. Although the MB and ME of monoterpenes simulation are increased, but the simulated monoterpenes flux show better agreement with observations (Figure 12). Therefore, it is clear that our calculation of activity factors is in a reasonable range, but the emission factor is the main source of uncertainties. The PFT level emission factors used in this study from Guenther et al. (2012) represents the globally averaged emission factor for PFTs, and it is relatively easy to use them with the satellite PFT products. Therefore, the most studies listed in Table 6 adopted the PFT/landuse level emission factors. Our validation showed that the accurate emission factor based on observations could largely improve the performance of the MEGAN model, but it also requires abundant efforts to conduct measurements. However, the measurements listed in Table 7 are still very limited for describing the spatial discrepancies of ecosystems in China, so we still used the default emission factors in MEGAN model for our national scale estimation. The estimations by Li et al. (2013, 2020) used the species level emission factors and Vegetation Atlas of China for 2007 to describe the spatial distribution of BVOC emission potentials, and they concluded the reason why their estimations were far higher than other studies is the high emission factors they adopted. Therefore, the same validations by using canopy-scale BVOC flux measurements are also needed for these studies to validate and constrain the emission factors they used.

Meteorological input is also a source of uncertainties for BVOC emission estimation. As shown in Figure 12, the modeled isoprene and monoterpenes fluxes are still generally higher than observations when observation-based emission factors were used. One potential reason for this phenomenon is the overestimation of temperature and radiation as described in Section 2.3. The sensitivity tests by Wang et al. (2011) showed that the about 1.89 ℃ discrepancy of temperature can result in -19.2 to 23.2% change of isoprene emission and -

16.2 to 18.5% change of monoterpenes emission for Pearl River Delta region in July, where is also a hotspot for BVOC emission in this study. They also found that 115.8 W m^{-2} discrepancy of DSW can result in -31.4 to 36.2% change of isoprene emission and -14.3 to 16.8% change of monoterpenes emission for the same region. The BVOC emission in this study might be overestimated because of the overestimated temperature and DSW in meteorological inputs. However, inaccurate emission factors could lead to over 100% uncertainties, which is more significant than the uncertainties induced by meteorological inputs.

4. Conclusion

Satellite observations have shown that China has led the global greening trend in recent decades (Chen et al., 2019). In this study, we investigated the impact of this greening trend on BVOC emission in China ~~during~~from 2001 to 2016. We used ~~the~~ long-term satellite vegetation products as inputs ~~for~~in the MEGAN ~~model~~. According to the model estimations, the ~~total BVOC emission in China had~~ vegetation development can lead to a significant increasing trend of 0.50% y^{-1}~~.09% yr-1 during~~ of total BVOC emission in China from 2001~~-~~ to 2016, and main BVOC classes of isoprene, monoterpene and sesquiterpene all had increasing trends of ~~1.35 % yr-1, 1.25 % yr-1~~0.64, 0.44 and ~~1.43 % yr-1,~~0.39 % y^{-1}. The BVOC emission level in 2016 can be 11.7% higher than that in 2001 because of higher tree cover fraction and biomass. The comparison among different scenarios showed that vegetation changes resulting from land cover management is the main driver of BVOC emission change in China. Climate variability contributed significantly to interannual variations but not the long-term trend~~.~~

On regional scales, there are strong increasing trends in 1) northeastern China, 2) Beijing and its surrounding areas, 3) the Qinling Mountains, ~~southern China~~ (4) Yunnan province, 5) Guangdong ~~and~~ Guangxi provinces~~)~~ and ~~southwestern China, while a~~ 6) Hainan island. A strong ~~negative trend was~~increasing trend of broadleaf tree cover fractions and LAIv were found ~~at~~ in these regions. The mean total tree cover fraction during the ~~boundary of Jiangxi and Hunan provinces.~~last four years (2013-2016) is 5.7-82.5 % higher than that of the first four years (2001-2004) for these regions, and the LAIv during 2013-2016 increased by 14.8 ~ 26.4 % comparing to that during 2001-2004 in these regions. Consequently, the average BVOC emission flux for the last four years (2013-2016) is 8.6%~19.3% higher than that for the first four years (2001-2004) in the sub-regions we defined driven by the same meteorological inputs. In the standard scenario~~, that considers both land cover and climate, the BVOC emission of year 2016 is 61.89% and 67.64% higher than that in 2001 in the Qinling Mountains and southern China, respectively; furthermore, the land cover change alone~~ of S1, a statistic significant increasing trend still could ~~lead to 40.40% and 47.44% increase of BVOC emission in the Qinling Mountains and southern China, respectively. Moreover, the vegetation change~~

Formatted: Font color: Text 1
Formatted: Font color: Text 1
Formatted: Font color: Text 1
Formatted: Font color: Text 1
Formatted: Font color: Text 1
Formatted: Font color: Text 1, Superscript
Formatted: Font color: Text 1
Formatted: Font color: Text 1
Formatted: Font color: Text 1
Formatted: Font color: Text 1
Formatted: Font color: Text 1
Formatted: Font color: Text 1
Formatted: Font color: Text 1
Formatted: Font color: Text 1
Formatted: Font color: Text 1
Formatted: Font color: Text 1
Formatted: Font color: Text 1
Formatted: Font color: Text 1

~~patterns are different~~be found in the ~~two regions. In the Qinling Mountains, the total vegetation cover rate obviously increased from 0.578 in 2001 to 0.683 in 2016, and all three main PFT categories, i.e. broadleaf trees, needleleaf trees and other vegetations, increased during 2001-2016.~~ sub-regions including Beijing and its surroundings, Yunnan province and Hainan island considering the climate variability. ~~In contrast there the total vegetation cover fraction only increased from 0.225 in 2001 to 0.242 in 2016 southern China, but this was due to the replacement of low BVOC emission potential PFTs, crops or grass, with forests that have much higher emission potential. There is also a significantly negative trend at the boundary region of Hunan and Jiangxi provinces (Figure 3) induced by deforestation during 2001-2010. However, the BVOC emission there has been in a increasing trend since 2011 with the recovery of the broadleaf tree forest.~~

We used the long-term record of satellite HCHO VC from the OMI sensor to ~~asses~~assess our estimation of isoprene emission in China during 2005-2016. The results indicated statistically significant positive correlation coefficients between the isoprene emission estimate and satellite HCHO VC in summer over the regions with high vegetation cover fraction including the northeast, central and southern China. In addition, isoprene emission and HCHO VC both had a statistically significant increasing trend in the south of China, mainly Guangxi Province, where there was a statistically significant positive correlation supporting the estimated variability of BVOC emission in China.

We conclude that uncertainties of this study mainly come from the emission factor, PFT and LAI inputs through comparing our results with other studies and flux measurements during 2010-2016 in China. The validation with flux measurements suggested that using the observation-based emission factor could largely improve the performance of model, but it also requires more much more efforts. The increase of BVOC reported by this study is expected to lead to a more complex situation for making the policies for controlling ozone pollution in China. The recent pollution control policies in China have effectively initiated the control of PM2.5 pollution, but the ozone pollution is still severe especially in urban areas ~~(Ma et al., 2019; Yu et al., 2019; Xu et al., 2019; Li et al., 2019). Although anthropogenic emission is still the dominant source of NMVOC in China and is ~70 % higher than the average biogenic emission in China, the BVOC still makes an important contribution to ozone pollution in mega cities including Beijing (Pang et al., 2009;Shao et al., 2009), Shang Hai (Geng et al., 2011), Guang Zhou (Situ et al., 2013) and Xi'an (Li et al., 2018) and may further increase in importance considering the continuing greening trend over China in the future~~.

Formatted: Font color: Text 1
Formatted: Font color: Text 1
Formatted: Font color: Text 1
Formatted: Font color: Text 1
Formatted: Font color: Text 1
Formatted: Font color: Text 1

Author Contribution

QW, LW and HW planned and organized the project. HW, JF and QX prepared the input datasets. HW modelled and analyzed the data. HW and QW wrote the manuscript. HW, AG and QW revised the manuscript. AG, XY, LN, XT, JL, JF and HC reviewed and provided key comments on the paper.

Data Availability

The source code of MEGAN v2.1 is available at https://bai.ess.uci.edu/. The MODIS MCD12C1 land cover product Version 6 and MODIS MCD15A2 LAI Version 6 and MODIS MOD44B VCF Version 6 datasets are available on the website of the Land Processes Distributed Active Archive Center (LP DAAC) at https://lpdaac.usgs.gov/dataset_discovery/modis/modis_products_table. The version 14 Level 3 OMI HCHO VC product were downloaded from the website of Tropospheric Emission Monitoring Internet Service (TEMIS) at http://h2co.aeronomy.be.

Competing Interests

The authors declare no competing financial interest.

Acknowledgements

The National Key R&D Program of China (2017YFC0209805 and 2016YFB0200800), the National Natural Science Foundation of China (41305121~~) and~~), the Fundamental Research Funds for the Central Universities and Beijing Advanced Innovation Program for Land Surface funded this work.

References

Arneth, A., Niinemets, Ü., Pressley, S., Bäck, J., Hari, P., Karl, T., Noe, S., Prentice, I., Serça, D., and Hickler, T.: Process-based estimates of terrestrial ecosystem isoprene emissions: incorporating the effects of a direct CO 2-isoprene interaction, Atmospheric Chemistry and Physics, 7, 31-53, 2007.

Bai, J., Baker, B., Liang, B., Greenberg, J., and Guenther, A.: Isoprene and monoterpene emissions from an Inner Mongolia grassland, Atmospheric Environment, 40, 5753-5758, https://doi.org/10.1016/j.atmosenv.2006.05.019, 2006.

Bai, J., Guenther, A., Turnipseed, A., and Duhl, T.: Seasonal and interannual variations in whole-ecosystem isoprene and monoterpene emissions from a temperate mixed forest in Northern China, Atmospheric Pollution Research, 6, 696-707, https://doi.org/10.5094/APR.2015.078, 2015.

Bai, J., Guenther, A., Turnipseed, A., Duhl, T., Yu, S., and Wang, B.: Seasonal variations in whole-ecosystem BVOC emissions from a subtropical bamboo plantation in China, Atmospheric Environment, 124, 12-21, https://doi.org/10.1016/j.atmosenv.2015.11.008, 2016.

Formatted: Font color: Text 1
Formatted: Font color: Text 1
Formatted: Font color: Text 1
Formatted: Font color: Text 1
Formatted: Font color: Text 1
Formatted: Font color: Text 1
Formatted: Font color: Text 1
Formatted: Font color: Text 1

Bai, J., Guenther, A., Turnipseed, A., Duhl, T., and Greenberg, J.: Seasonal and interannual variations in whole-ecosystem BVOC emissions from a subtropical plantation in China, Atmospheric Environment, 161, 176-190, 10.1016/j.atmosenv.2017.05.002, 2017.

Bauwens, M., Stavrakou, T., Müller, J. F., Van Schaeybroeck, B., De Cruz, L., De Troch, R., Giot, O., Hamdi, R., Termonia, P., Laffineur, Q., Amelynck, C., Schoon, N., Heinesch, B., Holst, T., Arneth, A., Ceulemans, R., Sanchez-Lorenzo, A., and Guenther, A.: Recent past (1979–2014) and future (2070–2099) isoprene fluxes over Europe simulated with the MEGAN–MOHYCAN model, Biogeosciences, 15, 3673-3690, 10.5194/bg-15-3673-2018, 2018.

Berrisford, P., Dee, D. P., Poli, P., Brugge, R., Mark, F., Manuel, F., Kållberg, P. W., Kobayashi, S., Uppala, S., and Adrian, S.: The ERA-Interim archive Version 2.0, ECMWF, Shinfield Park, Reading, 2011.

Bonan Gordon, B., Levis, S., Kergoat, L., and Oleson Keith, W.: Landscapes as patches of plant functional types: An integrating concept for climate and ecosystem models, Global Biogeochemical Cycles, 16, 5-1-5-23, 10.1029/2000GB001360, 2002.

Bryan, B. A., Gao, L., Ye, Y., Sun, X., Connor, J. D., Crossman, N. D., Stafford-Smith, M., Wu, J., He, C., Yu, D., Liu, Z., Li, A., Huang, Q., Ren, H., Deng, X., Zheng, H., Niu, J., Han, G., and Hou, X.: China's response to a national land-system sustainability emergency, Nature, 559, 193-204, 10.1038/s41586-018-0280-2, 2018.

Chen, C., Park, T., Wang, X., Piao, S., Xu, B., Chaturvedi, R. K., Fuchs, R., Brovkin, V., Ciais, P., Fensholt, R., Tømmervik, H., Bala, G., Zhu, Z., Nemani, R. R., and Myneni, R. B.: China and India lead in greening of the world through land-use management, Nature Sustainability, 2, 122-129, 10.1038/s41893-019-0220-7, 2019.

Chen, W. H., Guenther, A. B., Wang, X. M., Chen, Y. H., Gu, D. S., Chang, M., Zhou, S. Z., Wu, L. L., and Zhang, Y. Q.: Regional to Global Biogenic Isoprene Emission Responses to Changes in Vegetation From 2000 to 2015, Journal of Geophysical Research: Atmospheres, 123, 3757-3771, 10.1002/2017JD027934, 2018.

Chen, Y., Chen, L., Cheng, Y., Ju, W., Chen, H. Y. H., and Ruan, H.: Afforestation promotes the enhancement of forest LAI and NPP in China, Forest Ecology and Management, 462, 117990, https://doi.org/10.1016/j.foreco.2020.117990, 2020.

Claeys, M., Graham, B., Vas, G., Wang, W., Vermeylen, R., Pashynska, V., Cafmeyer, J., Guyon, P., Andreae, M. O., and Artaxo, P.: Formation of secondary organic aerosols through photooxidation of isoprene, Science, 303, 1173-1176, 2004.

De Smedt, I., Van Roozendael, M., Stavrakou, T., Müller, J. F., Lerot, C., Theys, N., Valks, P., Hao, N., and van der A, R.: Improved retrieval of global tropospheric formaldehyde columns from GOME-2/MetOp-A addressing noise reduction and instrumental degradation issues, Atmos. Meas. Tech., 5, 2933-2949, 10.5194/amt-5-2933-2012, 2012.

De Smedt, I., Stavrakou, T., Hendrick, F., Danckaert, T., Vlemmix, T., Pinardi, G., Theys, N., Lerot, C., Gielen, C., Vigouroux, C., Hermans, C., Fayt, C., Veefkind, P., Müller, J. F., and Van Roozendael, M.: Diurnal, seasonal and long-term variations of global formaldehyde columns inferred from combined OMI and GOME-2 observations, Atmos. Chem. Phys., 15, 12519-12545, 10.5194/acp-15-12519-2015, 2015.

Dimiceli, C., M. Carroll, R. Sohlberg, D.H. Kim, M. Kelly, J.R.G. Townshend. MOD44B MODIS/Terra Vegetation Continuous Fields Yearly L3 Global 250m SIN Grid V006. 2015, distributed by NASA EOSDIS Land Processes DAAC, https://doi.org/10.5067/MODIS/MOD44B.006. Accessed 2020-10-06.

Dobber, M., Kleipool, Q., Dirksen, R., Levelt, P., Jaross, G., Taylor, S., Kelly, T., Flynn, L., Leppelmeier, G., and Rozemeijer, N.: Validation of Ozone Monitoring Instrument level 1b data products, Journal of Geophysical Research: Atmospheres, 113, 10.1029/2007JD008665, 2008.

Friedl, M., D. Sulla-Menashe. MCD12C1 MODIS/Terra+Aqua Land Cover Type Yearly L3 Global 0.05Deg CMG V006. 2015, distributed by NASA EOSDIS Land Processes DAAC, https://doi.org/10.5067/MODIS/MCD12C1.006. Accessed 2020-08-28.

Formatted: Font color: Text 1

Formatted: Font color: Text 1

Formatted: Font color: Text 1

Fu, Y., and Liao, H.: Simulation of the interannual variations of biogenic emissions of volatile organic compounds in China: Impacts on tropospheric ozone and secondary organic aerosol, Atmospheric Environment, 59, 170-185, https://doi.org/10.1016/j.atmosenv.2012.05.053, 2012.

Geng, F., Tie, X., Guenther, A., Li, G., Cao, J., and Harley, P.: Effect of isoprene emissions from major forests on ozone formation in the city of Shanghai, China, Atmospheric Chemistry and Physics, 11, 10449-10459, 10.5194/acp-11-10449-2011, 2011.

Guenther, A., Hewitt, C. N., Erickson, D., Fall, R., Geron, C., Graedel, T., Harley, P., Klinger, L., Lerdau, M., McKay, W. A., Pierce, T., Scholes, B., Steinbrecher, R., Tallamraju, R., Taylor, J., and Zimmerman, P.: A global model of natural volatile organic compound emissions, Journal of Geophysical Research, 100, 8873, 10.1029/94jd02950, 1995.

Guenther, A., Karl, T., Harley, P., Wiedinmyer, C., Palmer, P., and Geron, C.: Estimates of global terrestrial isoprene emissions using MEGAN (Model of Emissions of Gases and Aerosols from Nature), Atmos. Chem. Phys, 6, 3181-3210, 2006.

Guenther, A. B., Monson, R. K., and Fall, R.: Isoprene and monoterpene emission rate variability: Observations with eucalyptus and emission rate algorithm development, Journal of Geophysical Research: Atmospheres, 96, 10799-10808, 10.1029/91JD00960, 1991.

Guenther, A. B., Zimmerman, P. R., Harley, P. C., Monson, R. K., and Fall, R.: Isoprene and monoterpene emission rate variability: Model evaluations and sensitivity analyses, Journal of Geophysical Research: Atmospheres, 98, 12609-12617, doi:10.1029/93JD00527, 1993.

Guenther, A. B., Jiang, X., Heald, C. L., Sakulyanontvittaya, T., Duhl, T., Emmons, L. K., and Wang, X.: The Model of Emissions of Gases and Aerosols from Nature version 2.1 (MEGAN2.1): an extended and updated framework for modeling biogenic emissions, Geoscientific Model Development, 5, 1471-1492, 10.5194/gmd-5-1471-2012, 2012.

~~Guenther, C.: Estimates of global terrestrial isoprene emissions using MEGAN (Model of Emissions of Gases and Aerosols from Nature), Atmospheric Chemistry and Physics, 6, 2006.~~

Hartley, A. J., MacBean, N., Georgievski, G., and Bontemps, S.: Uncertainty in plant functional type distributions and its impact on land surface models, Remote Sensing of Environment, 203, 71-89, https://doi.org/10.1016/j.rse.2017.07.037, 2017.

Heald, C. L., Wilkinson, M. J., Monson, R. K., Alo, C. A., Wang, G., and Guenther, A.: Response of isoprene emission to ambient CO2 changes and implications for global budgets, Global Change Biology, 15, 1127-1140, doi:10.1111/j.1365-2486.2008.01802.x, 2009.

Jin, X., and Holloway, T.: Spatial and temporal variability of ozone sensitivity over China observed from the Ozone Monitoring Instrument, Journal of Geophysical Research: Atmospheres, 120, 7229-7246, doi:10.1002/2015JD023250, 2015.

Kaiser, J., Jacob, D. J., Zhu, L., Travis, K. R., Fisher, J. A., González Abad, G., . . . Wisthaler, A. (2018). High-resolution inversion of OMI formaldehyde columns to quantify isoprene emission on ecosystem-relevant scales: application to the southeast US. Atmos. Chem. Phys., 18(8), 5483-5497. doi:10.5194/acp-18-5483-2018

Kavouras, I. G., Mihalopoulos, N., and Stephanou, E. G.: Formation of atmospheric particles from organic acids produced by forests, Nature, 395, 683-686, 1998.

Klinger, L. F., Li, Q. J., Guenther, A. B., Greenberg, J. P., Baker, B., and Bai, J. H.: Assessment of volatile organic compound emissions from ecosystems of China, Journal of Geophysical Research: Atmospheres, 107, ACH 16-11-ACH 16-21, 10.1029/2001jd001076, 2002.

Lathière, J., Hauglustaine, D. A., Friend, A. D., De Noblet-Ducoudré, N., Viovy, N., and Folberth, G. A.: Impact of climate variability and land use changes on global biogenic volatile organic compound emissions, Atmos. Chem. Phys., 6, 2129-2146, 10.5194/acp-6-2129-2006, 2006.

Formatted: Font color: Text 1

Formatted: Font color: Text 1

Formatted: Font: Times New Roman, Font color: Text 1

Lathière, J., Hewitt, C. N., and Beerling, D. J.: Sensitivity of isoprene emissions from the terrestrial biosphere to 20th century changes in atmospheric CO2 concentration, climate, and land use, Global Biogeochemical Cycles, 24, 10.1029/2009GB003548, 2010.

Lawrence, D. M., Oleson, K. W., Flanner, M. G., Thornton, P. E., Swenson, S. C., Lawrence, P. J., Zeng, X., Yang, Z. L., Levis, S., and Sakaguchi, K.: Parameterization improvements and functional and structural advances in Version 4 of the Community Land Model, Journal of Advances in Modeling Earth Systems, 3, 365-375, 2011.

Leemans, R., and Cramer, W. P.: The IIASA database for mean monthly values of temperature, precipitation, and cloudiness on a global terrestrial grid, INTERNATIONAL INSTITUTE FOR APPLIED SYSTEMS ANALYSIS, Laxenburg, Austria., 1991.

Levis, S., Wiedinmyer, C., Bonan, G. B., and Guenther, A.: Simulating biogenic volatile organic compound emissions in the Community Climate System Model, Journal of Geophysical Research: Atmospheres, 108, 10.1029/2002JD003203, 2003.

Li, K., Jacob, D. J., Liao, H., Shen, L., Zhang, Q., and Bates, K. H.: Anthropogenic drivers of 2013–2017 trends in summer surface ozone in China, Proceedings of the National Academy of Sciences, 116, 422, 10.1073/pnas.1812168116, 2019.

Li, L. Y., Chen, Y., and Xie, S. D.: Spatio-temporal variation of biogenic volatile organic compounds emissions in China, Environmental Pollution, 182, 157-168, https://doi.org/10.1016/j.envpol.2013.06.042, 2013.

Li, L. Y., and Xie, S. D.: Historical variations of biogenic volatile organic compound emission inventories in China, 1981–2003, Atmospheric Environment, 95, 185-196, https://doi.org/10.1016/j.atmosenv.2014.06.033, 2014.

Li, L., Yang, W., Xie, S., and Wu, Y.: Estimations and uncertainty of biogenic volatile organic compound emission inventory in China for 2008–2018, Science of The Total Environment, 733, 139301, https://doi.org/10.1016/j.scitotenv.2020.139301, 2020.

Li, N., He, Q., Greenberg, J., Guenther, A., Li, J., Cao, J., Wang, J., Liao, H., Wang, Q., and Zhang, Q.: Impacts of biogenic and anthropogenic emissions on summertime ozone formation in the Guanzhong Basin, China, Atmos. Chem. Phys., 18, 7489-7507, 10.5194/acp-18-7489-2018, 2018.

Ma, Z., Liu, R., Liu, Y., and Bi, J.: Effects of air pollution control policies on PM2.5 pollution improvement in China from 2005 to 2017: a satellite-based perspective, Atmos. Chem. Phys., 19, 6861-6877, 10.5194/acp-19-6861-2019, 2019.

Marais, E. A., Jacob, D. J., Kurosu, T., Chance, K., Murphy, J., Reeves, C., Mills, G., Casadio, S., Millet, D., and Barkley, M. P.: Isoprene emissions in Africa inferred from OMI observations of formaldehyde columns, Atmospheric Chemistry and Physics, 12, 6219-6235, 2012.

Messina, P., Lathière, J., Sindelarova, K., Vuichard, N., Granier, C., Ghattas, J., Cozic, A., and Hauglustaine, D. A.: Global biogenic volatile organic compound emissions in the ORCHIDEE and MEGAN models and sensitivity to key parameters, Atmos. Chem. Phys., 16, 14169-14202, 10.5194/acp-16-14169-2016, 2016.

Müller, J. F., Stavrakou, T., Wallens, S., De Smedt, I., Van Roozendael, M., Potosnak, M. J., . . . Guenther, A. B. (2008). Global isoprene emissions estimated using MEGAN, ECMWF analyses and a detailed canopy environment model. Atmos. Chem. Phys., 8(5), 1329-1341. doi:10.5194/acp-8-1329-2008

Myneni, R., Y. Knyazikhin, T. Park. MOD15A2H MODIS/Terra Leaf Area Index/FPAR 8-Day L4 Global 500m SIN Grid V006. 2015a, distributed by NASA EOSDIS Land Processes DAAC, https://doi.org/10.5067/MODIS/MOD15A2H.006. Accessed 2020-10-06.

Myneni, R., Y. Knyazikhin, T. Park. MCD15A2H MODIS/Terra+Aqua Leaf Area Index/FPAR 8-day L4 Global 500m SIN Grid V006. 2015b, distributed by NASA EOSDIS Land Processes DAAC, https://doi.org/10.5067/MODIS/MCD15A2H.006. Accessed 2020-10-06.

Formatted: Font color: Text 1

Formatted: Font color: Text 1

Formatted: Font: Times New Roman, Font color: Text 1

Formatted: Font color: Text 1

Formatted: Font color: Text 1

Palmer, P. I., Jacob, D. J., Fiore, A. M., Martin, R. V., Chance, K., and Kurosu, T. P.: Mapping isoprene emissions over North America using formaldehyde column observations from space, Journal of Geophysical Research: Atmospheres, 108, n/a-n/a, 10.1029/2002JD002153, 2003.

Pang, X., Mu, Y., Zhang, Y., Lee, X., and Yuan, J.: Contribution of isoprene to formaldehyde and ozone formation based on its oxidation products measurement in Beijing, China, Atmospheric Environment, 43, 2142-2147, http://dx.doi.org/10.1016/j.atmosenv.2009.01.022, 2009.

Penuelas, J., and Staudt, M.: BVOCs and global change, Trends Plant Sci, 15, 133-144, 10.1016/j.tplants.2009.12.005, 2010.

Peñuelas, J., Rutishauser, T., and Filella, I.: Phenology Feedbacks on Climate Change, Science, 324, 887, 10.1126/science.1173004, 2009.

Piao, S., Yin, G., Tan, J., Cheng, L., Huang, M., Li, Y., Liu, R., Mao, J., Myneni, R. B., Peng, S., Poulter, B., Shi, X., Xiao, Z., Zeng, N., Zeng, Z., and Wang, Y.: Detection and attribution of vegetation greening trend in China over the last 30 years, Global Change Biology, 21, 1601-1609, 10.1111/gcb.12795, 2015.

Ramankutty, N., and Foley, J. A.: Estimating historical changes in global land cover: Croplands from 1700 to 1992, Global Biogeochemical Cycles, 13, 997-1027, doi:10.1029/1999GB900046, 1999.

Sakulyanontvittaya, T., Duhl, T., Wiedinmyer, C., Helmig, D., Matsunaga, S., Potosnak, M., Milford, J., and Guenther, A.: Monoterpene and sesquiterpene emission estimates for the United States, Environmental science & technology, 42, 1623-1629, 2008.

Seinfeld, J. H., and Pandis, S. N.: Atmospheric Chemistry and Physics: From Air Pollution to Climate Change, 2nd Edition, 2012.

Shao, M., Lu, S., Liu, Y., Xie, X., Chang, C., Huang, S., and Chen, Z.: Volatile organic compounds measured in summer in Beijing and their role in ground - level ozone formation, Journal of Geophysical Research: Atmospheres, 114, 2009.

Sindelarova, K., Granier, C., Bouarar, I., Guenther, A., Tilmes, S., Stavrakou, T., Müller, J. F., Kuhn, U., Stefani, P., and Knorr, W.: Global data set of biogenic VOC emissions calculated by the MEGAN model over the last 30 years, Atmos. Chem. Phys., 14, 9317-9341, 10.5194/acp-14-9317-2014, 2014.

Situ, S., Guenther, A., Wang, X., Jiang, X., Turnipseed, A., Wu, Z., and Bai, J.: Impacts of seasonal and regional variability in biogenic VOC emissions on surface ozone in the Pearl River delta region, China, Atmospheric Chemistry and Physics, 13, 11803-11817, 2013.

Skamarock, W. C., Klemp, J. B., Dudhia, J., Gill, D. O., Barker, D. M., Duda, M. G., Huang, X.-y., Wang, W., and Powers, J. G.: A description of the advanced research WRF version 3, NCAR Technical Note NCAR/TN-475+STR, 2008.

Smedt, I. D., Stavrakou, T., Müller, J. F., R., J. v. d. A., and Roozendael, M. V.: Trend detection in satellite observations of formaldehyde tropospheric columns, Geophysical Research Letters, 37, L18808, 2010.

Stavrakou, T., Müller, J. F., Bauwens, M., De Smedt, I., Van Roozendael, M., Guenther, A., Wild, M., and Xia, X.: Isoprene emissions over Asia 1979-2012: impact of climate and land-use changes, Atmospheric Chemistry and Physics, 14, 4587-4605, 10.5194/acp-14-4587-2014, 2014.

Stavrakou, T., Müller, J. F., Bauwens, M., De Smedt, I., Van Roozendael, M., De Mazière, M., Vigouroux, C., Hendrick, F., George, M., Clerbaux, C., Coheur, P. F., and Guenther, A.: How consistent are top-down hydrocarbon emissions based on formaldehyde observations from GOME-2 and OMI?, Atmos. Chem. Phys., 15, 11861-11884, 10.5194/acp-15-11861-2015, 2015.

Stavrakou, T., Müller, J. F., Bauwens, M., Smedt, I., Roozendael, M., and Guenther, A.: Impact of Short-term Climate Variability on Volatile Organic Compounds Emissions Assessed Using OMI Satellite Formaldehyde Observations, Geophysical Research Letters, 0, 10.1029/2018GL078676, 2018.

Formatted: Font color: Text 1

Formatted: Font color: Text 1, English (United States)

Formatted: Font color: Text 1

Formatted: Font color: Text 1

Sulla-Menashe, D., and Friedl, M. A.: User guide to collection 6 MODIS land cover (MCD12Q1 and MCD12C1) product, USGS: Reston, VA, USA, 1-18, 2018.

Tang, X., Wang, Z., Zhu, J., Gbaguidi, A. E., Wu, Q., Li, J., and Zhu, T.: Sensitivity of ozone to precursor emissions in urban Beijing with a Monte Carlo scheme, Atmospheric Environment, 44, 3833-3842, http://dx.doi.org/10.1016/j.atmosenv.2010.06.026, 2010.

Tie, X., Li, G., Ying, Z., Guenther, A., and Madronich, S.: Biogenic emissions of isoprenoids and NO in China and comparison to anthropogenic emissions, Science of the total environment, 371, 238-251, 2006.

Unger, N.: Isoprene emission variability through the twentieth century, Journal of Geophysical Research: Atmospheres, 118, 13,606-613,613, 10.1002/2013JD020978, 2013.

Unger, N.: Human land-use-driven reduction of forest volatiles cools global climate, Nature Climate Change, 4, 907, 10.1038/nclimate2347 https://www.nature.com/articles/nclimate2347#supplementary-information, 2014.

Wang, H., Wu, Q., Liu, H., Wang, Y., Cheng, H., Wang, R., Wang, L., Xiao, H., and Yang, X.: Sensitivity of biogenic volatile organic compound emissions to leaf area index and land cover in Beijing, Atmos. Chem. Phys., 18, 9583-9596, 10.5194/acp-18-9583-2018, 2018.

Wang, X., Situ, S., Guenther, A., Chen, F. E. I., Wu, Z., Xia, B., and Wang, T.: Spatiotemporal variability of biogenic terpenoid emissions in Pearl River Delta, China, with high-resolution land-cover and meteorological data, Tellus B, 63, 241-254, 10.1111/j.1600-0889.2010.00523.x, 2011.

Xu, J., Tie, X., Gao, W., Lin, Y., and Fu, Q.: Measurement and model analyses of the ozone variation during 2006 to 2015 and its response to emission change in megacity Shanghai, China, Atmos. Chem. Phys., 19, 9017-9035, 10.5194/acp-19-9017-2019, 2019.

Yang, X., Wu, Q., Zhao, R., Cheng, H., He, H., Ma, Q., Wang, L., and Luo, H.: New method for evaluating winter air quality: PM2.5 assessment using Community Multi-Scale Air Quality Modeling (CMAQ) in Xi'an, Atmospheric Environment, 211, 18-28, https://doi.org/10.1016/j.atmosenv.2019.04.019, 2019.

Yuan, H., Dai, Y., Xiao, Z., Ji, D., and Shangguan, W.: Reprocessing the MODIS Leaf Area Index products for land surface and climate modelling, Remote Sensing of Environment, 115, 1171-1187, https://doi.org/10.1016/j.rse.2011.01.001, 2011.

Yu, M., Zhu, Y., Lin, C.-J., Wang, S., Xing, J., Jang, C., Huang, J., Huang, J., Jin, J., and Yu, L.: Effects of air pollution control measures on air quality improvement in Guangzhou, China, Journal of Environmental Management, 244, 127-137, https://doi.org/10.1016/j.jenvman.2019.05.046, 2019.

Zhang, Y., Peng, C., Li, W., Tian, L., Zhu, Q., Chen, H., Fang, X., Zhang, G., Liu, G., Mu, X., Li, Z., Li, S., Yang, Y., Wang, J., and Xiao, X.: Multiple afforestation programs accelerate the greenness in the 'Three North' region of China from 1982 to 2013, Ecological Indicators, 61, 404-412, https://doi.org/10.1016/j.ecolind.2015.09.041, 2016.

Zheng, B., Tong, D., Li, M., Liu, F., Hong, C., Geng, G., Li, H., Li, X., Peng, L., Qi, J., Yan, L., Zhang, Y., Zhao, H., Zheng, Y., He, K., and Zhang, Q.: Trends in China's anthropogenic emissions since 2010 as the consequence of clean air actions, Atmos. Chem. Phys., 18, 14095-14111, 10.5194/acp-18-14095-2018, 2018.

Zhu, L., Jacob, D. J., Keutsch, F. N., Mickley, L. J., Scheffe, R., Strum, M., González Abad, G., Chance, K., Yang, K., Rappenglück, B., Millet, D. B., Baasandorj, M., Jaeglé, L., and Shah, V.: Formaldehyde (HCHO) As a Hazardous Air Pollutant: Mapping Surface Air Concentrations from Satellite and Inferring Cancer Risks in the United States, Environmental Science & Technology, 51, 5650-5657, 10.1021/acs.est.7b01356, 2017a.

Formatted: Font color: Text 1

Formatted: Font color: Text 1

Zhu, L., Mickley, L. J., Jacob, D. J., Marais, E. A., Sheng, J., Hu, L., Abad, G. G., and Chance, K.: Long-term (2005–2014) trends in formaldehyde (HCHO) columns across North America as seen by the OMI satellite instrument: Evidence of changing emissions of volatile organic compounds, Geophysical Research Letters, 44, 7079-7086, 10.1002/2017GL073859, 2017b.

Table 1. Description of different scenarios used to estimate the BVOC emission.

	Land Cover	LAI	Meteorological conditions
S1	Annually updated	Annually updated	Annually updated
S2	Annually updated	Annually updated	Year 2001
S3	Year 2001	Year 2001	Annually updated
S4	Year 2016	Year 2016	Annually updated
S5	Year 2001	Annually updated	Year 2001

Table 2. The mean annual China emission (Tg) of different species during 2001 to 2016. The scenarios S1 to ~~S4~~S5 are described in Table 1.

	S1	S2	S3	S4	S5
Isoprene	15.94 (±1.12)	~~7.56~~15.40 (±0.~~74~~66)	~~7.40~~14.63 (±0.~~56~~76)	~~6.68~~16.70 (±0.~~32~~89)	~~8.68~~15.29 (±0.~~45~~54)
Monoterpenes	~~1.37~~3.99 (±0.~~12~~17)	~~1.35~~3.91 (±0.10)	~~1.24~~3.78 (±0.~~03~~12)	~~1.58~~4.12 (±0.~~05~~14)	3.9 (±0.08)
Sesquiterpenes	0.50 (±0.03)	0.~~16~~48 (±0.02)	0.~~16~~47 (±0.~~01~~02)	0.~~15~~51 (±0.~~01~~03)	0.~~19~~48 (±0.~~01~~02)
Other VOCs	~~6.73~~13.84 (±0.~~46~~78)	~~6.94~~13.95 (±0.~~24~~34)	~~6.16~~12.89 (±0.~~36~~66)	~~7.~~14.15 (±0.~~40~~73)	13.95 (±0.34)
Total BVOCs	34.27 (±2.06)	~~15.82~~33.74 (±1.~~29~~10)	~~15.85~~ (±0.~~91~~31.77 (±1.54)	~~14.23~~ (±0.~~70~~35.48 (±1.76)	~~17.59~~33.63 (±0.~~89~~95)

Table 3. ~~Comparison of isoprene~~The change and ~~monoterpene emissions (Tg)~~trend of annual emission flux (S1, S2 and S5), cover fractions of main PFTs, LAIv, growing season temperature and DSW in northeastern China ~~with previous estimations~~, Beijing and

Formatted ... [1]
Inserted Cells
Formatted: Font color: Text 1
Inserted Cells
Formatted: Font color: Text 1
Inserted Cells
Formatted: Font color: Text 1
Formatted: Font color: Text 1
Formatted: Font color: Text 1
Formatted: Font color: Text 1
Formatted: Font color: Text 1
Formatted: Font color: Text 1
Formatted ... [2]
Inserted Cells
Formatted ... [3]
Formatted ... [4]
Formatted ... [5]
Formatted ... [6]
Inserted Cells
Formatted: Font color: Text 1
Formatted ... [7]
Formatted: Font color: Text 1
Formatted ... [8]
Formatted ... [9]
Inserted Cells
Formatted: Font color: Text 1
Formatted ... [10]
Formatted ... [11]
Formatted ... [12]
Formatted ... [13]
Formatted: Font color: Text 1
Inserted Cells
Formatted ... [14]
Formatted ... [15]
Formatted ... [16]
Formatted ... [17]
Inserted Cells
Formatted: Font color: Text 1
Formatted ... [19]
Formatted ... [18]
Formatted: Font color: Text 1
Inserted Cells
Formatted: Font color: Text 1
Formatted: Font color: Text 1
Formatted: Font color: Text 1
Formatted ... [20]
Formatted ... [21]

its surrounding areas and the Qinling Mountains.

Reference	Isoprene	Monoterpene	Study period	Method or Model
Northeastern China		e		

	BVOC Emission (S2, g m^{-2})	BVOC Emission (S1, g m^{-2})	BVOC Emission (S5, g m^{-2})	LAIv (m^{-2} m^{-2})	BLT Cover Fraction	NLT Cover Fraction (%)	Shrub Cover Fraction (%)	Grass Cover Fraction (%)	Crop Cover Fraction (%)	2-m Temp (°C)	DSW (W m^{-2})
This study Average	7.56 3.37 (±0.74 13)	3.04 (±0.36)	3.25 (±0.06)	1.27 45 (±0.121)	2001 2016 21.37 (±1.56)	MEGAN 13.56 (±0.12)	5.97 (±0.16)	30.86 (±1.8)	25.85 (±0.3)	13.74 (±0.67)	224.5 (±6.98)
Stavrakou et al. (2014) Average (2001-2004)	7.17 3.21 (±0.30 05)	2.9 (±0.32)	2007 2012 3.19 (±0.06)	MEGAN MOHYCAN 1.34 (±0.05)	19.37 (±0.51)	13.57 (±0.04)	6.06 (±0.15)	33.1 (±0.61)	25.71 (±0.21)	13.89 (±0.41)	227.54 (±5.22)
Average (2013-2016)	3.52 (±0.06)	3.07 (±0.36)	3.3 (±0.05)	1.55 (±0.12)	23.1 (±0.04)	13.45 (±0.13)	5.87 (±0.04)	28.7 (±0.18)	26.22 (±0.25)	13.42 (±0.59)	218.39 (±4.74)
Trend	0.02***a	0.01	0.01**	0.02**	0.31***	-0.01	-0.03**	-0.37***	0.06***	-0.03	-0.73**

Beijing & its surrounding areas

	BVOC Emission (S2, g m^{-2})	BVOC Emission (S1, g m^{-2})	BVOC Emission (S5, g m^{-2})	LAIv (m^{-2} m^{-2})	BLT Cover Fraction	NLT Cover Fraction (%)	Shrub Cover Fraction (%)	Grass Cover Fraction (%)	Crop Cover Fraction (%)	2-m Temp (°C)	DSW (W m^{-2})
Average	2.94 (±0.21)	2.58 (±0.25)	2.76 (±0.08)	1.24 (±0.1)	4.96 (±1.17)	0.61 (±0.25)	2.74 (±0.63)	58.18 (±1.58)	27.48 (±1.33)	17.68 (±0.65)	251.09 (±3.22)
Average (2001-2004)	2.7 (±0.14)	2.41 (±0.09)	2.67 (±0.12)	1.13 (±0.11)	3.83 (±0.16)	0.35 (±0.03)	1.99 (±0.11)	58.73 (±0.07)	29.44 (±0.33)	17.87 (±0.6)	250.47 (±4.56)
Average (2013-2016)	3.22 (±0.08)	2.81 (±0.29)	2.81 (±0.04)	1.3 (±0.08)	6.66 (±0.44)	0.97 (±0.14)	3.6 (±0.27)	55.84 (±1.26)	26.51 (±0.41)	17.52 (±0.75)	250.42 (±1.95)
Trend	0.04***	0.03*	0.01**	0.01*	0.23***	0.04***	0.13***	-0.18*	-0.26***	-0.03	0.02

Qinling Mountains

Formatted: Font color: Text 1
Deleted Cells
Deleted Cells
Deleted Cells
Deleted Cells
Formatted ... 23
Formatted ... 22
Formatted Table
Inserted Cells
Formatted ... 29
Inserted Cells
Inserted Cells
Inserted Cells
Inserted Cells
Inserted Cells
Inserted Cells
Formatted ... 24
Formatted ... 25
Formatted ... 26
Formatted ... 30
Formatted ... 31
Formatted ... 32
Formatted ... 27
Formatted ... 35
Formatted ... 36
Formatted ... 28
Formatted ... 33
Formatted ... 34
Formatted ... 37
Inserted Cells
Inserted Cells
Formatted ... 39
Formatted ... 40
Formatted ... 42
Formatted ... 43
Formatted ... 38
Formatted ... 41
Formatted ... 44
Formatted ... 45
Formatted ... 46
Formatted ... 47

	BVOC Emission (S2, g m^{-2})	BVOC Emission (S1, g m^{-2})	BVOC Emission (S5, g m^{-2})	LAIv (m^{-2} m^{-2})	BLT Cover Fraction	NLT Cover Fraction (%)	Shrub Cover Fraction (%)	Grass Cover Fraction (%)	Crop Cover Fraction (%)	2-m Temp (°C)	DSW (W m^{-2})
Average	9.25 (±0.38)	9.29 (±0.93)	9.10 (±0.28)	1.8 (±0.19)	44.08 (±1.52)	12.25 (±0.17)	14.05 (±0.64)	14.67 (±0.67)	12.15 (±0.25)	20.78 (±0.58)	219.93 (±9.01)
Average (2001-2004)	8.84 (±0.25)	8.91 (±0.38)	8.85 (±0.25)	1.59 (±0.17)	42.18 (±0.32)	12.48 (±0.11)	14.84 (±0.29)	15.51 (±0.26)	12.31 (±0.32)	20.83 (±0.25)	220.28 (±9.41)
~~Li et al~~ Average (2013-2016)	~~20.79~~71 (±0.22)	~~4.9~~75 (±1.64)	~~20039.3 9~~ (±0.22)	~~MEGAN~~2.01 (±0.12)	45.91 (±0.27)	12.07 (±0.03)	13.26 (±0.14)	13.84 (±0.16)	11.95 (±0.10)	20.75 (±0.91)	221.26 (±12.30)
Trend	0.06***	0.07	0.04**	0.03***	0.32***	-0.03***	-0.13***	-0.14***	-0.04**	-0.01	-0.11

a: p<0.1; **: p<0.05; ***: p<0.01;

Table 4. The change and trend of annual emission flux (S1, S2 and S5), cover fractions of main PFTs, LAIv, growing season temperature and DSW in Yunnan province, Guangxi-Guangdong provinces and Hainan island.

Yunnan provincc

	BVOC Emission (S2, g m^{-2})	BVOC Emission (S1, g m^{-2})	BVOC Emission (S5, g m^{-2})	LAIv (m^{-2} m^{-2})	BLT Cover Fraction (%)	NLT Cover Fraction (%)	Shrub Cover Fraction (%)	Grass Cover Fraction (%)	Crop Cover Fraction (%)	2-m Temp (°C)	DSW (W m^{-2})
Average	6.79 (±0.26)	7.28 (±0.54)	6.67 (±0.21)	2.23 (±0.17)	32.7 (±0.83)	14.92 (±0.32)	17.25 (±0.12)	21.83 (±0.52)	9.86 (±0.71)	18.54 (±0.31)	224.71 (±5.64)
Average (2001-2004)	6.53 (±0.28)	6.76 (±0.45)	6.57 (±0.30)	2.02 (±0.19)	32.1 (±0.19)	14.51 (±0.04)	17.22 (±0.14)	22.45 (±0.20)	10.34 (±0.53)	18.35 (±0.30)	219.18 (±6.70)
Average (2013-2016)	7.09 (±0.09)	7.92 (±0.35)	6.94 (±0.04)	2.4 (±0.02)	33.93 (±0.58)	15.33 (±0.1)	17.2 (±0.17)	21.12 (±0.30)	8.92 (±0.25)	18.7 (±0.47)	227.49 (±2.65)
Trend	0.04***a	0.1***	0.02**	0.03***	0.15***	0.07***	0	-0.11***	-0.17***	0.03**	0.42

Guangxi-Guangdong provinces

Inserted Cells
Inserted Cells
Formatted: Caption, Centered, Space After: 10 pt
Formatted: Font: Times New Roman, 7.5 pt, Font color: Text 1
Inserted Cells
Inserted Cells
Inserted Cells
Inserted Cells
Inserted Cells
Formatted: Font: Times New Roman, 7.5 pt, Bold, Font color: Text 1, English (United Kingdom)
Formatted: Font: Times New Roman, 7.5 pt, Bold, Font color: Text 1, English (United Kingdom)
Formatted: Caption, Centered, Space After: 10 pt
Formatted: Font: Times New Roman, 7.5 pt, Bold, Font color: Text 1, English (United Kingdom)
Formatted: Font: Times New Roman, 7.5 pt, Bold, Font color: Text 1, English (United Kingdom)
Formatted: Caption, Centered, Space After: 10 pt
Formatted: Caption, Centered, Space After: 10 pt
Formatted: Font: Times New Roman, 7.5 pt, Bold, Font color: Text 1, English (United Kingdom)
Formatted: Caption, Centered, Space After: 10 pt
Formatted: Font: Times New Roman, 7.5 pt, Font color: Text 1

	BVOC Emission (S2, g m^{-2})	BVOC Emission (S1, g m^{-2})	BVOC Emission (S5, g m^{-2})	LAIv (m^2 m^{-2})	BLT Cover Fraction (%)	NLT Cover Fraction (%)	Shrub Cover Fraction (%)	Grass Cover Fraction (%)	Crop Cover Fraction (%)	2-m Temp (°C)	DSW (W m^{-2})
Average	15.53 (±0.79)	16.23 (±1.59)	15.57 (±0.67)	2.24 (±0.22)	32.92 (±1.6)	9.08 (±0.27)	19.13 (±0.38)	20.47 (±0.60)	9.89 (±0.70)	26.32 (±0.67)	258.72 (±7.32)
Average (2001-2004)	15.06 (±1.09)	15.84 (±1.70)	15.23 (±1.23)	2.1 (±0.35)	32.2 (±0.57)	9.3 (±0.02)	19.41 (±0.04)	21.02 (±0.03)	9.89 (±0.57)	26.36 (±0.25)	258.74 (±9.25)
Average (2013-2016)	16.36 (±0.37)	17.03 (±1.99)	15.92 (±0.29)	2.44 (±0.09)	35.24 (±0.88)	8.69 (±0.19)	18.57 (±0.31)	19.62 (±0.32)	9.03 (±0.16)	26.31 (±0.99)	256.36 (±4.26)
Trend	0.13***	0.14	0.05	0.03**	0.32***	-0.05***	-0.06***	-0.12***	-0.14**	0.02	-0.24

Hainan Island

	BVOC Emission (S2, g m^{-2})	BVOC Emission (S1, g m^{-2})	BVOC Emission (S5, g m^{-2})	LAIv (m^2 m^{-2})	BLT Cover Fraction (%)	NLT Cover Fraction (%)	Shrub Cover Fraction (%)	Grass Cover Fraction (%)	Crop Cover Fraction (%)	2-m Temp (°C)	DSW (W m^{-2})
Average	17.79 (±0.73)	17.98 (±1.40)	17.57 (±0.51)	2.43 (±0.20)	39.44 (±1.46)	0	17.41 (±0.14)	22.2 (±1.12)	8.67 (±0.56)	27.3 (±0.47)	257.51 (±4.55)
Average (2001-2004)	17.16 (±0.72)	17.51 (±1.04)	17.27 (±0.80)	2.3 (±0.26)	38.07 (±0.52)	0	17.46 (±0.18)	23.63 (±0.04)	8.79 (±0.33)	27.38 (±0.22)	259.79 (±7.28)
Average (2013-2016)	18.68 (±0.27)	19.44 (±1.89)	18.07 (±0.24)	2.64 (±0.14)	41.11 (±0.23)	0	17.31 (±0.08)	20.9 (±0.28)	8.14 (±0.07)	27.41 (±0.78)	258.39 (±3.95)
Trend	0.13***	0.12*	0.06**	0.03*	0.27***	**0**	-0.02	-0.22***	-0.07**	0	-0.13

a: p<0.1; **: p<0.05; ***: p<0.01;

Table 5. Comparison of isoprene and monoterpene emissions (Tg) in China with previous studies.

Data Source	Isoprene	Monoterpene	Study period	Method or Model
This study	15.94 (±1.12)	3.99 (±0.17)	2001-2016	MEGAN
Stavrakou et al. (2014)	7.17 (±0.30)	-	2007-2012	MEGAN-MOHYCAN
Li et al. (2013)	23.4	5.6	2003	MEGAN
Li et al. (2020)	33.21	6.35	2008-2018	MEGAN
CAMS-GLOB-BIO v1.1 (Sindelarova et al., 2014)	7.67	3.04	2001-2016	MEGEN
CAMS-GLOB-BIO v3.1 (Sindelarova et al., 2014)	8.54	3.23	2001-2016	MEGAN
Fu and Liao (2012)	10.87	3.21	2001-2006	GEOS-Chem-MEGAN
Tie et al. (2006)	7.7	3.16	2004	Guenther et al. (1993)
Klinger et al. (2002)	4.65	3.97	2000	Guenther et al. (1995)
Guenther et al. (1995)	17	4.87	1990	Guenther et al. (1995)

Formatted: Font color: Text 1
Formatted: Centered
Formatted Table
Formatted: Font color: Text 1
Formatted: Centered
Formatted: Font color: Text 1
Formatted: Centered
Formatted: Font color: Text 1
Formatted: Centered

Table 6. Comparison of inputs for BVOC estimation with previous studies.

Reference	Emission Factor Type	Emission Factor Reference	PFT/Land use	LAI/Biomass	Meteorology	Model/Algorithms
This study	PFT level emission factors	Guenther et al. (2012)	MODIS MCD12C1 v6	MODIS MCD15A2H v5	WRF Model v3.9	MEGANv2.1
Stavrakou et al. (2014)	PFT level emission factors	Guenther et al. (2006)	Ramankutty and Foley (1999)	MODIS MOD15A2 v5	ERA-Interim Dataset	MEGAN-MOHYCAN
Li et al. (2013)	Vegetation genera/species level emission factors	Li et al. (2013)	Vegetation Atlas of China for year 2007	MEGAN database for 2003	MM5 Model v3.7	MEGAN
Li et al. (2020)	Vegetation genera/species level emission factors	Li et al. (2013)	Vegetation Atlas of China for year 2007	Estimations based on surveys and statistics	WRF Model v3.8	MEGAN
CAMS-GLOB-BIO v1.1 (Sindelarova et al., 2014)	PFT level emission factors	Guenther et al. (2012)	16 plant functional types consistent with the Community Land Model	MODIS MOD15A2 v5	ERA-Interim Dataset	MEGAN
CAMS-GLOB-BIO v3.1 (Sindelarova et al., 2014)	PFT level emission factors	Guenther et al. (2012)	16 plant functional types consistent with the Community Land Model	MODIS MOD15A2 v5	ERA-5 Dataset	MEGAN
Fu and Liao (2012)	PFT level emission factors	Guenther et al. (1995) Lathière et al. (2006) Levis et al. (2003) Bai et al. (2006)	MODIS MCD12Q1 v5	MODIS MOD15A2 v5	GEOS-4 Meteorology	GEOS-Chem-MEGAN
Tie et al. (2006)	Landuse level emission factors	Landuse-based emission rates	USGS 1km land use data	/	WRF model	Guenther et al. (1993)
Klinger et al. (2002)	Vegetation genera/species level emission factors	Klinger et al. (2002)	Province-level Forest Inventory	/	Monthly meteorology database by (Leemans and Cramer, 1991)	Guenther et al. (1995)
Guenther et al. (1995)	PFT level emission factors	Guenther et al. (1995)	Grided Global Ecosystem Types	Estimations from NPP	Monthly meteorology database	Guenther et al. (1995)

				by (Leemans and Cramer, 1991)	

Table 7. Detailed descriptions of the flux measurements used in this study and corresponding campaigns.

Reference	Site Location	Sample Collection Periods	Ecosystem Type	Isoprene Emission Factor (mg m^{-2} h^{-1})	Monoterpenes Emission Factor (mg m^{-2} h^{-1})
Bai et al. (2015)	Changbai Mountain (42°24′ N, 128°6′)	28 June -9 July 2010; 19 July -30 July 2010; 12 Aug.- 25 Aug. 2010; 19 June - 30 June 2011; 10 July -16 July 2011; 22 July - 29 July 2011; 5 Sep. - 8 Sep. 2011.	Mixed forest	4.3	0.32
Bai et al. (2016)	An Ji, Zhejiang (30°40′15″ N, 119°40′15″)	7 July-13 July 2012; 20 Aug.-26 Aug. 2012; 25 Sep.-1 Oct. 2012; 28 Oct.- 5 Nov. 2012.	Moso bamboo forest	3.3	0.008
Bai et al. (2017)	Taihe, Jiangxi (26°44′48″ N, 115°04′13″)	22 May -28 May 2013; 29 June - 6 July 2013; 6 Aug. -13 Aug. 2013; 7 Sep. -11 Sep. 2013; 18 Jan. -19 Jan. 2014; 23 July - 27 July 2014; 2 Nov. - 7 Nov. 2015; 31 Dec. 2015 -4 Jan. 2016.	Subtropical Pinus forest	0.71	1.65

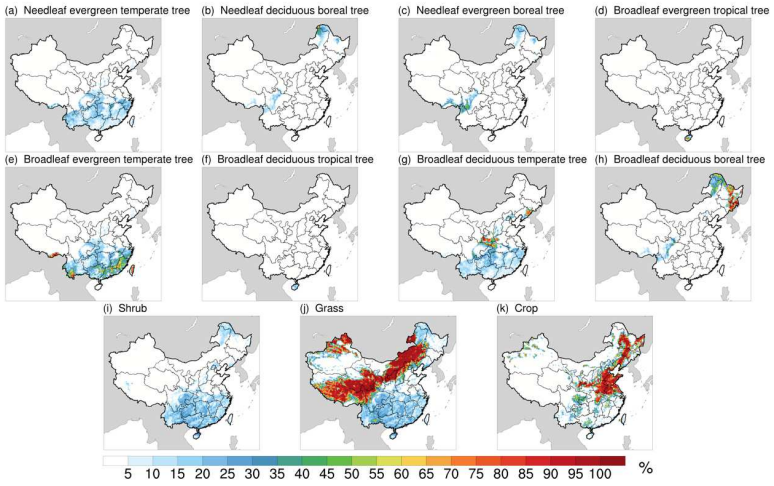

Figure 1. The cover factions of different PFTs for the year 2016.

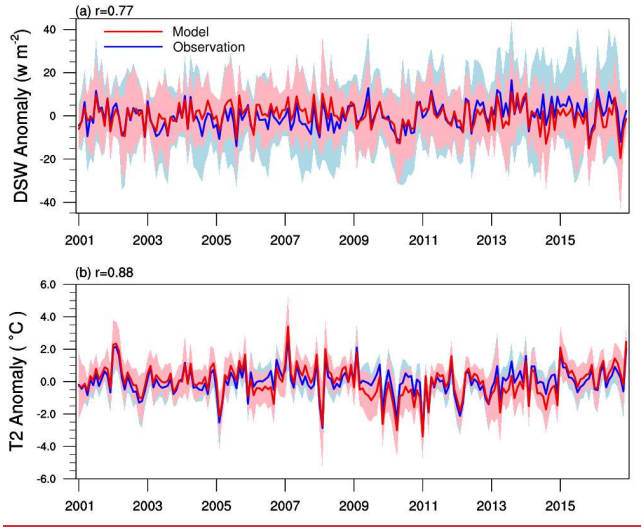

Figure 2. The comparison of monthly anomaly of downward shortwave (DSW) radiation (a) and 2-meter temperature (T2) (b) for model simulation and in-situ observation and the filled areas present the standard deviations among 98 sites for DSW and 697 sites for T2.

Formatted: Width: 21.59 cm, Height: 27.94 cm

Formatted: Font color: Text 1

Formatted: Font color: Text 1

Formatted: Font color: Text 1

Formatted: Font color: Text 1

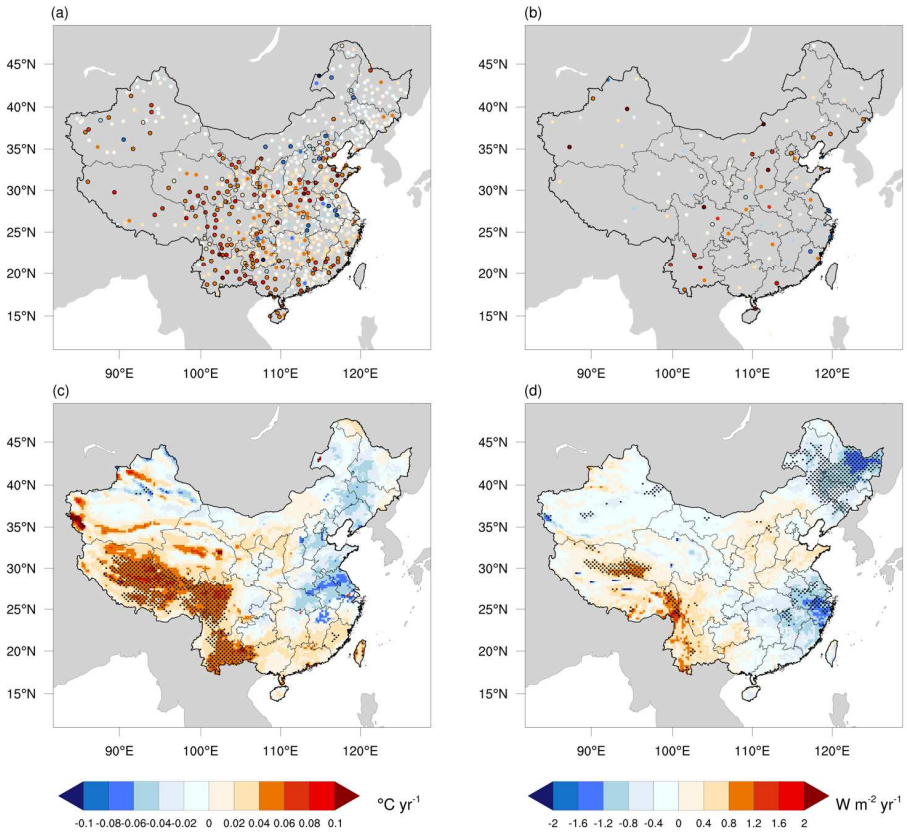

Figure 3. The trend of growing season averaged 2-meter temperature (T2) and downward shortwave radiation (DSW). (a) and (b) are for in-situ T2 and DSW, respectively, and the sites with statistically significant trend are marked by black circles. (c) and (d) are for the WRF simulated T2 and DSW, respectively, and the regions with statistically significant trend are illustrated by shadow.

Formatted: Font color: Text 1

Formatted: Font color: Text 1

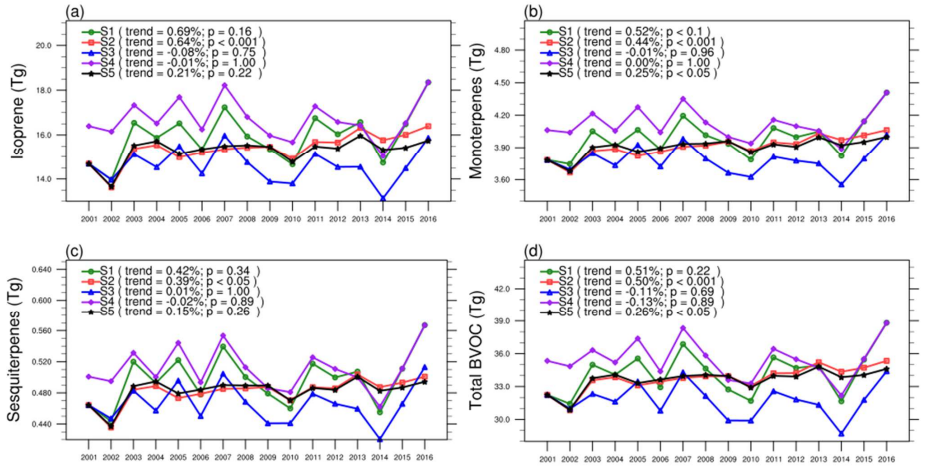

Figure 4. Annual BVOC emissions in China during 2001 to 2016 for four scenarios (S1-S4S5) described in Table 1. The increasing trends and the probabilities (p) using the Mann-Kendall test are shown in the legend.

Formatted: Font color: Text 1

Formatted: Font color: Text 1

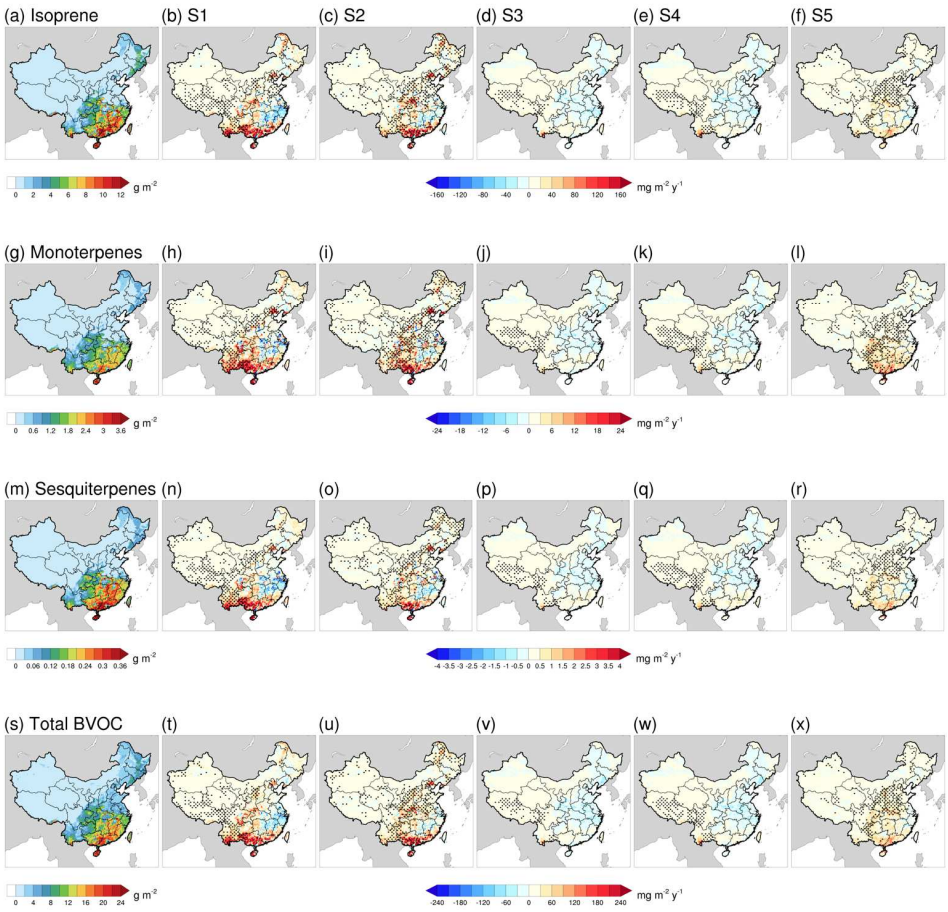

Figure 5. The horizontal distributions of isoprene, monoterpenes, sesquiterpenes and total BVOCs emissions of China in 2001 are showed in figure (a), (~~f~~), (~~kg~~), (m) and (~~ps~~), respectively. The rest columns of figures present the changing trend of isoprene (b-~~e~~f), monoterpenes (~~g~~-~~jh~~-l), sesquiterpenes (~~l~~-~~o~~n-~~r~~) and total BVOCs (~~q~~-t-x) in S1, S2, S3, S4 and ~~S4~~S5, respectively. The Mann-Kendall test were used to ~~filter~~mark the grids where the p is ~~lowers~~maller than 0.~~9~~1.

Formatted: Font color: Text 1
Formatted: Font color: Text 1
Formatted: Space After: 0 pt, No widow/orphan control
Formatted: Font color: Text 1
Formatted: Font color: Text 1
Formatted: Font color: Text 1
Formatted: Font color: Text 1
Formatted: Font color: Text 1
Formatted: Font color: Text 1
Formatted: Font color: Text 1
Formatted: Font color: Text 1
Formatted: Font color: Text 1
Formatted: Font color: Text 1
Formatted: Font color: Text 1
Formatted: Font color: Text 1

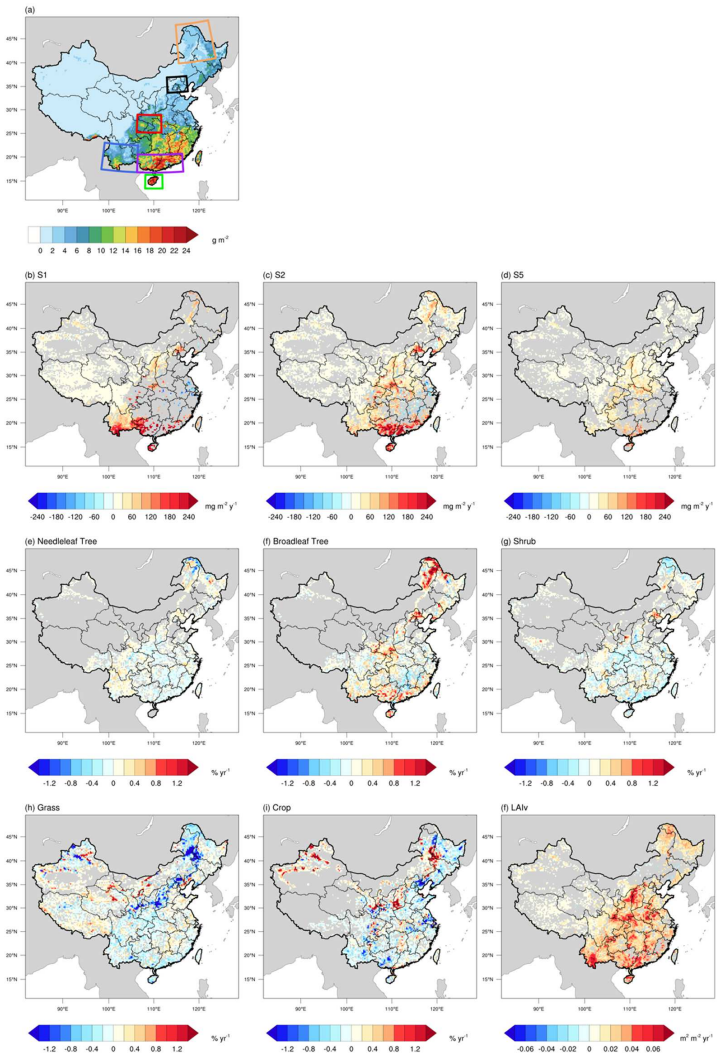

Figure 6. Spatial distribution of BVOC emission in 2001 (a) and the changing trends of annual emission flux (S1, S2 and S5), cover fractions of main PFTs and LAIv. The Mann-Kendall test were used to filter the grids where the p is greater than 0.1.

Formatted: Font color: Text 1

Formatted: Font color: Text 1

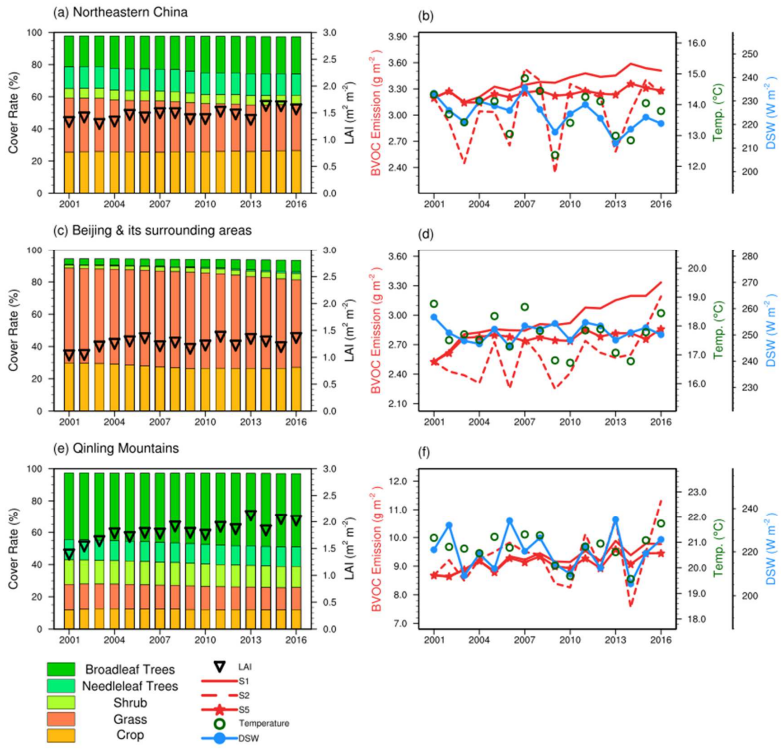

Figure 7. The annual changes of PFTs, the annual emission ~~rate~~amount of BVOC and LAI in (a) ~~the Qinling Montains, (b) southern of~~ northeastern China, (b) Beijing and its surroundings, and the (c) ~~the Jiang Xi and Hu Nan province border.~~Qinling mountains. The solid ~~and~~, dashed and marked line represents the mean emission flux rate of total BVOC in S1, S2 and ~~S2~~S5, respectively.

Formatted: Font color: Text 1
Formatted: Font color: Text 1
Formatted: Font color: Text 1
Formatted: Font color: Text 1
Formatted: Font color: Text 1
Formatted: Font color: Text 1
Formatted: Font color: Text 1
Formatted: Font color: Text 1
Formatted: Font color: Text 1
Formatted: Font color: Text 1

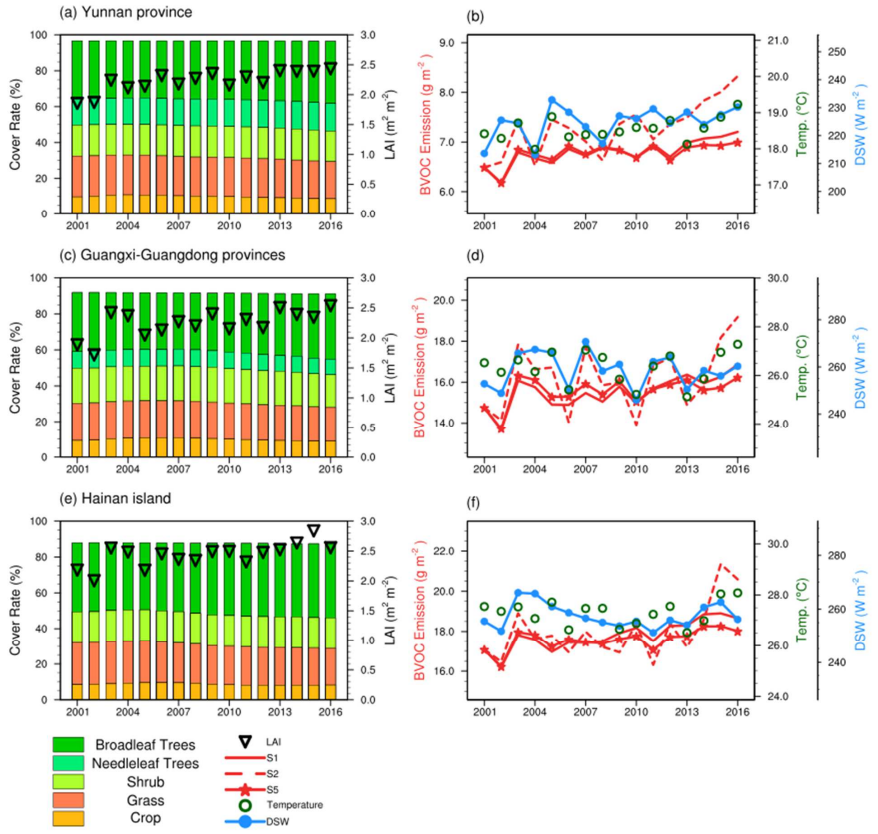

Figure 8. The annual changes of PFTs, the annual emission amount of BVOC and LAI in (a) southwestern China, (b) southern, and (c) Hainan island. The solid, dashed and marked line represents the mean emission flux rate of total BVOC in S1, S2 and S5, respectively.

Formatted: Font color: Text 1

Formatted: Font color: Text 1

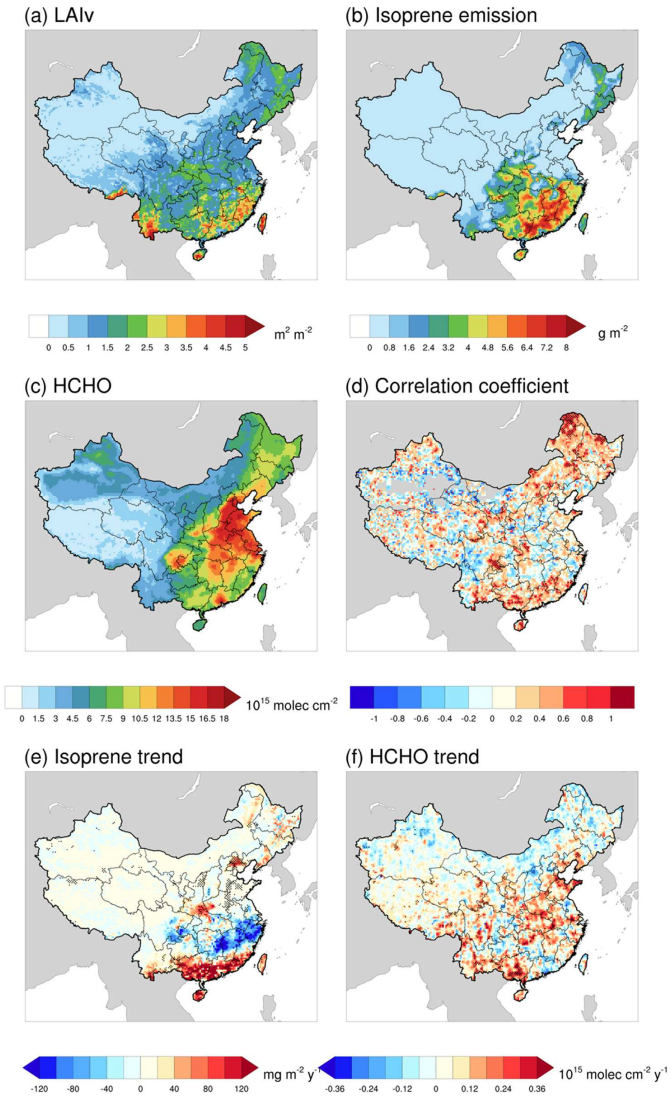

Figure 9. Comparison of estimated isoprene annual emission with the satellite derived tropospheric HCHO vertical column concentration by OMI during 2005-2016. (a), (b) and (c) illustrate the spatial ~~distributions~~patterns of ~~growing season~~annual mean ~~LAI~~LAIv, isoprene emission and HCHO vertical columns (VC) by OMI respectively. (d) presents the spatial distribution of the correlation ~~efficient~~coefficient between summertime isoprene emission and HCHO VC. (e) and (f) shows the increasing trend of isoprene and HCHO VC during 2005-2016.

Formatted: Font color: Text 1
Formatted: Font color: Text 1
Formatted: Font color: Text 1
Formatted: Font color: Text 1
Formatted: Font color: Text 1

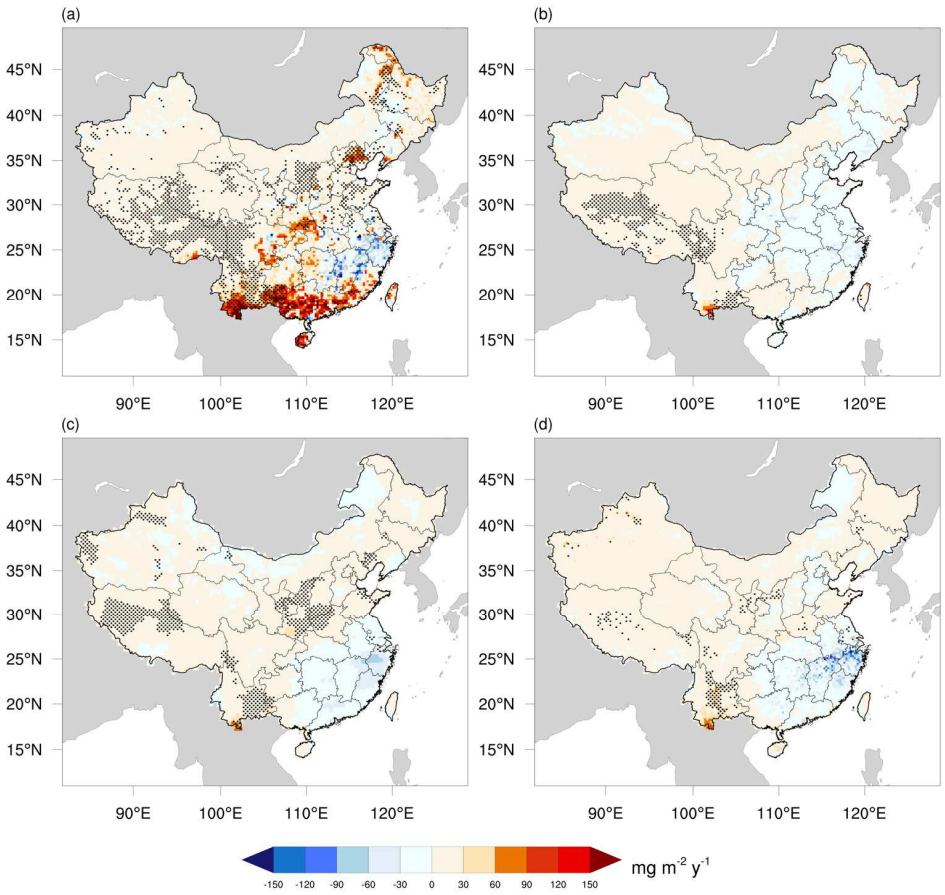

Figure 10. Comparison of ~~BVOC~~the trend of isoprene emission ~~with anthropogenic VOC (Zheng et al., 2018~~between this study (S1) and ~~NOx emission in China~~other estimations during ~~2010~~2001-2016. ~~The dashed lines represent the average emission of NOx(orange), AVOC (blue), BVOC(green) during 2010 to 2016.~~(a) and (b) is for S1 and S3 respectively. in this study, and (c) and (d) are for CAMS-GLOB-BIO v 1.1 and CAM-GLOB-BIO v3.1, respectively. The Mann-Kendall test were used to mark the grids where the p is smaller than 0.1.

Formatted: Font color: Text 1
Formatted: Font color: Text 1
Formatted: Font color: Text 1
Formatted: Font color: Text 1
Formatted: Font color: Text 1
Formatted: Font color: Text 1
Formatted: Font color: Text 1
Formatted: Font color: Text 1

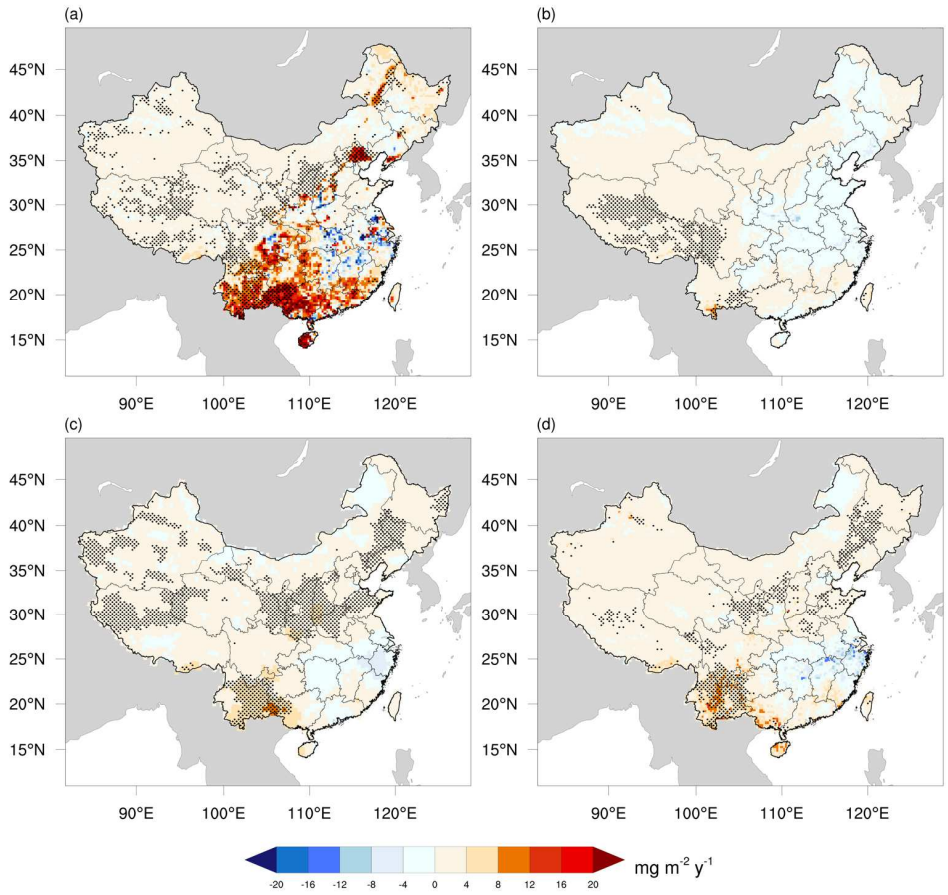

Figure 11. Comparison of the trend of monoterpenes emission between this study (S1) and other estimations during 2001-2016. (a) and (b) is for S1 and S3, respectively, in this study, and (c) and (d) are for CAMS-GLOB-BIO v 1.1 and CAM-GLOB-BIO v3.1, respectively. The Mann-Kendall test were used to mark the grids where the p is smaller than 0.1.

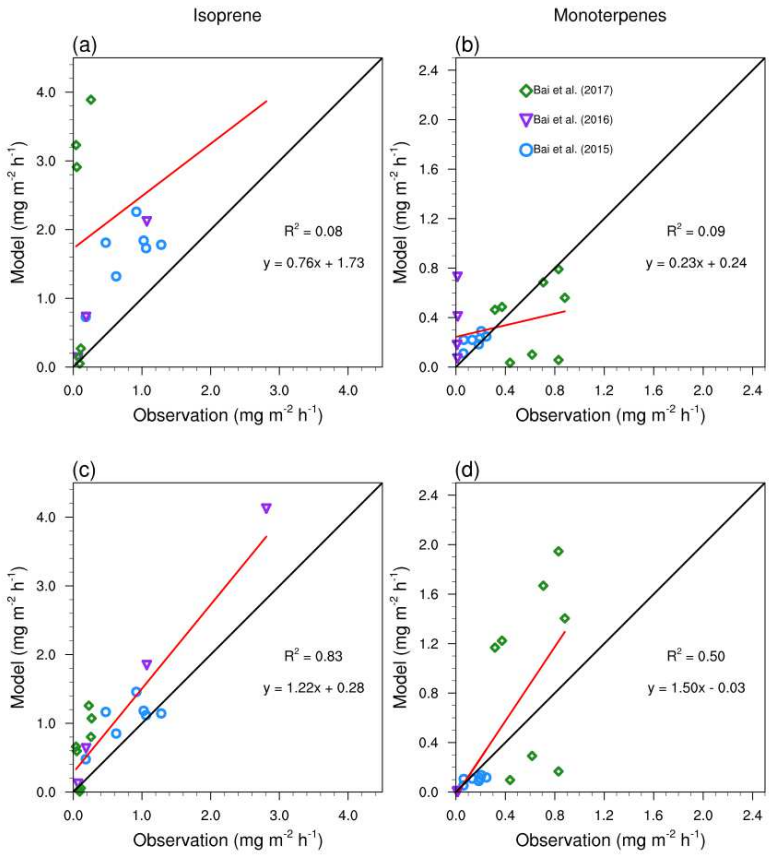

Figure 12. Validation of the model with flux measurements in China. (a) and (b) show the performance of the MEGAN model with the default emission factors (N=19). (c) and (d) show the performance of the MEGAN model with the emission factors derived from observations (N=19).

Formatted: Font color: Text 1

Page 25: [1] Formatted Author 23/10/2020 20:37:00

Font color: Text 1

Page 25: [1] Formatted Author 23/10/2020 20:37:00

Font color: Text 1

Page 25: [1] Formatted Author 23/10/2020 20:37:00

Font color: Text 1

Page 27: [2] Formatted Author 23/10/2020 20:37:00

Font color: Text 1

Page 27: [2] Formatted Author 23/10/2020 20:37:00

Font color: Text 1

Page 27: [2] Formatted Author 23/10/2020 20:37:00

Font color: Text 1

Page 27: [2] Formatted Author 23/10/2020 20:37:00

Font color: Text 1

Page 27: [3] Formatted Author 23/10/2020 20:37:00

Font color: Text 1

Page 27: [3] Formatted Author 23/10/2020 20:37:00

Font color: Text 1

Page 27: [4] Formatted Author 23/10/2020 20:37:00

Font color: Text 1

Page 27: [4] Formatted Author 23/10/2020 20:37:00

Font color: Text 1

Page 27: [5] Formatted Author 23/10/2020 20:37:00

Font color: Text 1

Page 27: [5] Formatted Author 23/10/2020 20:37:00

Font color: Text 1

Page 27: [6] Formatted Author 23/10/2020 20:37:00

Font color: Text 1

Page 27: [6] Formatted Author 23/10/2020 20:37:00

Font color: Text 1

Page 27: [7] Formatted Author 23/10/2020 20:37:00

Font color: Text 1

Page 27: [7] Formatted Author 23/10/2020 20:37:00

Font color: Text 1

Page 27: [8] Formatted Author 23/10/2020 20:37:00

Font color: Text 1

Page 27: [8] Formatted Author 23/10/2020 20:37:00

Font color: Text 1

Page 27: [9] Formatted Author 23/10/2020 20:37:00

Font color: Text 1

Page 27: [9] Formatted Author 23/10/2020 20:37:00

Font color: Text 1

Page 27: [10] Formatted Author 23/10/2020 20:37:00

Font color: Text 1

Page 27: [10] Formatted Author 23/10/2020 20:37:00

Font color: Text 1

Page 27: [11] Formatted Author 23/10/2020 20:37:00

Font color: Text 1

Page 27: [11] Formatted Author 23/10/2020 20:37:00

Font color: Text 1

Page 27: [12] Formatted Author 23/10/2020 20:37:00

Font color: Text 1

Page 27: [12] Formatted Author 23/10/2020 20:37:00

Font color: Text 1

Page 27: [13] Formatted Author 23/10/2020 20:37:00

Font color: Text 1

Page 27: [13] Formatted Author 23/10/2020 20:37:00

Font color: Text 1

Page 27: [14] Formatted Author 23/10/2020 20:37:00

Font color: Text 1

Page 27: [14] Formatted Author 23/10/2020 20:37:00

Font color: Text 1

Page 27: [15] Formatted Author 23/10/2020 20:37:00

Font color: Text 1

Page 27: [15] Formatted Author 23/10/2020 20:37:00

Font color: Text 1

Page 27: [16] Formatted Author 23/10/2020 20:37:00

Font color: Text 1

Page 27: [16] Formatted Author 23/10/2020 20:37:00

Font color: Text 1

Page 27: [17] Formatted Author 23/10/2020 20:37:00

Font color: Text 1

Page 27: [17] Formatted Author 23/10/2020 20:37:00

Font color: Text 1

Page 27: [17] Formatted Author 23/10/2020 20:37:00

Font color: Text 1

Page 27: [18] Formatted Author 23/10/2020 20:37:00

Font color: Text 1

Page 27: [18] Formatted Author 23/10/2020 20:37:00

Font color: Text 1

Page 27: [19] Formatted Author 23/10/2020 20:37:00

Font color: Text 1

Page 27: [19] Formatted Author 23/10/2020 20:37:00

Font color: Text 1

Page 27: [20] Formatted Author 23/10/2020 20:37:00

Space After: 0 pt, No widow/orphan control, Keep with next

Page 27: [21] Formatted Author 23/10/2020 20:37:00

Font color: Text 1

Page 27: [21] Formatted Author 23/10/2020 20:37:00

Font color: Text 1

Page 27: [21] Formatted Author 23/10/2020 20:37:00

Font color: Text 1

Page 27: [21] Formatted Author 23/10/2020 20:37:00

Font color: Text 1

Page 27: [21] Formatted Author 23/10/2020 20:37:00

Font color: Text 1

Page 28: [22] Formatted Author 23/10/2020 20:37:00

Caption, Centered, Space After: 10 pt

Page 28: [23] Formatted Author 23/10/2020 20:37:00

Font: Times New Roman, 7.5 pt, Bold, Font color: Text 1, English (United Kingdom)

Page 28: [24] Formatted Author 23/10/2020 20:37:00

Caption, Centered, Space After: 10 pt

Page 28: [25] Formatted Author 23/10/2020 20:37:00

Font: Times New Roman, 7.5 pt, Bold, Font color: Text 1, English (United Kingdom)

Page 28: [26] Formatted Author 23/10/2020 20:37:00

Font: Times New Roman, 7.5 pt, Font color: Text 1

Page 28: [27] Formatted Author 23/10/2020 20:37:00

Caption, Centered, Space After: 10 pt

Page 28: [28] Formatted Author 23/10/2020 20:37:00

Font: Times New Roman, 7.5 pt, Font color: Text 1

Page 28: [29] Formatted Author 23/10/2020 20:37:00

Font: Times New Roman, 7.5 pt, Font color: Text 1

Page 28: [30] Formatted Author 23/10/2020 20:37:00

Font: Times New Roman, 7.5 pt, Font color: Text 1

Page 28: [31] Formatted Author 23/10/2020 20:37:00

Caption, Centered, Space After: 10 pt

Page 28: [32] Formatted Author 23/10/2020 20:37:00

Font: Times New Roman, 7.5 pt, Font color: Text 1

Page 28: [33] Formatted Author 23/10/2020 20:37:00

Caption, Centered, Space After: 10 pt

Page 28: [34] Formatted Author 23/10/2020 20:37:00

Font: Times New Roman, 7.5 pt, Bold, Font color: Text 1, English (United Kingdom)

Page 28: [35] Formatted Author 23/10/2020 20:37:00

Caption, Centered, Space After: 10 pt

Page 28: [36] Formatted Author 23/10/2020 20:37:00

Font: Times New Roman, 7.5 pt, Bold, Font color: Text 1, English (United Kingdom)

Page 28: [37] Formatted Author 23/10/2020 20:37:00

Caption, Centered, Space After: 10 pt

Page 28: [38] Formatted Author 23/10/2020 20:37:00

Font: Times New Roman, 7.5 pt, Bold, Font color: Text 1, English (United Kingdom)

Page 28: [39] Formatted Author 23/10/2020 20:37:00

Font: Times New Roman, 7.5 pt, Font color: Text 1

Page 28: [40] Formatted Author 23/10/2020 20:37:00

Caption, Centered, Space After: 10 pt

Page 28: [41] Formatted Author 23/10/2020 20:37:00

Font: Times New Roman, 7.5 pt, Font color: Text 1

Page 28: [42] Formatted Author 23/10/2020 20:37:00

Caption, Centered, Space After: 10 pt

Page 28: [43] Formatted Author 23/10/2020 20:37:00

Font: Times New Roman, 7.5 pt, Bold, Font color: Text 1, English (United Kingdom)

Page 28: [44] Formatted Author 23/10/2020 20:37:00

Caption, Centered, Space After: 10 pt

Page 28: [45] Formatted Author 23/10/2020 20:37:00

Font: Times New Roman, 7.5 pt, Font color: Text 1

Page 28: [46] Formatted Author 23/10/2020 20:37:00

Caption, Centered, Space After: 10 pt

Page 28: [47] Formatted Author 23/10/2020 20:37:00

Font: Times New Roman, 7.5 pt, Bold, Font color: Text 1, English (United Kingdom)

Table S1. Look-up table for mapping the IGBP legend to eight main vegetations categories.

Name	Value	Description	Main Category Percentage
Needleleaf Evergreen Forest	1	Dominated by evergreen conifer trees (canopy >2m).	100% NET
Broadleaf Evergreen Forest	2	Dominated by evergreen broadleaf and palmate trees (canopy >2m).	100% BET
Needleleaf Deciduous Forest	3	Dominated by deciduous needleleaf (larch) trees (canopy >2m).	100% NDT
Broadleaf Deciduous Forest	4	Dominated by deciduous broadleaf trees (canopy >2m).	100% BDT
Mixed Forests	5	Dominated by neither deciduous nor evergreen (40-60% of each) tree type (canopy >2m).	100% Mixed Forests
Closed Shrublands	6	Dominated by woody perennials (1-2m height) >60% cover.	100% Shrub
Open Shrublands	7	Dominated by woody perennials (1-2m height) 10-60% cover.	60% Shrub 40% Grass
Woody Savannas	8	Tree cover 30-60% (canopy >2m).	60% Mixed Forest 20% Shrub 20% Grass
Savannas	9	Tree cover 10-30% (canopy >2m).	30% Mixed Forest 35% Shrub 35% Grass
Grasslands	10	Dominated by herbaceous annuals (<2m).	100% Grass
Permanent Wetlands	11	Permanently inundated lands with 30-60% water cover and >10% vegetated cover.	40% Grass
Croplands	12	At least 60% of area is cultivated cropland.	100% Crop

Urban and Built-up Lands	13	At least 30% impervious surface area including building materials, asphalt, and vehicles.	None
Cropland/Natural Vegetation Mosaics	14	Mosaics of small-scale cultivation 40-60% with natural tree, shrub, or herbaceous vegetation.	60% Crop 20% Shrub 20% Grass
Permanent Snow and Ice	15	At least 60% of area is covered by snow and ice for at least 10 months of the year.	None
Barren	16	At least 60% of area is non-vegetated barren (sand, rock, soil) areas with less than 10% vegetation.	None

Table 2. The climatic criteria for mapping main vegetation categories to CLM PFTs.

Main Category	Mapping Condition	CLM PFT
NET	T_c>-19 °C and GDD > 1200	100% NET Temperate
	T_c≤-19 °C or GDD ≤ 1200	100% NET Boreal
BET	T_c>15.5 °C	100% BET Tropical
	T_c≤15.5 °C	100% BET Temperate
NDT	None	100% NDT
BDT	T_c>15.5 °C	100% BDT Tropical
	-15.5 °C <T_c≤15.5 °C or GDD>1200	100% BDT Temperate
	T_c≤-15.5 °C or GDD ≤ 1200	100% BDT Boreal
Mixed Forest	T_c>15.5 °C	50% BET Tropical
		50% BDT Tropical
	-15.5 °C<T_c≤15.5 °C and GDD>1200	33.33% NET Temperate
		33.33% BET Temperate
		33.33% BDT Temperate
	T_c≤-15.5 °C or GDD ≤ 1200	33.33% NDT
		33.33% NET Boreal
		33.33% BDT Boreal

Shrub	T_c>-19 °C and GDD > 1200	100% BDS Temperate
	T_c≤-19 °C or GDD ≤ 1200	100% BDS Boreal
Grass	GDD<1000	100% C3 Arctic
	GDD>1000 and (Tc ≤ 22°C or Pmon≤25 mm)	100% C3
	GDD>1000 and Tc > 22°C and Pmon >25 mm	100% C4
Crop	None	100% Crop

Table S3. The physical schemes for the WRF simulation.

Physical mechanism	Scheme
Microphysics	WSM 3-class simple ice scheme
Long-wave radiation	RRTM scheme
Short-wave radiation	Duhbia scheme
Land Surface	Noah Land Surface Model
PBL Scheme	YSU scheme
Cumulus parameter	Kain-Fritsch (new Eta) scheme

Formatted Table

Formatted: English (United States)